Title
Nanotechnology Approaches for Arabidopsis and Chlamydomonas Chloroplast Bioengineering

Author
Newkirk, Gregory Michael

Publication Date
2023

UNIVERSITY OF CALIFORNIA
RIVERSIDE

Nanotechnology Approaches for *Arabidopsis* and *Chlamydomonas* Chloroplast Bioengineering

A Dissertation submitted in partial satisfaction
of the requirements for the degree of

Doctor of Philosophy

in

Microbiology

by

Gregory Michael Newkirk

September 2023

Dissertation Committee:
Dr. Juan Pablo Giraldo, Chairperson
Dr. Robert Jinkerson
Dr. Ian Wheeldon

The Dissertation of Gregory Michael Newkirk is approved:

Committee Chairperson

University of California, Riverside

Acknowledgments

The text of this dissertation in full, is a reprint of the material as it appears in Newkirk, G. M., Wu, H., Santana, I. & Giraldo, J. P. Catalytic Scavenging of Plant Reactive Oxygen Species In Vivo by Anionic Cerium Oxide Nanoparticles. *J. Vis. Exp.* (2018). This work was supported by the National Science Foundation under grant no. 1911763 to Juan Pablo Giraldo.

The text of this dissertation in full, is a reprint of the material as it appears in Newkirk, G. M., de Allende, P., Jinkerson, R. E. & Giraldo, J. P. Nanotechnology Approaches for Chloroplast Biotechnology Advancements. *Front. Plant Sci.* **12**, 1496 (2021), This work was supported by the University of California, Riverside and USDA National Institute of Food and Agriculture, Hatch project 1009710 to J.P.G. This material is based upon work supported by the National Science Foundation under Grant No. 1817363 to J.P.G. All authors listed have made a substantial, direct and intellectual contribution to the work, and approved it for publication.

With chapter 4, Gregory Newkirk, Juan Pablo Giraldo and Robert Jinkerson conceived the idea and designed the experiments. Gregory Newkirk performed the experiments. Su-ji Jeon performed nanoparticle characterizations. Supreetha Sivaraj helped advise and analyzed biocompatibility assays. Pedro De Allende helped with confocal microscopy and algae strain maintenance. Hye-in Kim and Christopher Castillo. advised on and performed nanoparticle characterizations.

All authors contributed to writing the manuscript. Gregory Newkirk is supported by a fellowship by the Department of Defense National Science and Engineering Graduate Fellowship Program. This work was supported by the National Science Foundation under the Center for Sustainable Nanotechnology, CHE-2001611. The CSN is part of the Centers for Chemical Innovation Program.

The co-authors listed in these publications directed and supervised the research, which forms the basis for this dissertation.

Dedications

To my family.

To the Giraldo Lab.

To future researchers.

ABSTRACT OF THE DISSERTATION

Nanotechnology Approaches for *Arabidopsis* and *Chlamydomonas* Chloroplast Bioengineering

by

Gregory Michael Newkirk

Doctor of Philosophy, Graduate Program in Microbiology
University of California, Riverside, September 2023
Dr. Juan Pablo Giraldo, Chairperson

Nanotechnology approaches to deliver biomolecules to chloroplasts has been applied to land plants, but not well studied in algae. It was found that little is known about how nanomaterial size, charge, and plant biomolecule coatings influence interactions with green algae and its outer algae matrix. Intellectual merit for this research, explored in Chapter 1, included environmental sustainability of industrial runoff and chloroplast transformation for use in synthetic biology. Broader impacts of nanotechnology apply to chloroplast biotechnology would be increased plant productivity, enhanced lipid production for renewable biofuels, and more sustainable biodegradable materials. These nanotechnology approaches, explored in Chapter 2, can lead to new abilities for plants, or bolster existing abilities, such as dealing with the reactive oxygen species created from abiotic or biotic stressors. To enable chloroplast biotechnology through nanomaterial *in situ* approaches, cerium oxide nanoparticles,

outlined in Chapter 3, were fabricated to scavenge reactive oxygen species within chloroplasts of *Arabidopsis* and confocal microscopy with colocalization analysis was used for scavenging confirmation.

In Chapter 4, we delivered DNA to the chloroplasts of algae with single-walled carbon nanotubes coated with a polymer. Carbon nanotubes were coated and bound to single-stranded DNA. Varying polymer lengths and mass ratios of DNA:coated-nanotube were characterized for their size and charge, and those characteristics were analyzed against the green algae *Chlamydomonas reinhardtii* with and without a cell wall. Assays were used to analyze the impact the polymer-coated single-walled carbon nanotubes impact on production of reactive oxygen species, living cell enzymatic activity, and total carotenoid production over four days. To confirm that the DNA biomolecule was being uptaken to the algae chloroplast after a one hour exposure, a dye was bound to the DNA (Dye-DNA). With confocal microscopy, the Dye-DNA was confirmed to colocalize within the chloroplast due to chlorophyll autofluorescence, with a Manders colocalization analysis and ANOVA tests for statistical significance. Our results indicate that the higher charged nanoparticle was able to deliver Dye-DNA at a higher rate than the lower charged nanoparticle, confirming previous hypotheses and models seen in land plants.

Together we demonstrated biomolecule delivery to algal chloroplasts and biocompatibility of DNA and polymer-coated single-walled carbon nanotubes in the model organism green algae *Chlamydomonas reinhardtii*. With this, we can move forward with applications to chloroplast transformation into algae, furthering our understanding and capabilities of synthetic biology for chloroplast biotechnology advancements.

Table of Contents

List of Figures

Supplemental figure list: Chapter 4

List of Tables

Chapter 1: Introduction

Microbial Nanotechnology

Chloroplasts, the home of photosynthesis in plants, are at the center of food production, biofuel renewability, and sustainable biodegradable material production. New tools from molecular and synthetic biology are creating large mutant libraries that may be beneficial for enhanced photosynthetic productivity, e.g. RuBisCO mutants, but the main bottleneck is the chloroplast efficiency rate (Bock, 2015). Current chloroplast transformation rates are limiting because the large carriers are not capable of being targeted to specific organelles and are not customizable based on the organism of interest (Wang et al., 2019). Targeting is important for specific organelles but also to target specific species living within a microbial community, since single culturing specific species is incredibly difficult (Stewart, 2012). In addition, these techniques require monocultures of the organism of choice, and the vast majority cannot be grown in the lab. Microbiology research has expanded dramatically recently, touching every aspect of life, especially the human microbiome-brain connection and the plant root rhizosphere link to productivity (Gwak & Chang, 2021; Philippot et al., 2013). All of these new networks and ways of microbial communication hint at new ways of understanding circuits of regulation to create more and more advanced molecules like biopharmaceuticals (Waheed et al., 2015). Environmental microbes are being exposed to industrial human-derived runoff, causing lethal algal blooms, all the while over 50% of the oxygen in the atmosphere is from microbial aquatic communities (Batley et al., 2013; Gilbert &

Neufeld, 2014; Wells et al., 2015). New microbial defense mechanisms are being retooled for molecular biology that have revolutionized our way of genome engineering through CRISPR-Cas systems (Doudna & Charpentier, 2014). Microbiology remains one of the largest unexplored frontiers in the field of biology, and new tools are needed to explore these communities (Albertsen et al., 2013). Therefore, there is a need for a universal delivery carrier for biomolecules to chloroplasts for increased chloroplast transformation rates and a need to study the nanoparticle uptake characteristics of algae.

Nanotechnology-mediated delivery of biomolecules may be a solution for chloroplast transformation rates while bolstering research into the nanoparticle characteristics that are impacting the environment. Quantum dots have been targeted to chloroplasts with chemical cargo (Santana et al., 2020). Nanomaterials offer tunable and easily modifiable characteristics for advanced modeling of size and charge for entry into land plant cells (Wong et al. 2016; Hu et al. 2020; Santana et al. 2022). Single-walled carbon nanotubes have delivered plasmid DNA to the chloroplasts of land plants and was confirmed by a fluorescent protein reporter (Kwak et al., 2019).

If nanotechnology can deliver biomolecules to chloroplasts, it provides broader impacts into algae, land plants, cyanobacteria, and microbial communities (Figure 1.1). Thus, this dissertation highlights methods and strategies to interface nanomaterials within chloroplasts, engineer nanomaterials for biomolecule delivery into algal chloroplasts, and research the nanoparticle characteristics that impact the uptake into the algal cell.

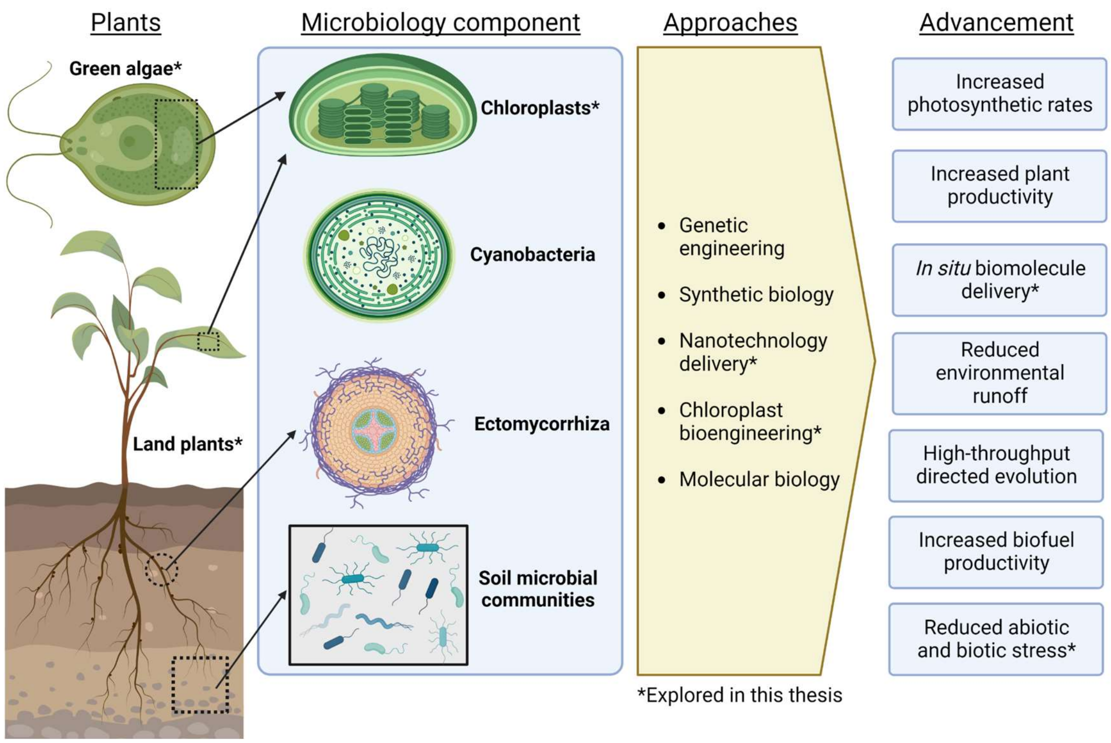

Figure 1.1. Application of plant nanotechnology tools to improve chloroplast biotechnology and microbiology. Applications explored include green algae and land plant chloroplast biotechnology through nanotechnology delivery for reducing abiotic stress and *in situ* biomolecule delivery.

Thesis overview

My aims and objectives for my Dissertation are to:

I. Review nanotechnology advancements for chloroplast biotechnology
II. Develop methods to deliver and image nanomaterials inside chloroplasts of land plants for enabling chloroplast biotechnology
III. Assess the structural elements of algae and nanomaterial properties that impact uptake into algal chloroplasts
IV. Establish assays for delivering genetic material to *Chlamydomonas reinhardtii* chloroplasts

The work discussed here will address methods to interface nanomaterials with chloroplasts and microbes. We will address significant bottlenecks in chloroplast bioengineering by developing nanomaterials can enhance photosynthetic function and that can deliver biomolecules to algal chloroplasts. Lastly, we will assess nanomaterial size and charge in terms of uptake to algal chloroplasts and biocompatibility on the cell. These aims are critical steps in using nanomaterials as a technology to study new unculturable microbial communities and bioengineering microorganisms for enhanced productivity or functions.

Chloroplast Nanobiotechnology

The second chapter is a detailed review of the capability of nanotechnology to improve chloroplast biotechnology research. Current knowledge gaps remain on nanomaterial size, charge, and plant-biocompatible coatings despite recent advances with isolated chloroplasts, plant protoplasts, and plant leaves (Hu et al., 2020; Lew et al., 2018; Wong et al., 2016). Unexplored are the questions surrounding the outer algae matrix and plant cuticle, and their role in the biomolecule-associated nanoparticle coronas formed. In plant cells, nanoparticles up to 18 nm were able to penetrate cotton leaf cells while nanoparticles up to 8 nm were able to penetrate maize leaf cells through application by foliar delivery (Hu et al., 2020). The current model for encompassing nanomaterial entry into the chloroplast is lipid exchange envelope penetration (LEEP), where highly charged nanoparticles with high aspect ratios are capable of entering at a higher rate than ones with a lower charge (Wong et al., 2016).

For ideal applications into synthetic biology research, a universal chassis could efficiently delivery biomolecules directly to chloroplasts. Unfortunately, current chloroplast transformation approaches are only reproducible and stable in ten species and are mediated by 0.6-1.6 μm microcarriers that are not targetable to organelles, unmodifiable outer coatings, and require forced mechanical entry (Bock, 2015; Yu et al., 2017). Despite these limitations in transformation efficiency, chloroplast biotechnology has been bolstered with synthetic riboswitches, site-specific-enabled recombinase, and metabolic pathway engineering through synthetic operons (Lu et al., 2013; Tungsuchat-

Huang et al., 2011; Verhounig et al., 2010). However, any type of large mutant library is incompatible with current chloroplast biotechnology approaches due to the low transformation efficiency (Aigner et al., 2017). Therefore, new biomolecule delivery approaches must be explored for chloroplast biotechnology advancement.

In wild-type plants, nanotechnology approaches have enabled biomolecule delivery to nuclei, chloroplasts, and chemical delivery targeted to chloroplasts. Single-walled carbon nanotubes (SWCNT) have mediated transient nuclear expression of exogenous DNA through fluorescent protein reporters (Demirer et al., 2019). Quantum dots and plasmid-bound SWCNT with a chloroplast targeting peptide were capable of delivering chemical cargoes (Santana et al. 2020; Santana et al. 2022). Mature *Eruca sativa*, *Nasturtium officinale*, *Nicotiana tabacum*, and *Spinacia oleracea* expressed fluorescent protein within the chloroplasts from exogenous DNA delivery (Kwak et al., 2019). Taken together, biomolecule delivery has been demonstrated in land plants but has yet to been explored in algae. This review was published in *Frontiers in Plant Science* (Newkirk et al., 2021).

Nanobioengineered Chloroplasts for Abiotic Stress

Chapter three details the protocol used to synthesize a cerium oxide nanoparticle that was used to scavenge reactive oxygen species inside *Arabidopsis thaliana* chloroplasts and confirmed through colocalization analysis with confocal microscopy. These nanomaterial-based tools and research was motivated by the increasing need to help plants deal with abiotic stresses caused by anthropogenic climate change. The delivered nanoparticle was capable of reducing the ROS levels *in planta* by 52% compared to negative controls. Additionally, hydroxyl radicals were shown to be reduced which have no known plant enzyme scavenger. Upon the addition of abiotic stresses, 61% higher Rubisco carboxylation, 67% carbon assimilation, and 19% higher quantum yield of photosystem II than wildtype plants (Wu et al., 2017, 2018).

Thus, the protocol published provides a reproducible and highly detailed method to nanobioengineer chloroplasts to deal with abiotic stresses and the ROS generated thereof. Recent applications of this protocol have been to help coral reef microbes *Symbiodiniaceae* deal with abiotic stresses (Roger et al., 2022). This work was published in the Journal of Visualized Experiments (Newkirk et al., 2018).

Nanotechnology-enabled Biomolecule Delivery to Algal Chloroplasts

With food demands rising and current algal biofuel production not capable of meeting the increasing demands for a renewable alternative to fossil fuel, there is an increasing need for a highly efficient chloroplast transformation. Current chloroplast transformation rates are so poor that directed evolution experiments with RuBisCO must be done in bacterial systems instead of algae (Wilson et al., 2018; Wilson & Whitney, 2017). If chloroplast biotechnology is enabled with current synthetic biology approaches, food, biofuel, and bioplastic research would be bolstered (Maliga & Bock, 2011; Mayfield & Golden, 2015). Of these nanotechnology approaches, the best one for biomolecule delivery to chloroplasts has been shown to be single-walled carbon nanotubes (Giraldo et al., 2019; Wang et al., 2019). Covered in the positively-charged polyethylenimine (PEI) polymer, DNA is capable of being delivery biomolecules *in planta* (Demirer et al., 2019). Previous studies have shown *Chlamydomonas reinhardtii* interacting with nanoparticles through the lens of environmental toxicology, and not as an applied technology for synthetic biology.

Previous research with *Chlamydomonas reinhardtii*, the green algae and eukaryotic model organism, exposed to single-walled carbon nanotube has looked at the inhibition on growth and photosynthetic ability. SWCNT that were not functionalized or coated showed no inhibitory impacts on growth or quantum yield (Matorin et al., 2010). However, that is hard to take into account, considering how poorly the nanoparticles were characterized. Conversely, salmon sperm DNA, at a 1:1 ratio, was bound to sodium choclate-coated SWCNTs and found after 10 days to have no inhibitory effect on growth of *Chlamydomonas reinhardtii (Williams et al., 2014)*. Again, *Chlamydomonas reinhardtii* was exposed to SWCNT and it was shown that the nanomaterial can protect against photoinhibition (Antal et al., 2022). All together, the current state of algal nanotechnology calls into question the biocompatibility of functionalized nanomaterial that can deliver biomolecules, like that of PEI-coated SWCNT in land plants. With algae being closely related to land plants, this provides an interesting research opportunity to apply land plant entry models that have already been established like lipid exchange envelope penetration mechanism and others that have found size limiations (Hu et al., 2020; Wong et al., 2016).

The fourth chapter utilized knowledge and chemical engineering prowess demonstrated in Chapters two and three to develop single-walled carbon nanotube-mediated delivery of biomolecules to algal chloroplasts. Furthermore, we developed high throughput assays to assess the biocompatibility of multiple coatings at various concentrations and ratios of biomolcule:nanomaterial. This chapter demonstrates a functionalized nanomaterial coated with biomolecule-capable delivery colocalizing a Cy3-ssGT_{15} (Dye-DNA). Coatings are tested for biocompatibility through tests for reactive oxygen species, living cell enzymatic assays, total carotenoid after a four-day exposure, and biomolecule Dye-DNA biomolecule delivery confirmed through confocal microscopy for colocalization with the chloroplast autofluorescence. This protocol and assays could be extrapolated to new coatings or ratios for enhanced uptake, or to test the biomolecule delivery of plasmid DNA for algal chloroplast transformation.

Conclusion

Photosynthesis is a key step that encircles food, fuel, and materials that humans need to use sustainably and renewably in the future. Improved productivity of land plants can be mediated with new technologies: nanotechnology-mediated biosensors, biomolecule delivery, photosynthetic augmentation, and new capabilities to deal with stressors (Giraldo et al., 2019). All of these land plant approaches would be further improved with an algal model species that could be worked with at higher efficiencies. Algae provides high throughput automated liquid handling and mutant screening capabilities that is not possible through land plants(Newkirk et al., 2021). This work provides the basis for algal nanotechnology approaches for synthetic biology advancements in the field of chloroplast biotechnology for the advancement of biofuel, biomaterial, and food engineering.

References

Aigner, H., Wilson, R. H., Bracher, A., Calisse, L., Bhat, J. Y., Hartl, F. U., & Hayer-Hartl, M. (2017). Plant RuBisCo assembly in E. coli with five chloroplast chaperones including BSD2. *Science*, *358*(6368), 1272–1278. https://doi.org/10.1126/science.aap9221

Albertsen, M., Hugenholtz, P., Skarshewski, A., Nielsen, K. L., Tyson, G. W., & Nielsen, P. H. (2013). Genome sequences of rare, uncultured bacteria obtained by differential coverage binning of multiple metagenomes. *Nature Biotechnology*, *31*(6), 533–538. https://doi.org/10.1038/nbt.2579

Antal, T. K., Volgusheva, A. A., Kukarskikh, G. P., Lukashev, E. P., Bulychev, A. A., Margonelli, A., Orlanducci, S., Leo, G., Cerri, L., Tyystjärvi, E., & Lambreva, M. D. (2022). Single-walled carbon nanotubes protect photosynthetic reactions in Chlamydomonas reinhardtii against photoinhibition. *Plant Physiology and Biochemistry: PPB / Societe Francaise de Physiologie Vegetale*, *192*, 298–307. https://doi.org/10.1016/j.plaphy.2022.10.009

Batley, G. E., Kirby, J. K., & McLaughlin, M. J. (2013). Fate and risks of nanomaterials in aquatic and terrestrial environments. *Accounts of Chemical Research*, *46*(3), 854–862. https://doi.org/10.1021/ar2003368

Bock, R. (2015). Engineering plastid genomes: methods, tools, and applications in basic research and biotechnology. *Annual Review of Plant Biology*, *66*, 211–241. https://doi.org/10.1146/annurev-arplant-050213-040212

Demirer, G. S., Zhang, H., Matos, J. L., Goh, N. S., Cunningham, F. J., Sung, Y., Chang, R., Aditham, A. J., Chio, L., Cho, M.-J., Staskawicz, B., & Landry, M. P. (2019). High aspect ratio nanomaterials enable delivery of functional genetic material without DNA integration in mature plants. *Nature Nanotechnology*. https://doi.org/10.1038/s41565-019-0382-5

Doudna, J. A., & Charpentier, E. (2014). The new frontier of genome engineering with CRISPR-Cas9. *Science*, *346*(6213), 1258096. https://doi.org/10.1126/science.1258096

Gilbert, J. A., & Neufeld, J. D. (2014). Life in a World without Microbes. *PLoS Biology*, *12*(12), e1002020. https://doi.org/10.1371/journal.pbio.1002020

Giraldo, J. P., Wu, H., Newkirk, G. M., & Kruss, S. (2019). Nanobiotechnology approaches for engineering smart plant sensors. *Nature Nanotechnology*, *14*(6), 541–553. https://doi.org/10.1038/s41565-019-0470-6

Gwak, M.-G., & Chang, S.-Y. (2021). Gut-Brain Connection: Microbiome, Gut Barrier, and Environmental Sensors. *Immune Network*, *21*(3), e20. https://doi.org/10.4110/in.2021.21.e20

Hu, P., An, J., Faulkner, M. M., Wu, H., Li, Z., Tian, X., & Giraldo, J. P. (2020). Nanoparticle Charge and Size Control Foliar Delivery Efficiency to Plant Cells and Organelles. *ACS Nano*, *14*(7), 7970–7986. https://doi.org/10.1021/acsnano.9b09178

Kwak, S.-Y., Lew, T. T. S., Sweeney, C. J., Koman, V. B., Wong, M. H., Bohmert-Tatarev, K., Snell, K. D., Seo, J. S., Chua, N.-H., & Strano, M. S. (2019). Chloroplast-selective gene delivery and expression in planta using chitosan-complexed single-walled carbon nanotube carriers. *Nature Nanotechnology*. https://doi.org/10.1038/s41565-019-0375-4

Lew, T. T. S., Wong, M. H., Kwak, S.-Y., Sinclair, R., Koman, V. B., & Strano, M. S. (2018). Rational Design Principles for the Transport and Subcellular Distribution of Nanomaterials into Plant Protoplasts. *Small* , e1802086. https://doi.org/10.1002/smll.201802086

Lu, Y., Rijzaani, H., Karcher, D., Ruf, S., & Bock, R. (2013). Efficient metabolic pathway engineering in transgenic tobacco and tomato plastids with synthetic multigene operons. *Proceedings of the National Academy of Sciences of the United States of America*, *110*(8), E623–E632. https://doi.org/10.1073/pnas.1216898110

Maliga, P., & Bock, R. (2011). Plastid biotechnology: food, fuel, and medicine for the 21st century. *Plant Physiology*, *155*(4), 1501–1510. https://doi.org/10.1104/pp.110.170969

Matorin, D. N., Karateyeva, A. V., Osipov, V. A., Lukashev, E. P., Seifullina, N. K., & Rubin, A. B. (2010). Influence of carbon nanotubes on chlorophyll fluorescence parameters of green algae Chlamydomonas reinhardtii. *Nanotechnologies in Russia*, *5*(5), 320–327. https://doi.org/10.1134/S199507801005006X

Mayfield, S., & Golden, S. S. (2015). Photosynthetic bio-manufacturing: food, fuel, and medicine for the 21st century. *Photosynthesis Research*, *123*(3), 225–226. https://doi.org/10.1007/s11120-014-0063-z

Newkirk, G. M., de Allende, P., Jinkerson, R. E., & Giraldo, J. P. (2021). Nanotechnology Approaches for Chloroplast Biotechnology Advancements. *Frontiers in Plant Science*, *12*, 1496. https://doi.org/10.3389/fpls.2021.691295

Newkirk, G. M., Wu, H., Santana, I., & Giraldo, J. P. (2018). Catalytic Scavenging of Plant Reactive Oxygen Species In Vivo by Anionic Cerium Oxide Nanoparticles. *Journal of Visualized Experiments: JoVE*, *138*. https://doi.org/10.3791/58373

Philippot, L., Raaijmakers, J. M., Lemanceau, P., & van der Putten, W. H. (2013). Going back to the roots: the microbial ecology of the rhizosphere. *Nature Reviews. Microbiology*, *11*(11), 789–799. https://doi.org/10.1038/nrmicro3109

Roger, L. M., Russo, J. A., Jinkerson, R. E., Giraldo, J. P., & Lewinski, N. A. (2022). Engineered nanoceria alleviates thermally induced oxidative stress in free-living Breviolum minutum (Symbiodiniaceae, formerly Clade B). In *Frontiers in Marine Science* (Vol. 9). https://doi.org/10.3389/fmars.2022.960173

Santana, I., Jeon, S.-J., Kim, H.-I., Islam, M. R., Castillo, C., Garcia, G. F. H., Newkirk, G. M., & Giraldo, J. P. (2022). Targeted Carbon Nanostructures for Chemical and Gene Delivery to Plant Chloroplasts. ACS Nano. https://doi.org/10.1021/acsnano.2c02714

Santana, I., Wu, H., Hu, P., & Giraldo, J. P. (2020). Targeted delivery of nanomaterials with chemical cargoes in plants enabled by a biorecognition motif. *Nature Communications*, *11*(1), 2045. https://doi.org/10.1038/s41467-020-15731-w

Stewart, E. J. (2012). Growing unculturable bacteria. *Journal of Bacteriology*, *194*(16), 4151–4160. https://doi.org/10.1128/JB.00345-12

Tungsuchat-Huang, T., Slivinski, K. M., Sinagawa-Garcia, S. R., & Maliga, P. (2011). Visual spectinomycin resistance (aadA(au)) gene for facile identification of transplastomic sectors in tobacco leaves. *Plant Molecular Biology*, *76*(3-5), 453–461. https://doi.org/10.1007/s11103-010-9724-2

Verhounig, A., Karcher, D., & Bock, R. (2010). Inducible gene expression from the plastid genome by a synthetic riboswitch. *Proceedings of the National Academy of Sciences of the United States of America*, *107*(14), 6204–6209. https://doi.org/10.1073/pnas.0914423107

Waheed, M. T., Ismail, H., Gottschamel, J., Mirza, B., & Lössl, A. G. (2015). Plastids: The Green Frontiers for Vaccine Production. *Frontiers in Plant Science*, *6*, 1005. https://doi.org/10.3389/fpls.2015.01005

Wang, J. W., Grandio, E. G., Newkirk, G. M., Demirer, G. S., Butrus, S., Giraldo, J. P., & Landry, M. P. (2019). Nanoparticle mediated genetic engineering of plants [Review of *Nanoparticle mediated genetic engineering of plants*]. *Molecular Plant*. https://doi.org/10.1016/j.molp.2019.06.010

Wells, M. L., Trainer, V. L., Smayda, T. J., Karlson, B. S. O., Trick, C. G., Kudela, R. M., Ishikawa, A., Bernard, S., Wulff, A., Anderson, D. M., & Cochlan, W. P. (2015). Harmful algal blooms and climate change: Learning from the past and present to forecast the future. *Harmful Algae*, *49*, 68–93. https://doi.org/10.1016/j.hal.2015.07.009

Williams, R. M., Taylor, H. K., Thomas, J., Cox, Z., Dolash, B. D., & Sooter, L. J. (2014). The Effect of DNA and Sodium Cholate Dispersed Single-Walled Carbon Nanotubes on the Green Algae Chlamydomonas reinhardtii. *Journal of Nanoscience and Nanotechnology*, *2014*. https://doi.org/10.1155/2014/419382

Wilson, R. H., Martin-Avila, E., Conlan, C., & Whitney, S. M. (2018). An improved Escherichia coli screen for Rubisco identifies a protein-protein interface that can enhance CO2-fixation kinetics. *The Journal of Biological Chemistry*, *293*(1), 18–27. https://doi.org/10.1074/jbc.M117.810861

Wilson, R. H., & Whitney, S. M. (2017). Improving CO2 Fixation by Enhancing Rubisco Performance. In M. Alcalde (Ed.), *Directed Enzyme Evolution: Advances and Applications* (pp. 101–126). Springer International Publishing. https://doi.org/10.1007/978-3-319-50413-1_4

Wong, M. H., Misra, R. P., Giraldo, J. P., Kwak, S.-Y., Son, Y., Landry, M. P., Swan, J. W., Blankschtein, D., & Strano, M. S. (2016). Lipid Exchange Envelope Penetration (LEEP) of Nanoparticles for Plant Engineering: A Universal Localization Mechanism. *Nano Letters*, *16*(2), 1161–1172. https://doi.org/10.1021/acs.nanolett.5b04467

Wu, H., Shabala, L., Shabala, S., & Giraldo, J. P. (2018). Hydroxyl radical scavenging by cerium oxide nanoparticles improves Arabidopsis salinity tolerance by enhancing leaf mesophyll potassium retention. *Environmental Science: Nano*, *5*(7), 1567–1583. https://doi.org/10.1039/C8EN00323H

Wu, H., Tito, N., & Giraldo, J. P. (2017). Anionic Cerium Oxide Nanoparticles Protect Plant Photosynthesis from Abiotic Stress by Scavenging Reactive Oxygen Species. *ACS Nano*, *11*(11), 11283–11297. https://doi.org/10.1021/acsnano.7b05723

Yu, Q., Lutz, K. A., & Maliga, P. (2017). Efficient Plastid Transformation in Arabidopsis. *Plant Physiology*, *175*(1), 186–193. https://doi.org/10.1104/pp.17.00857

Chapter 2: Nanotechnology Approaches for Chloroplast Biotechnology Advancements

Gregory M. Newkirk[1,2], Pedro de Allende[1], Robert E. Jinkerson[1,3] and Juan Pablo Giraldo[1*]

[1] Department of Botany and Plant Sciences, University of California, Riverside, Riverside, CA, United States

[2] Department of Microbiology and Plant Pathology, University of California, Riverside, Riverside, CA, United States

[3] Department of Chemical and Environmental Engineering, University of California, Riverside, Riverside, CA, United States

Abstract

Photosynthetic organisms are sources of sustainable foods, renewable biofuels, novel biopharmaceuticals, and next-generation biomaterials essential for modern society. Efforts to improve the yield, variety, and sustainability of products dependent on chloroplasts are limited by the need for biotechnological approaches for high-throughput chloroplast transformation, monitoring chloroplast function, and engineering photosynthesis across diverse plant species. The use of nanotechnology has emerged as a novel approach to overcome some of these limitations. Nanotechnology is enabling advances in the targeted delivery of chemicals and genetic elements to chloroplasts,

nanosensors for chloroplast biomolecules, and nanotherapeutics for enhancing chloroplast performance. Nanotechnology-mediated delivery of DNA to the chloroplast has the potential to revolutionize chloroplast synthetic biology by allowing transgenes, or even synthesized DNA libraries, to be delivered to a variety of photosynthetic species. Crop yield improvements could be enabled by nanomaterials that enhance photosynthesis, increase tolerance to stresses, and act as nanosensors for biomolecules associated with chloroplast function. Engineering isolated chloroplasts through nanotechnology and synthetic biology approaches are leading to a new generation of plant-based biomaterials able to self-repair using abundant CO2 and water sources and are powered by renewable sunlight energy. Current knowledge gaps of nanotechnology-enabled approaches for chloroplast biotechnology include precise mechanisms for entry into plant cells and organelles, limited understanding about nanoparticle-based chloroplast transformations, and the translation of lab-based nanotechnology tools to the agricultural field with crop plants. Future research in chloroplast biotechnology mediated by the merging of synthetic biology and nanotechnology approaches can yield tools for precise control and monitoring of chloroplast function in vivo and ex vivo across diverse plant species, allowing increased plant productivity and turning plants into widely available sustainable technologies.

Introduction

Chloroplast biotechnology has the potential to help alleviate the main challenges of this century by lowering renewable biofuels cost, increasing food production, and increasing productivity per plant. Currently, the cost of renewable energy through biofuels is not competitive against fossil fuels (Medipally et al., 2015; Mu et al., 2020; Lo et al., 2021; Scown et al., 2021). The current goal of the Bioenergy Technologies Office Advanced Algal Systems program within the Department of Energy is $2.5–3 gallon of gas equivalent for renewable algal biofuels by 2030, while current gasoline prices remain relatively low at $2.18 per gallon (BETO Publications, 2020; Fuel Prices, n.d.). Additionally, due to the rapidly growing world population, food production must increase by more than 50% in the coming decades with a more limited amount of arable and productive land and under a changing climate (Hatfield et al., 2011; Xu et al., 2013; Masson-Delmotte et al., 2018; Lowry et al., 2019). The "Green Revolution" in plant and molecular biology led to a significant increase in food productivity (Long et al., 2015). However, chloroplast biotechnology efforts toward increasing food production have been impaired by the inability to take full advantage of emergent research progress in synthetic biology and nanotechnology.

Stifling the ability to explore synthetic biology tools for the advancement of chloroplast biotechnology are the low chloroplast transformation rate, low number of species capable of having their chloroplast genomes transformed, and labor intensive culturing of calli – unorganized plant cells – and screening of phenotypes for homoplasy.

When compared to the rates of nuclear transformation within the same plant species, chloroplast transformation is a significant limitation. In-depth reviews of chloroplast transformation have been written by Day and Goldschmidt-Clermont (2011) and Bock (2015). Since its introduction, particle bombardment has been the standard method of chloroplast transformation across multiple plant species (Przibilla et al., 1991). This method attaches DNA to microparticles of gold or tungsten and, using a biolistic delivery system, propels the DNA-attached particle, via high-pressure helium gas, toward the plant cell. A significant downside to particle bombardment is that it requires specialized equipment and has a low transformation throughput. Accessibility, however, is limited to those plants for which protoplasts can be readily obtained (O'Neill et al., 1993). A more recent addition to the chloroplast transformation toolkit, a glass-bead vortex method has been demonstrated for green algae, but it does have lower rates when compared to particle bombardment (Economou et al., 2014; Wannathong et al., 2016). Despite these advances, relatively few plant species can have their chloroplast transformed with Arabidopsis being a very recent addition by Yu et al. in the Maliga Lab (Yu et al., 2017). Land plants routinely need species-specific bombardment procedures, vectors, and selectable markers. Increasing the number of species amenable to chloroplast transformation would have a significant research impact on broadening the number of crop plants that can be made more productive by bioengineering. A further hurdle is that any current chloroplast transformation method creates heterogenous chloroplast genomes, which must subsequently be driven to homoplasy. Chloroplast genome replication, through cell division, is one way of producing and confirming a homogenous chloroplast genome. However, continuous calli culturing is a laborious and tedious manual process. Chloroplast transformation problems could be alleviated by a biomolecule delivery chassis that targets specific germline or meristematic plant cells and removes the tissue culture bottleneck. The benefits of a universal chloroplast transformation tool for diverse plant species could improve research in plant biology and have significant impacts on agriculture, the biopharmaceutical industry, and sustainable materials.

Advances in chloroplast biotechnology have broader impacts on medicine, fuel, food, bioplastics, and chemicals and may open new frontiers of crop development (Maliga and Bock, 2011). These chloroplast products become compartmentalized, which means they have unique abilities to produce advanced biopharmaceuticals like cancer-killing immunotoxins that would normally kill eukaryotic cells (Tran et al., 2013). Also, algal chloroplasts can produce high-value proteins like human growth hormones (Wannathong et al., 2016). Several reviews of biopharmaceuticals capable of being made within chloroplasts include Adem et al. (2017) and Dyo and Purton (2018). Additionally, chloroplasts can produce renewable fuel that is environmentally sustainable by utilizing carbon within the atmosphere rather than ecological carbon sinks (Medipally et al., 2015). A significant advantage of algae biofuels is that the biodiesel produced can work with existing gas infrastructure with slight modifications. The benefits of algal biofuels from advances in synthetic biology have been reviewed by Georgianna and Mayfield (2012). Chloroplast biotechnology advances also are leading to improvements in food crop productivity (Parry et al., 2013) of algae-based food products (Dawczynski et al., 2007). There are new frontiers of materials made from non-petroleum-based foam, where bioplastics are being used to make algae-based products from the starch made within chloroplasts (Mathiot et al., 2019). Through synthetic biology and the addition of artificial intelligence algorithms via deep learning, there could be even more opportunities for novel chemicals and crop improvements (Wang et al., 2020). To fulfill these chloroplast biotechnology breakthroughs, knowledge gaps in our current understanding of delivering synthetic biology tools must be addressed and molecular biology tools developed to be universal and more efficient.

Nanotechnology is providing tools to enable plant biology researchers for a better understanding of chloroplast molecular biology and genetics, by offering modular delivery chassis for chemicals and biomolecules, nanosensors, and nanotherapeutics that are customizable with targeted and controlled capabilities. Nanomaterials are particles within a size range of 1–100 nanometer scale and varying shapes, aspect ratios, charge, and surface chemistry. These nanoparticles can also be made up of diverse materials for biological applications including silica, gold, carbon, and polymers. Nanoparticles can be coated or loaded with biomolecules for delivery of cargo that can be targeted to plant cells and organelles, such as chloroplasts, by modifying their size and charge (Avellan et al., 2019; Hu et al., 2020) and biorecognition coatings (Santana et al., 2020). For example, single-walled carbon nanotubes (SWCNTs) can be coated with a single-stranded DNA for delivery to chloroplasts (Giraldo et al., 2014) with polyethylenimine for an overall positive charge to facilitate binding and release of plasmid DNA into the nucleus of a mature land plant (Demirer et al., 2019b) or with chitosan for the delivery and plasmid DNA to the chloroplast of a mature land plant (Kwak et al., 2019).

Nanoparticles can also be fabricated with fluorescent properties such as carbon nanotubes and quantum dots for research on plant signaling, stress communication, and environmental monitoring (Giraldo et al., 2019). While knowledge of nanoparticle interactions with plants has increased in technological prowess, research into studying and engineering plants with nanomaterials are still in infancy.

This review focuses on nanotechnology uses that advance our understanding of chloroplast biotechnology (Figure 2.1). We discuss the current knowledge of the interactions between chloroplasts and nanomaterials, how plastid synthetic biology can synergize with nanotechnology approaches, nanomaterials' impact on crop performance monitoring and improvement, and how nanotechnology can turn chloroplasts into manufacturing technologies.

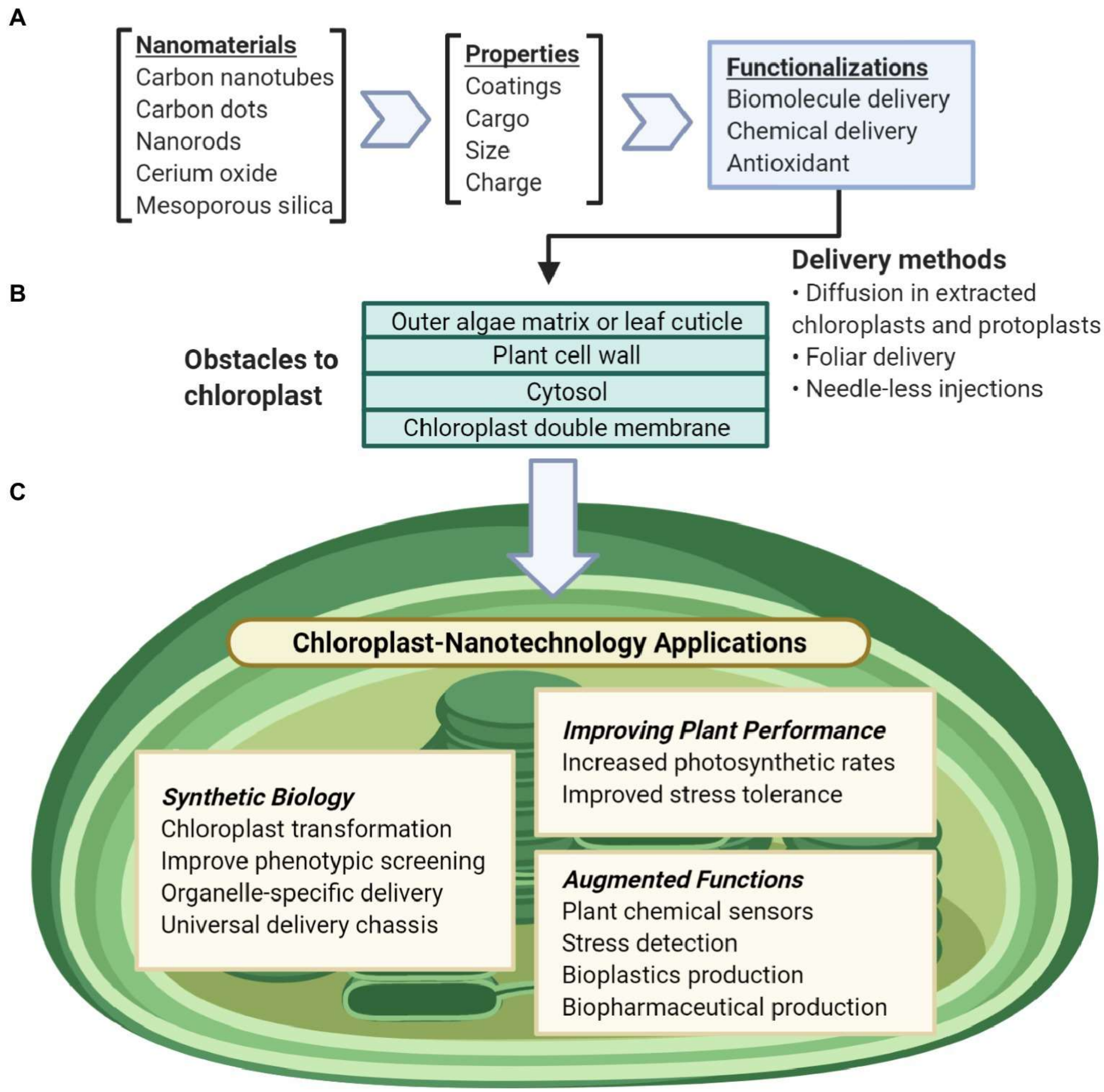
A
Nanomaterials
Carbon nanotubes
Carbon dots
Nanorods
Cerium oxide
Mesoporous silica
Properties
Coatings
Cargo
Size
Charge
Functionalizations
Biomolecule delivery
Chemical delivery
Antioxidant
Delivery methods
• Diffusion in extracted chloroplasts and protoplasts
• Foliar delivery
• Needle-less injections
B
Obstacles to chloroplast
Outer algae matrix or leaf cuticle
Plant cell wall
Cytosol
Chloroplast double membrane
C
Chloroplast-Nanotechnology Applications
Improving Plant Performance
Increased photosynthetic rates
Improved stress tolerance
Synthetic Biology
Chloroplast transformation
Improve phenotypic screening
Organelle-specific delivery
Universal delivery chassis
Augmented Functions
Plant chemical sensors
Stress detection
Bioplastics production
Biopharmaceutical production

Figure 2.1. Overview of nanotechnology approaches for chloroplast biotechnology. (A) Nanomaterial properties can be modularly tuned for a variety of functions including biomolecule and chemical delivery, biosensors, antioxidants. (B) Nanomaterials can be delivered to chloroplasts in liquid suspensions by passive intake without mechanical aid or through needleless-syringes and foliar spray. To reach the chloroplast, these particles pass through obstacles of the plant cell including the outer leaf cuticle or the glycoprotein-rich extracellular matrix of algae, the plant cell wall, the plant cell membrane, the cell cytosol, and lastly the chloroplast double membranes. (C) Nanotechnology applications for understanding and engineering chloroplasts include synthetic biology research, improving chloroplast function, or enabling non-native abilities for chloroplasts.

Chloroplast-Nanoparticle Interactions

Nanoparticle interactions with chloroplasts for biotechnology applications have been researched with isolated chloroplasts (Wong et al., 2016), plant protoplasts (Lew et al., 2018), and in leaves of land plants (Hu et al., 2020), but knowledge gaps remain on how nanomaterial properties, such as size, charge, hydrophobicity, and plant biomolecule coatings and coronas, influence interactions with land plants and green algae biosurfaces including the plant cuticle and cell wall and outer algae matrix, respectively. Although recent studies have improved our understanding of translocation of nanoparticles through chloroplast galactolipid-based membranes, how nanoparticle and membrane physical and chemical properties impact uptake into chloroplasts is not well understood.

Plant cell and organelle biosurfaces represent obstacles for delivering nanoparticles with their cargo into chloroplasts (Figure 2.2). Current standard particle delivery methods, such as particle bombardment, rely on pressure and force to deliver microcarriers to the chloroplast genome (Economou et al., 2014). More recently, nanomaterials have been delivered to chloroplasts by spontaneous penetration of lipid membranes via diffusion in vitro, leaf infiltration using a needleless syringe, and topical foliar delivery mediated by surfactants (Giraldo et al., 2014; Wong et al., 2016; Lew et al., 2018; Hu et al., 2020).

The main barriers for entry into the chloroplast genome that nanoparticles must overcome are the plant cell wall, the plant cell membrane, the cytosol, and the chloroplast double membrane; in algae, there can also be an outer epilithic algal matrix (Kramer et al., 2014). Each of these plant biosurfaces represents various physical and chemical barriers that can limit nanoparticle uptake by size, charge, hydrophobicity, and other properties.

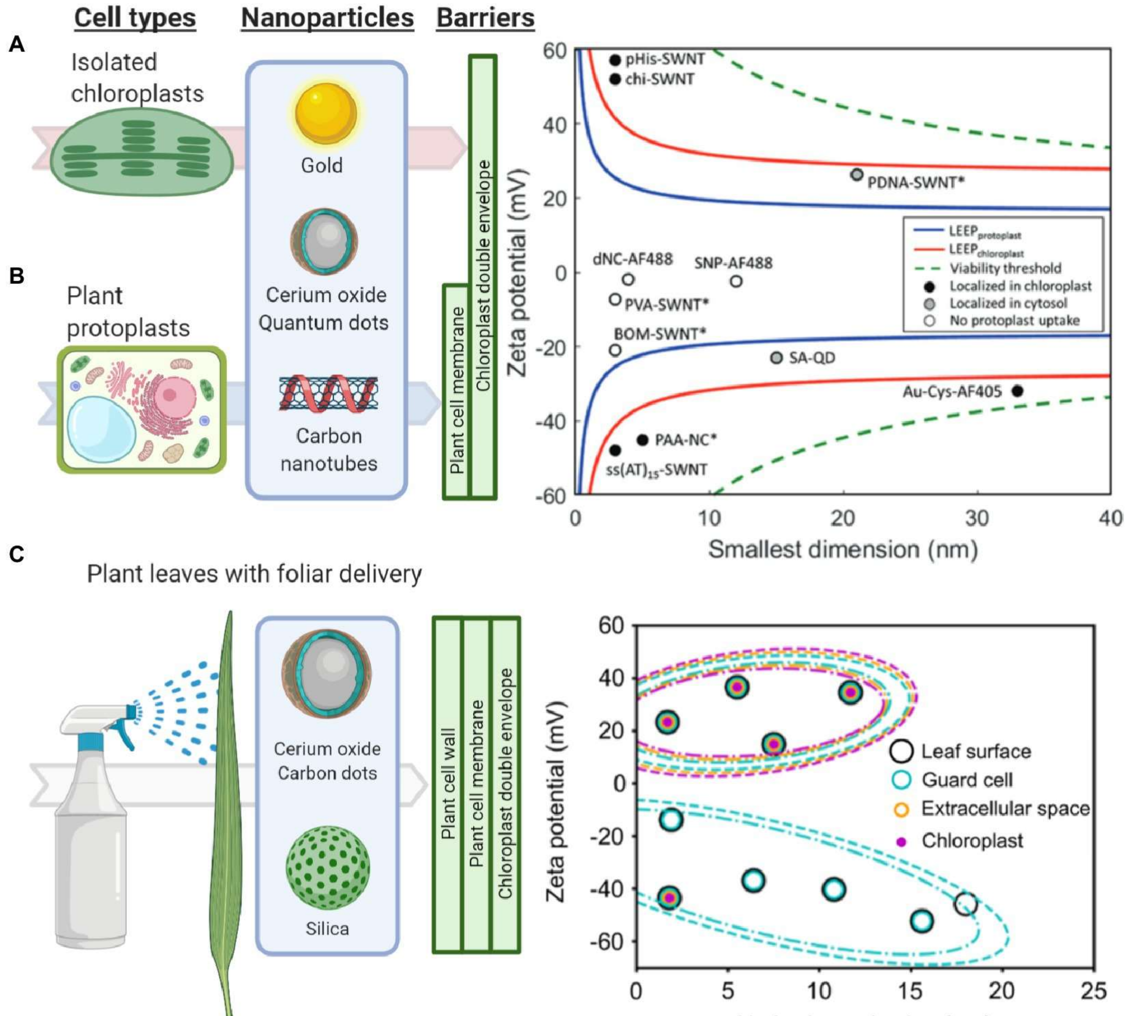
Cell types
Nanoparticles
Barriers
A
Isolated chloroplasts
Gold
Chloroplast double envelope
B
Plant protoplasts
Cerium oxide
Quantum dots
Carbon nanotubes
Plant cell membrane
pHis-SWNT
chi-SWNT
PDNA-SWNT*
dNC-AF488
SNP-AF488
PVA-SWNT*
BOM-SWNT*
SA-QD
Au-Cys-AF405
PAA-NC*
ss(AT)15-SWNT
LEEPprotoplast
LEEPchloroplast
Viability threshold
Localized in chloroplast
Localized in cytosol
No protoplast uptake
Zeta potential (mV)
Smallest dimension (nm)
C
Plant leaves with foliar delivery
Cerium oxide
Carbon dots
Silica
Plant cell wall
Plant cell membrane
Chloroplast double envelope
Leaf surface
Guard cell
Extracellular space
Chloroplast
Zeta potential (mV)
Hydrodynamic size (nm)

Figure 2.2. Understanding and modeling nanoparticle-chloroplast interactions. (A) The lipid exchange envelope penetration (LEEP) model was developed on isolated plant chloroplasts. It predicts that highly charged nanoparticles localize within chloroplasts while more neutrally charged nanoparticles are unable to enter these organelles (Reprinted with permission from Wong et al., 2016). (B) Similarly, the LEEP model for isolated plant protoplasts that includes a plant cell membrane as a barrier, predicts that nanomaterial charge magnitude determines whether particles enter plant protoplasts or localize in the cytosol or chloroplasts (Reprinted with permission from Lew et al., 2018). (C) Systematic studies of foliar delivery of nanoparticles of various sizes and charges in planta indicated that there is a size limit for uptake in leaf cells in which highly positively charged nanoparticles were more efficiently delivered into these organelles (Reprinted with permission from Hu et al., 2020).

The plant cell wall comprises pectin, cross-linking glycan, and cellulose microfibrils (Barros et al., 2015) and is the first significant barrier to entry into the plant cell. The role of plant cell wall pore size, charge, and hydrophobicity have in limiting nanoparticle entry into cells has been recently reported but is not well understood. Nanoparticles up to 18 nm were capable of permeating cotton leaf cells, while nanoparticles larger than 8 nm could not permeate the maize leaf cells (Hu et al., 2020). This study, based on high spatial and temporal resolution confocal fluorescence microscopy, suggests that hydrophilic nanoparticles with a positive charge and less than 20 or 10 nm depending on plant type and leaf anatomy are more efficiently delivered into plant cells and chloroplasts. However, other studies have observed amphiphilic nanoparticles up to 40 nm to translocate across leaf cells and into other plant organs (Avellan et al., 2019). Additionally, studies of poly- and mono-dispersed poly(lactic-co-glycolic) acid nanoparticles have reported that the cell wall inhibits uptake in grapevine cells over 50 nm while the plasma membrane is permeable from 500 to 600 nm with the same nanoparticles (Palocci et al., 2017).

The cell membrane, which is a lipid bilayer composed of phospholipids, carbohydrates, and proteins, represents another barrier of entry into plant cells. Highly charged nanoparticles have been reported to cross both the plasma membrane and chloroplast envelopes (Giraldo et al., 2014; Wong et al., 2016; Lew et al., 2018). Passive penetration rather than energy-dependent endocytosis is hypothesized as the mechanism for nanoparticle uptake. The lipid exchange envelope penetration (LEEP) model proposes a disruption of the lipid bilayer by the ionic cloud surrounding nanoparticles (Figure

2.2B; Lew et al., 2018). Modeling studies of nanoparticle uptake by chloroplasts highlight the importance of nanoparticle charge. However, these models need to incorporate a variety of biosurfaces in plants such as plant cell wall, where nanoparticles encounter in planta. Furthermore, nanoparticles with varying hydrophobicities and biomolecules coatings and coronas have not been accounted for in the modeling efforts of chloroplast nanoparticle interactions. Recent evidence suggests that nanoparticles coated with a chloroplast guiding peptide do not require the high charge predicted by the LEEP model for targeting chloroplasts at high levels of more than 75% in Arabidopsis leaf mesophyll cells (Santana et al., 2020).

After crossing the cell wall and membrane, nanoparticles must then pass through the cytosol, containing a variety of different biomolecules, including proteins. Nanoparticles passing through the cytosol are expected to be coated with biomolecule coronas, but this is poorly understood within plants. Recently, Prakash and Deswal (2020) demonstrated that gold nanoparticles interfaced with plant extracts from *Brassica juncea* formed protein coronas increasing the nanoparticle surface charge by approximately 30% after 36 h of interaction. Mass spectrometry showed that 27% of the hard corona formation around the gold nanoparticle comes from the plant energy-yielding pathways including glycolysis, photosynthesis, and ATP synthesis (Prakash and Deswal, 2020). In comparison, a study on nanoparticle coronas with human plasma highlights that irrespective of the nanoparticle material, the coronas formed were dependent on size and surface engineering (Lundqvist et al., 2008). Research performed in mouse models reports that the wild-type Tobacco mosaic virus had a higher accumulation of proteins than synthetic nanoparticles, promoting faster clearance from the body (Pitek et al., 2016). This study also found that the choice of targeting ligand and surface engineering, e.g., coatings, can drastically alter the distribution and biocompatibility of the nanoparticles in living systems. These studies in non-plant systems indicate that protein, lipid, and carbohydrate coronas should be crucial to tune interactions with plant cells and organelles.

The last obstacles to reaching the chloroplast are its double lipid bilayers, referred to as the chloroplast membranes. The chloroplast membranes are formed by galactolipids and are highly dynamic (Block et al., 2007). Chemical interactions of nanomaterials with phospholipid-based membranes of eukaryotic cells have been thoroughly studied (Sanchez et al., 2012; Wu et al., 2013; Wang et al., 2016; Lew et al., 2018). However, there are no studies of nanomaterial interactions with the galactolipid-based membranes that form the majority of the chloroplast envelopes. Highly positively or negatively charged nanoparticles interact with the exposed lipids, allowing diffusion and eventual kinetic trapping into isolated chloroplasts without mechanical aid (Figure 2.2A; Wong et al., 2016). These nanoparticles can be larger than chloroplast porin's diameter of 2.5–3 nm, and channel proteins, including mechanosensitive channels, have the largest diameter in chloroplast membranes (Ganesan et al., 2018). High and low aspect ratio nanomaterials, such as carbon nanotubes and carbon dots, respectively, are capable of penetrating plant cells and chloroplasts with high efficiency (Giraldo et al., 2014; Wong et al., 2016; Hu et al., 2020; Santana et al., 2020). However, the role of nanomaterial aspect ratio on entry into cells and chloroplasts has not been systematically explored with nanomaterials having precise control of aspect ratios. Gold, silica, and polymer nanostructures could aid in understanding the role of nanoparticle aspect ratio on interactions with chloroplast envelopes.

Nanotechnology Cargo Delivery Approaches to Enable Chloroplast Synthetic Biology

Developing a universal and efficient chassis for biomolecule delivery into chloroplasts may unleash synthetic biology research progress into novel photosynthetic organisms, their molecular pathways and enable high-value biomolecule production. The advanced regulatory and expression logic systems constructed through synthetic biology are stymied by the inability to deliver biomolecules to chloroplasts. Ideally, this delivery chassis would cause little to no toxicity to the organism and have the ability to carry a variety of biomolecules (Vazquez-Vilar et al., 2018).

Current approaches to deliver DNA to chloroplasts through force via particle bombardment work for a small number of organisms – nine species are shown with stable and reproducible plastid transformation (Bock, 2015) plus recently Arabidopsis thaliana (Yu et al., 2017) – but cannot be targeted to specific organelles. The standard gold or tungsten microcarriers used for chloroplast transformation in the gene gun system are 0.6–1.6 μm in diameter (Figure 2.3). These microcarriers have coatings that are not fully customizable, cannot be directed to specific organelles, or used without forced mechanical aid. Despite these limitations of current microcarriers and low transformation efficiency, synthetic biology has made enormous strides in plant biology research.

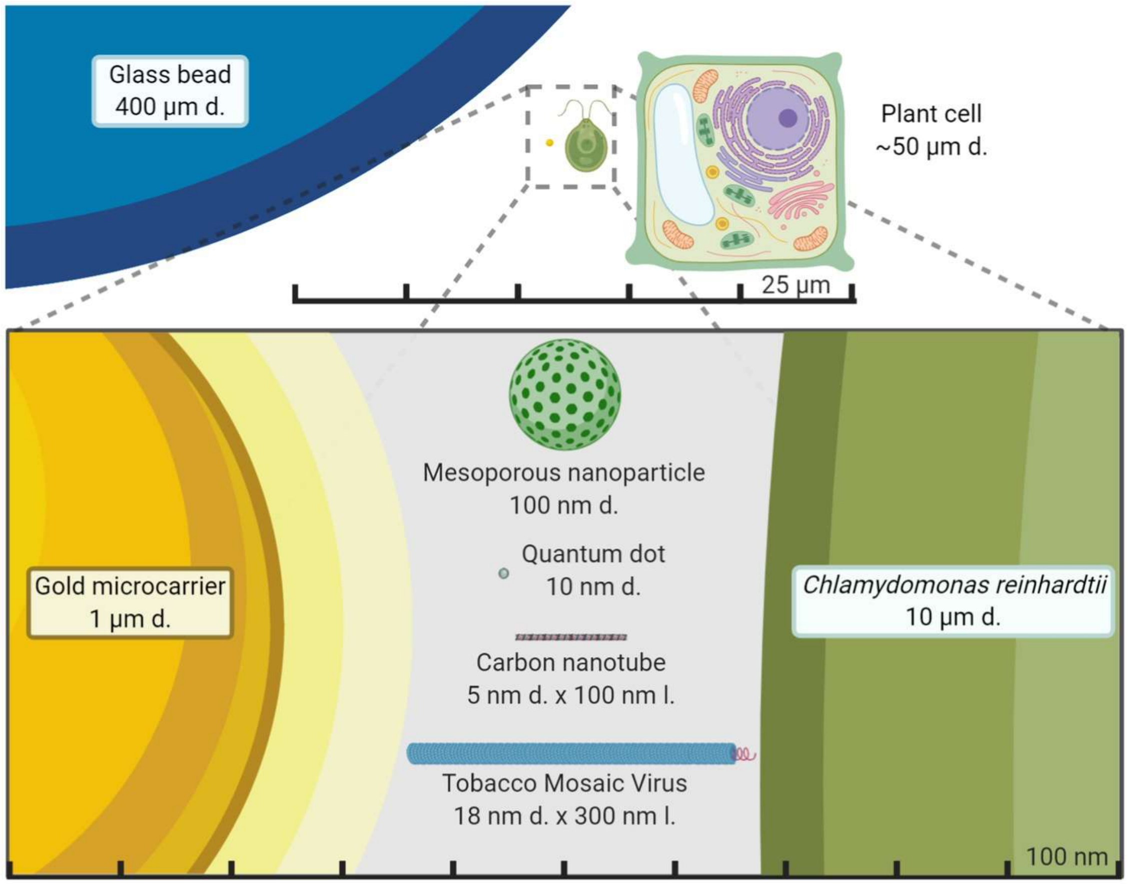

Figure 2.3. Size comparison of nanomaterials to other exogenous biomolecule delivery systems. Average plant cell and the green alga *Chlamydomonas reinhardtii* size are compared to chloroplast transformation carriers in the micrometer and nanometer scale. Gold microcarriers are standardly used in chloroplast transformations of both land plants and green algae through particle bombardment while the glass beads are used in a vortex-based protocol for *C. reinhardtii*. It becomes starkly apparent just how smaller nanoparticles are compared to standard microcarriers and potentially less disruptive for plant cells. The figure is made to scale.

Despite being a relatively new field of research, synthetic biology has enabled the discovery of multiple new chemicals, exploration of advanced protein expression regulation, and production of novel high-value proteins like biopharmaceuticals within chloroplasts. These advancements in chloroplast biotechnology have been discussed in seminal reviews (Bock, 2015; Boehm and Bock, 2019). New research that is enabling chloroplast biotechnology includes the ability to monitor the expression of proteins in vivo through a luciferase reporter (Matsuo et al., 2006), gene activation can be enabled through a site-specific recombinase (Tungsuchat-Huang et al., 2011), a synthetic riboswitch (Verhounig et al., 2010), and metabolic pathway engineering is possible through synthetic multigene operons (Lu et al., 2013). These approaches may, in the future, be used in combination with nanotechnology approaches within diverse wild-type plants, for which currently there are no transformation and genome modification protocols available. Containing these new molecular and genetic regulatory mechanisms and proteins are possible through chloroplast biotechnology. As shown in the green algae *Chlamydomonas reinhardtii*, codon reassignment allows an additional avenue for biocontainment (Young and Purton, 2016). Biocontainment within chloroplasts may allow researchers to rapidly and specifically produce proteins within wild-type strains at specific time periods for a better understanding of nuclear-chloroplast protein expression and regulation. In addition, synthetic biology may be further enabled by a chloroplast transformation with large mutant libraries for the entire plastid genome. Facile in vivo assembly of chloroplast transformation vectors have been developed for plastid engineering (Wu et al., 2017a). The first fully exogenous plastid transformation has been completed in *C. reinhardtii* (O'Neill et al., 2012). The in situ ability of nanotechnology DNA delivery may enable new directed evolution approaches to screen large mutant libraries. Synthetic biology has made strides in research in a short amount of time, and new research done in nanotechnology may help to bolster it into new plant species.

Nanotechnology approaches are allowing the genetic modification for the expression of proteins and the specific delivery of cargoes to chloroplasts in wild-type plants. Chloroplast transformations currently must be performed with somatic or embryonic plant callus material and must be screened for heterogeneity in their genomes. This callus culturing stage requires manual labor and lengthy growth periods. New nanotechnology approaches are focusing on using mature land plants for the expression of exogenous DNA, which in turn may lead to the development of chloroplast transformations without calli culturing through targeted delivery into germline or meristematic tissues. Nuclear expression of exogenous DNA mediated by SWCNT has been assessed with a green fluorescent protein (Demirer et al., 2019a). Interestingly, the nuclear genomes seemed to not have been transformed as the incorporation of the exogenous DNA was not observed. A yellow fluorescent protein has also been transiently expressed from chloroplasts in mature Eruca sativa, Nasturtium officinale, Nicotiana tabacum, and Spinacia oleracea plants through SWCNT mediated delivery of exogenous plasmid DNA (Figure 2.4A; Kwak et al., 2019).

One major advantage of nanoparticles is the ability to functionalize them with biomolecules for targeted and controlled delivery. A chloroplast targeting peptide allowed quantum dots to selectively target these organelles and to deliver chemical cargoes (Figure 2.4B; Santana et al., 2020). These nanotechnology advances in biomolecule delivery can act as promising tools for plant biology research and widespread use in crop biotechnology.

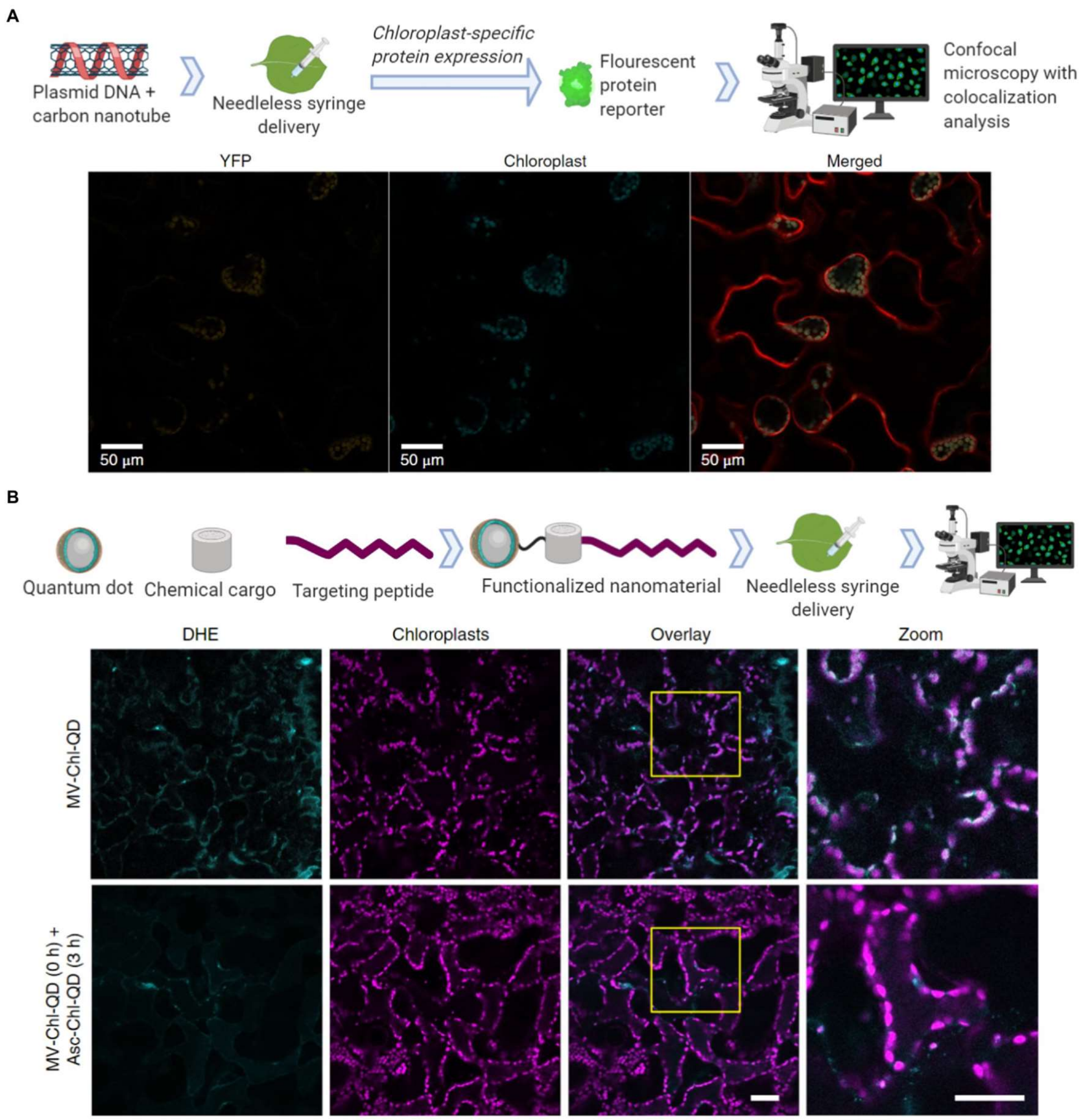
A
Plasmid DNA +
carbon nanotube
Needleless syringe
delivery
Chloroplast-specific
protein expression
Flourescent
protein
reporter
Confocal
microscopy with
colocalization
analysis
YFP
Chloroplast
Merged
50 µm
50 µm
50 µm
B
Quantum dot
Chemical cargo
Targeting peptide
Functionalized nanomaterial
Needleless syringe
delivery
DHE
Chloroplasts
Overlay
Zoom
MV-Chl-QD
MV-Chl-QD (0 h) +
Asc-Chl-QD (3 h)

Figure 2.4. Nanomaterial mediated delivery of DNA and chemical cargoes to chloroplasts. (A) Single-walled carbon nanotubes coated with chitosan carry plasmid DNA to chloroplasts. The nanomaterials are infiltrated into leaf mesophyll cells with a needless syringe. Confocal microscopy was then used for colocalization analysis 2–3 days post-infiltration by measuring the chloroplast-specific fluorescent protein (YFP) expressed within the mesophyll cells of tobacco plants (Material from Kwak et al., 2019). (B) Quantum dots with molecular baskets target the delivery of a chemical cargo to chloroplasts guided by a peptide recognition motif (Chl-QD). These functionalized nanomaterials were then loaded with methyl viologen (paraquat; MV-Chl-QD) to generate superoxide anion within chloroplasts or ascorbic acid (Asc-Chl-QD) to scavenge the superoxide anion. By monitoring reactive oxygen species (ROS) through the DHE dye using confocal microscopy, the targeted nanomaterials were shown to specifically induce and scavenge ROS in vivo in chloroplasts. Scale bar, 40 μM (Material from Santana et al., 2020).

Crop Improvements Through Chloroplast Nanobiotechnology

Agriculture demands more precise monitoring of plant health, increasing crop productivity, and efficiently delivering agrochemicals with lessening amounts of harmful environmental runoff. Chloroplasts are sites of photosynthesis, assimilation of nutrients, including nitrogen and phosphorus (Merchant et al., 2006; Carmo-Silva et al., 2015), and function as signaling organelles involved in plant stress responses (Van Aken et al., 2016; Su et al., 2019). More precise monitoring and improvement of photosynthesis, nutrient delivery to the sites of assimilation, stress responses, and plant health would allow higher crop yields. Some of these needs were met in the "Green Revolution" with molecular biology and genetics advancements that allowed higher crop productivity. However, chloroplast transformation-based approaches have not been reproducibly developed in most crops that feed the world (Bock, 2015).

Recent advances in nanosensors research may allow nanotechnology-based devices that monitor plant's health in real-time before detrimental symptoms occur. A full review of this topic discusses nanotechnology approaches for smart plant sensors (Giraldo et al., 2019), including nanosensors for monitoring plant health, detecting molecules related to photosynthesis, and reporting chemicals in the environment to electronic imaging devices already in use in phenotyping and agricultural operations. Current standard technologies that monitor plant function, stress, and photosynthesis rely on remote sensing tools to measure chlorophyll fluorescence or gas analyzers to quantify CO2 assimilation (Pérez-Bueno et al., 2019). Recently, carbon nanotubes were functionalized to sense H_2O_2, a key signaling molecule generated by chloroplasts and associated with plant stress (Wu et al., 2020). The H2O2 was monitored in real-time and within the plant physiological range through a near-infrared camera (Figures 5A,B). Multiplexed sensing of several plants signaling molecules associated with plant health, such as NO, glucose, and $Ca2^+$, among others, could allow for both monitoring plant stress status and identification of types of stress experienced. New research in nanotechnology has demonstrated the ability to use fluorescent quantum dots to monitor glucose, a direct product of chloroplast photosynthesis, through a Raspberry Pi camera in laboratory conditions in wild-type Arabidopsis plants (Figure 2.5C; Li et al., 2018). Previous approaches were only able to monitor glucose through genetically modified plant model systems. Plants embedded with nanosensors can also be engineered into environmental sensors for chemicals in groundwater with the use of remote near-infrared cameras. These plant nanosensors can detect small amounts of molecules in the environment such as those present in explosives (Wong et al., 2017). Although carbon nanotubes and quantum dots raise environmental toxicity concerns, improved knowledge in plant-nanoparticle interactions is leading to more precise control of the spatial and temporal distribution of nanomaterials in plant organs, such as leaves, for reducing exposure to humans and the environment (Wang et al., 2008; Williams et al., 2014). Alternatively, sentinel plants with nanosensors may be deployed throughout an area to determine what other plants within that crop field are experiencing.

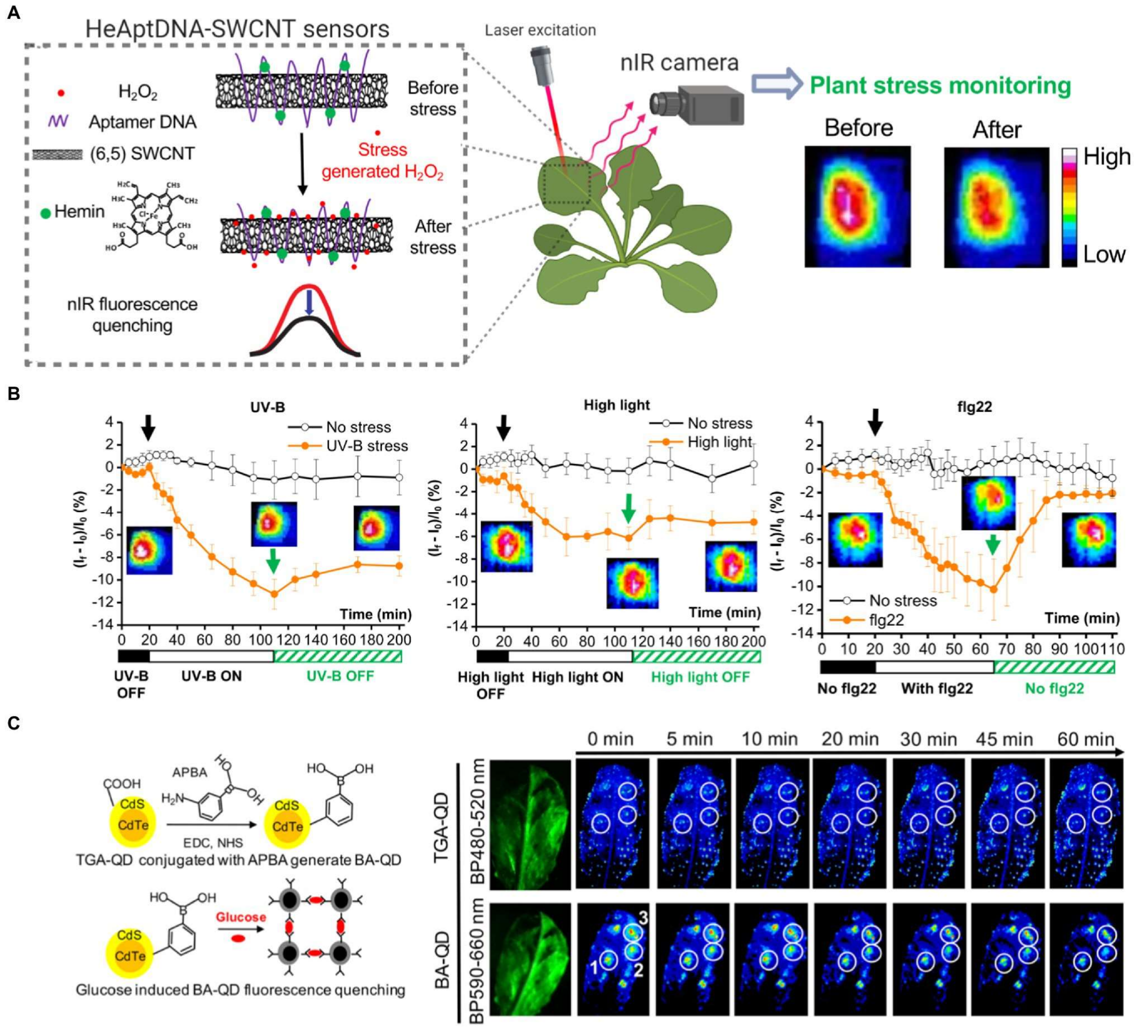
A
HeAptDNA-SWCNT sensors
H_2O_2
Aptamer DNA
(6,5) SWCNT
Hemin
Before stress
Stress generated H_2O_2
After stress
nIR fluorescence quenching
Laser excitation
nIR camera
Plant stress monitoring
Before
After
High
Low
B
UV-B
No stress
UV-B stress
High light
High light
flg22
$(I_f - I_0)/I_0$ (%)
Time (min)
UV-B OFF
UV-B ON
UV-B OFF
High light OFF
High light ON
High light OFF
No flg22
With flg22
No flg22
C
APBA
EDC, NHS
TGA-QD conjugated with APBA generate BA-QD
Glucose
Glucose induced BA-QD fluorescence quenching
0 min
5 min
10 min
20 min
30 min
45 min
60 min
TGA-QD
BP480-520 nm
BA-QD
BP590-660 nm

Figure 2.5. Plant health monitoring by nanotechnology-based sensors. (A) Single-walled carbon nanotubes (SWCNTs) can be functionalized with aptamer DNA and hemins to detect H2O2, a signaling molecule associated with plant stress. SWCNT sensors report H2O2 in real-time by quenching in NIR fluorescence intensity The nanosensor fluorescence changes are monitored by a NIR imaging before and after the stress event. This standoff detection via NIR imaging can report stress events within the plant physiological range of H2O2 (10–100 µm; Wu et al., 2020). (B) SWCNT-based nanosensors allow early detection of stresses from UV-B, high light, and a pathogen-related peptide (flg22; Reprinted with permission from Wu et al., 2020). (C) Boronic acid-coated quantum dots (BA-QDs) can act as glucose sensors, a principal product of chloroplast photosynthesis. Standoff glucose detection of *A. thaliana* is enabled by nanosensors excited through UV light and imaged with a Raspberry Pi camera (Reprinted with permission from Li et al., 2018). Thioglycolic acid-coated quantum dots (TGA-QD) act as internal controls that do not respond to glucose.

Bolstering chloroplast biotechnology through nanotechnology also may come through engineering photosynthesis in plants. Semiconducting SWCNTs have been shown to increase photosynthetic activity in mature plants (Figure 6A; Giraldo et al., 2014). The mechanisms of increased photosynthetic rates in land plants suggest that expanding the range of chloroplast pigment absorption to the near-infrared is a route for improving photosynthesis and is an avenue for new research. Nanotechnology approaches are enabling the improvement of wild-type plants without genetic modification by increasing their ability to scavenge reactive oxygen species (ROS) that are accumulated under abiotic and biotic stresses. Cerium oxide nanoparticles catalytically reduce hydroxyl radicals in A. thaliana leaves, a novel ability in plants (Figure 6B; Wu et al., 2018). This augmented hydroxyl radical scavenging capability improves plant stress tolerance by enhancing potassium mesophyll retention, which is a key trait associated with salt stress. Stressed plants interfaced with cerium oxide nanoparticles have higher carbon assimilation rates, photosystem II quantum yields, and quantum efficiency of CO2 relative to controls without nanoparticles (Figures 6C–F; Wu et al., 2017b, 2018). Reducing ROS through nanomaterials is a promising mechanism for improving or maintaining plant productivity under stress environments in the field. While both of these examples are in the lab environment with a plant model species, they give an important stepping stone to future applications in the field in crop plant species.

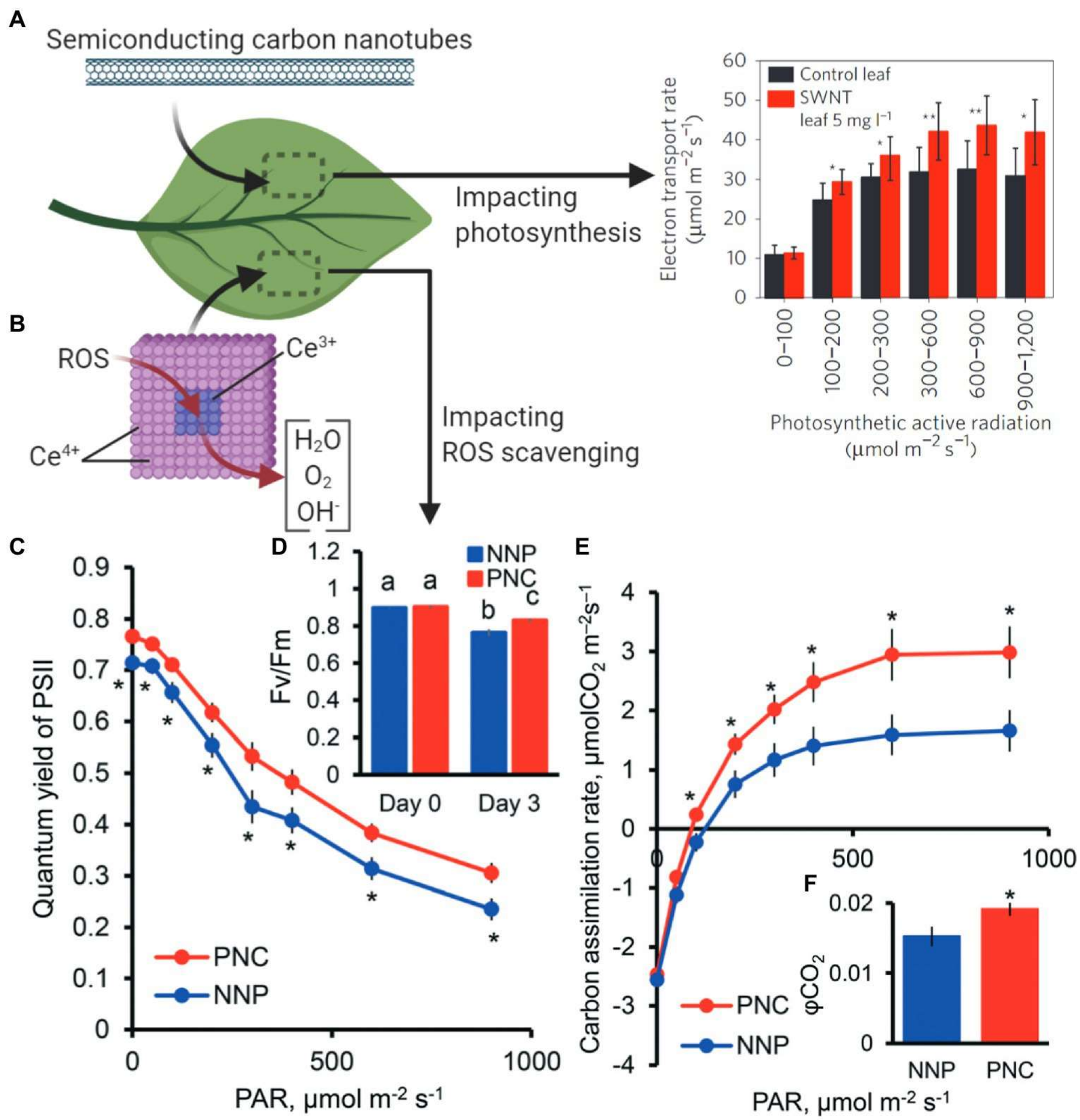
A
Semiconducting carbon nanotubes
Impacting photosynthesis
Electron transport rate (μmol m−2 s−1)
Control leaf
SWNT leaf 5 mg l−1
0–100
100–200
200–300
300–600
600–900
900–1,200
Photosynthetic active radiation (μmol m−2 s−1)
B
ROS
Ce3+
Ce4+
H2O
O2
OH-
Impacting ROS scavenging
C
Quantum yield of PSII
PNC
NNP
PAR, μmol m-2 s-1
D
Fv/Fm
NNP
PNC
Day 0
Day 3
E
Carbon assimilation rate, μmolCO2 m−2s−1
PNC
NNP
PAR, μmol m-2 s-1
F
φCO2
NNP
PNC

Figure 2.6. Nanotechnology approaches to improve plant photosynthesis. (A) SWCNTs interfaced with plant leaves increase chloroplast photosynthetic activity (Material from Giraldo et al., 2014). (B) Cerium oxide nanoparticles catalytically scavenge reactive oxygen species (ROS) in chloroplasts, resulting in enhanced light and carbon reactions of photosynthesis. Stressed plants with poly acrylic-coated cerium oxide nanoparticles (PNC) have higher (C) PSII quantum yields, (D) maximum PSII efficiency (Fv/Fm), (E) carbon assimilation rates, and (F) quantum yield of CO_2 relative to controls without nanoparticles (NNP; Reproduced from Wu et al., 2018 with permission from the Royal Society of Chemistry). *$p < 0.05$; **$p < 0.01$. Different lower case letters mean significant differences at $p < 0.05$.

Future Research in Chloroplast Nanobiotechnology

Research into chloroplast biotechnology through nanotechnology approaches may take guidance from previous research breakthroughs in the biomedical field, lead to new discoveries through improved synthetic biology tools, and enable innovative ways of human-plant interactions, all while managing environmental impacts for applications in crops. Future chloroplast nanobiotechnology applications will range from targeted delivery of agrochemicals, plastid transformation and genome editing, nanosensors for monitoring signaling molecules, improvement of plant photosynthesis, and turning plants into biomanufacturing devices (Table 2.1).

Table 2.1. Strengths and weaknesses of nanotechnology approaches for chloroplast biotechnology advancements.

Chloroplast nanobiotechnology applications	Strengths	Weaknesses	Areas of improvement
Chemical delivery	- Targeted delivery - Less runoff into environment - Improvement of agrochemical suspensions	- Environmental impact of biocompatible nanomaterials for targeted delivery is unknown	- Biodegradability studies of targeted nanomaterials - Controlled chemical release
Gene delivery	- Species independent - Gene delivery without specialized equipment - *In situ* gene delivery	- Potential limitation of plasmid DNA size per nanoparticle - Only transient expression shown - Only proof of concept, with GFP expression	- Stable plastid genome transformation enabled by nanomaterials - Targeted gene delivery to chloroplasts for applied research - Inducible expression of exogenous DNA - Overcoming the bottleneck of selectable markers
Nanosensors	- Real-time monitoring of plant signaling molecules - High sensitivity down to single molecule level - Do not photobleach - Near infrared imaging - Species independent	- Available for only a few plant signaling molecules to date - Most studies performed in laboratory conditions	- Targeted sensor delivery to chloroplasts - Multiplexed sensing of plant signaling molecules
Photosynthesis	- Enhancement of light and carbon reactions of photosynthesis - Protecting chloroplast photosynthetic machinery from oxidative stress	- Environmental toxicity of some types of nanomaterials used to boost photosynthesis - Most studies performed in laboratory conditions	- Targeted delivery of nanoparticles to chloroplasts - Develop more biocompatible and biodegradable nanomaterials that improve photosynthesis
Biomanufacturing	- Use of plants as widely accessible, solar powered manufacturing technology - Scalable, low cost manufacturing of biopharmaceuticals and bioplastics *in situ*	- Research and development at very early stage	- Proof of concept of turning plants into biomanufacturing devices using nanotechnology

To enable these future applications of nanotechnology for chloroplast biotechnology advancements will require improving our understanding of chloroplast-nanoparticle interactions. The role of nanomaterial hydrophobicity, aspect ratios, and biomolecule coatings on nanoparticle delivery to chloroplasts is not well understood. Hydrophobicity has been reported to play a role in altering the distribution of gold nanoparticles in plant leaves (Avellan et al., 2019). Recent studies have also explored how shapes of DNA nanostructures influence the delivery of siRNA-based gene silencing biomolecules in plant leaves (Zhang et al., 2020). Peptide coatings have recently been reported to more precisely guide nanoparticles to chloroplasts in plants (Santana et al., 2020). Future studies in these areas will be a significant step forward in understanding the underlying mechanisms of nanoparticle entry into plant cells and chloroplasts.

Chloroplast transformation is a limiting factor that, if alleviated, could fundamentally transform plant biotechnology research. Plant chloroplast transformation efficiencies are so low that researchers studying RuBisCO, the key protein responsible for CO2 assimilation during photosynthesis, have relied on bacterial systems instead of using plant or algae systems (Wilson et al., 2018). With efficient chloroplast transformation rates, large libraries could be used for the directed evolution of photosynthetic proteins; genome shuffling could be performed with the entire photosynthetic pathway; entire plastid genomes could be synthesized and mutated for increased photosynthetic abilities. For example, directed protein evolution is a strategy that takes advantage of large mutant libraries and yields mutants with a beneficial trait (Zhu et al., 2010; Sinha and Shukla, 2019). Recent research has enabled the simultaneous multiplexed synthesis of 7,000 synthetic genes for two essential genes in Escherichia coli (Plesa et al., 2018). While chloroplast transformation efficiencies may never achieve the efficiency of bacteria transformation, the most robust directed evolution experiment of a single chloroplast gene, RuBisCO's rbcL, in *C. reinhardtii* was able to yield 80,000 library variants that were selected and screened across multiple chloroplast transformations (Zhu et al., 2010). While researching chloroplast transformation efficiencies, we found that there was a lack of standardization across research articles. Therefore, we are recommending reporting the following parameters to increase the scientific value and reproducibility of chloroplast transformations. Chloroplast transformations should be reported with raw data for (1) the amount and type of DNA used, (2) age and origin of calli, or cell count for algae, (3) amount of calli per plate bombarded, or algae cell count per transformation replicate, (4) transformants per replicate and total number before and after genetic screening, and (5) the transformation efficiency.

New synthetic biology applications and evolutionary strategies could help to bioengineer chloroplast genomes with, for example, improved efficiency through pathway engineering using robust mutant libraries and directed protein evolution. Synthetic genomics, i.e., the construction of chromosomes, is emerging in the last decade as an exciting frontier for minimizing genomes, constructing mosaic chromosomes of two or more species reengineering organelles (Coradini et al., 2020). Synthetic genomics approaches will be bolstered by nanoparticle gene delivery due to the ability to tune characteristics of the delivery chassis, deliver a wider array of genes for more applications at once, and allow gene delivery to precise organelles. In addition, nanotechnology approaches may be employed for CRISPR-Cas genetic engineering of plants (Demirer et al., 2021). With the chloroplast's DNA repair mechanism nearly exclusively homology-driven, current approaches for plastid genetic engineering rely on delivering antibiotic markers with homologous arms for integration. However, a large problem with chloroplast biotechnology is the lack of strong selectable markers, like spectinomycin, necessary for marker excision through repeated rounds of transformation for chloroplast genetic engineering (Bock, 2015). In the future, CRISPR delivered by nanoparticles may enable new strategies of inducible silencing and increasing expression of exogenous DNA for pathway engineering that move beyond the bottleneck of strong selectable markers.

Nanomaterials can be used to deliver genes that encode proteins that act as sensors or the nanoparticle itself can be used as a sensor, and these approaches could lead to new applications in chloroplast biotechnology research. Through tunable characteristics and various types of nanoparticles, genes can be delivered that detect other proteins in wild-type plant species. For example, nanotechnology approaches for gene delivery of fluorescence resonance energy transfer (FRET) sensors to mature plants without previous genetic modification. In the future, multiplexed sensing of signaling molecules associated with chloroplast function may be possible. Currently, with *C. reinhardtii*, multiplexed stress-based imaging is possible through fluorescent-activated cell sorting (Béchet et al., 2017). In terms of applications to land plants, nanosensors already offer approaches to monitor chloroplast ROS, glucose, and nitric oxide (Giraldo et al., 2019). These plant signaling molecules may be able to be monitored simultaneously for the actuation of devices that promote plant health that are integrated into artificial intelligence deep learning algorithms.

Research into photosynthesis would be bolstered by nanotechnology approaches that allow targeted delivery of nanoparticles that manipulate chloroplast function. Biomolecule delivery of DNA or RNA (Wang et al., 2019) will expand research in the lab into chloroplasts of land plants that are not currently capable of being transformed. While nanotechnology approaches for plant research is a new field, nanoparticles have been used in mammalian systems to deliver biomolecules for the past decades (Shahiwala et al., 2007; Woodward et al., 2007). Their applications may give insights to future research directions in plants. CRISPR/Cas9 genome editing in mammalian cells through mRNA delivery has been demonstrated over the span of months (Liu et al., 2019). Applications in the field of nanoparticles for improving plant photosynthesis under stress will also require studies on environmental toxicity, the longevity of nanoparticles in the environment, and exposure of those nanoparticles to products for human consumption.

Plants and their chloroplasts potential are just beginning to be explored in terms of manufacturing of biopharmaceuticals, fuels, and materials. Plant chloroplasts within our homes may become 3D printers for high-value biopharmaceuticals (Maliga and Bock, 2011; Jin and Daniell, 2015). Polyhydroxybutyrate, a biodegradable polyester, can be made within the chloroplast and is being researched as a bioplastic (McQualter et al., 2016). Plants themselves could be used as a platform for self-repairing of infrastructure

(Lu, 2020). A new class of materials made with extracted spinach chloroplasts stabilized with antioxidant cerium oxide nanoparticles can self-repair using glucose created from photosynthesis (Kwak et al., 2018). Algae and their chloroplasts enable a unique opportunity for renewable biofuels to take advantage of existing gasoline infrastructure and create jet fuel (Mayfield and Golden, 2015). In terms of legislation that is further enabling renewable algal biofuels, algae has officially been included in the latest 2018 Farm Bill in the United States, which enables algae agriculture to receive federal financial assistance for biomass cultivation, farm insurance, loans, carbon capture research and creates a new USDA Algae Agriculture Research Program (Conaway, 2018). These future applications for plants may fundamentally revolutionize our relationship with plants from providing food and materials to intricate partners that facilitate technology access to the world.

Conclusion

Nanotechnology offers promising new approaches for some of the hardest challenges in chloroplast biotechnology research. Nanoparticle and plant cell interactions are still an emerging field that needs to be studied, but research has shown promising results in nanoparticles getting past plant cell barriers to their organelles. Knowledge gaps still exist in the exact mechanism of entry of nanoparticles into plant cells and chloroplast envelopes to determine the characteristics needed for a universal delivery cassette for biomolecules that would be applicable across diverse plant species. With current knowledge of plant-nanoparticle interactions, successful nanoparticle-based biomolecule delivery to chloroplasts has been possible. Using these targeted and controlled delivery technologies to bolster the number of applicable species or increase the efficiency of chloroplast transformations is yet to be seen. If increased chloroplast transformation efficiencies were to be realized, emerging synthetic biology-based strategies, such as directed protein evolution, may be able to be deployed within plastid genomes to unlock new potential in productivity and augmented manufacturing capabilities in chloroplasts. Additionally, nanomaterials have already been used to enable chloroplast biotechnology advancements such as sensing specific compounds, increasing photosynthetic rates, and decreasing stress-related molecules' accumulation. Taken together, chloroplast biology and biotechnology research have challenges that can be uniquely addressed with nanotechnology approaches for increasing crop productivity and realizing the next generation of chloroplast-related biomanufacturing.

References

Adem, M., Beyene, D., & Feyissa, T. (2017). Recent achievements obtained by chloroplast transformation. *Plant Methods*, *13*(1), 30. https://doi.org/10.1186/s13007-017-0179-1

Avellan, A., Yun, J., Zhang, Y., Spielman-Sun, E., Unrine, J. M., Thieme, J., Li, J., Lombi, E., Bland, G., & Lowry, G. V. (2019). Nanoparticle Size and Coating Chemistry Control Foliar Uptake Pathways, Translocation, and Leaf-to-Rhizosphere Transport in Wheat. *ACS Nano*. https://doi.org/10.1021/acsnano.8b09781

Barros, J., Serk, H., Granlund, I., & Pesquet, E. (2015). The cell biology of lignification in higher plants. *Annals of Botany*, *115*(7), 1053–1074. https://doi.org/10.1093/aob/mcv046

Béchet, Q., Laviale, M., Arsapin, N., Bonnefond, H., & Bernard, O. (2017). Modeling the impact of high temperatures on microalgal viability and photosynthetic activity. *Biotechnology for Biofuels*, *10*, 136. https://doi.org/10.1186/s13068-017-0823-z

BETO Publications. (n.d.). Retrieved April 2, 2021, from https://www.energy.gov/eere/bioenergy/beto-publications

Block, M. A., Douce, R., Joyard, J., & Rolland, N. (2007). Chloroplast envelope membranes: a dynamic interface between plastids and the cytosol. *Photosynthesis Research*, *92*(2), 225–244. https://doi.org/10.1007/s11120-007-9195-8

Bock, R. (2015). Engineering plastid genomes: methods, tools, and applications in basic research and biotechnology. *Annual Review of Plant Biology*, *66*, 211–241. https://doi.org/10.1146/annurev-arplant-050213-040212

Boehm, C. R., & Bock, R. (2019). Recent Advances and Current Challenges in Synthetic Biology of the Plastid Genetic System and Metabolism. *Plant Physiology*, *179*(3), 794–802. https://doi.org/10.1104/pp.18.00767

Carmo-Silva, E., Scales, J. C., Madgwick, P. J., & Parry, M. A. J. (2015). Optimizing Rubisco and its regulation for greater resource use efficiency. *Plant, Cell & Environment*, *38*(9), 1817–1832. https://doi.org/10.1111/pce.12425

Agriculture Improvement Act of 2018, 2, House of Representatives, 115th Congress (2018). https://www.congress.gov/bill/115th-congress/house-bill/2

Coradini, A. L. V., Hull, C. B., & Ehrenreich, I. M. (2020). Building genomes to understand biology. *Nature Communications*, *11*(1), 6177. https://doi.org/10.1038/s41467-020-19753-2

Davis, M. E. (2006). Nanoparticles for systemic medicines and imaging agents. 10.1038/nature11479

Giraldo, J. P., Landry, M. P., Faltermeier, S. M., McNicholas, T. P., Iverson, N. M., Boghossian, A. A., Reuel, N. F., Hilmer, A. J., Sen, F., Brew, J. A., & Strano, M. S. (2014). Plant nanobionics approach to augment photosynthesis and biochemical sensing. *Nature Materials*, *13*(4), 400–408. https://doi.org/10.1038/nmat3890

Giraldo, J. P., Wu, H., Newkirk, G. M., & Kruss, S. (2019). Nanobiotechnology approaches for engineering smart plant sensors. *Nature Nanotechnology*, *14*(6), 541–553. https://doi.org/10.1038/s41565-019-0470-6

Hatfield, J. L., Boote, K. J., Kimball, B. A., Ziska, L. H., Izaurralde, R. C., Ort, D., Thomson, A. M., & Wolfe, D. (2011). Climate Impacts on Agriculture: Implications for Crop Production. *Agronomy Journal*, *103*(2), 351–370. https://doi.org/10.2134/agronj2010.0303

Hu, P., An, J., Faulkner, M. M., Wu, H., Li, Z., Tian, X., & Giraldo, J. P. (2020). Nanoparticle Charge and Size Control Foliar Delivery Efficiency to Plant Cells and Organelles. *ACS Nano*, *14*(7), 7970–7986. https://doi.org/10.1021/acsnano.9b09178

Jin, S., & Daniell, H. (2015). The Engineered Chloroplast Genome Just Got Smarter. *Trends in Plant Science*, *20*(10), 622–640. https://doi.org/10.1016/j.tplants.2015.07.004

Kramer, M. J., Bellwood, D. R., & Bellwood, O. (2014). Large-scale spatial variation in epilithic algal matrix cryptofaunal assemblages on the Great Barrier Reef. *Marine Biology*, *161*(9), 2183–2190. https://doi.org/10.1007/s00227-014-2495-6

Kwak, S.-Y., Giraldo, J. P., Lew, T. T. S., Wong, M. H., Liu, P., Yang, Y. J., Koman, V. B., McGee, M. K., Olsen, B. D., & Strano, M. S. (2018). Polymethacrylamide and Carbon Composites that Grow, Strengthen, and Self-Repair using Ambient Carbon Dioxide Fixation. *Advanced Materials* , *30*(46), e1804037. https://doi.org/10.1002/adma.201804037

Kwak, S.-Y., Lew, T. T. S., Sweeney, C. J., Koman, V. B., Wong, M. H., Bohmert-Tatarev, K., Snell, K. D., Seo, J. S., Chua, N.-H., & Strano, M. S. (2019). Chloroplast-selective gene delivery and expression in planta using chitosan-complexed single-walled carbon nanotube carriers. *Nature Nanotechnology*. https://doi.org/10.1038/s41565-019-0375-4

Lew, T. T. S., Wong, M. H., Kwak, S.-Y., Sinclair, R., Koman, V. B., & Strano, M. S. (2018). Rational Design Principles for the Transport and Subcellular Distribution of Nanomaterials into Plant Protoplasts. *Small* , e1802086. https://doi.org/10.1002/smll.201802086

Li, J., Wu, H., Santana, I., Fahlgren, M., & Giraldo, J. P. (2018). Standoff Optical Glucose Sensing in Photosynthetic Organisms by a Quantum Dot Fluorescent Probe. *ACS Applied Materials & Interfaces*, *10*(34), 28279–28289. https://doi.org/10.1021/acsami.8b07179

Liu, J., Chang, J., Jiang, Y., Meng, X., Sun, T., Mao, L., Xu, Q., & Wang, M. (2019). Fast and Efficient CRISPR/Cas9 Genome Editing In Vivo Enabled by Bioreducible Lipid and Messenger RNA Nanoparticles. *Advanced Materials* , e1902575. https://doi.org/10.1002/adma.201902575

Long, S. P., Marshall-Colon, A., & Zhu, X.-G. (2015). Meeting the global food demand of the future by engineering crop photosynthesis and yield potential. *Cell*, *161*(1), 56–66. https://doi.org/10.1016/j.cell.2015.03.019

Lo, S. L. Y., How, B. S., Leong, W. D., Teng, S. Y., Rhamdhani, M. A., & Sunarso, J. (2021). Techno-economic analysis for biomass supply chain: A state-of-the-art review. *Renewable and Sustainable Energy Reviews*, *135*, 110164. https://doi.org/10.1016/j.rser.2020.110164

Lowry, G. V., Avellan, A., & Gilbertson, L. M. (2019). Opportunities and challenges for nanotechnology in the agri-tech revolution. *Nature Nanotechnology*, *14*(6), 517–522. https://doi.org/10.1038/s41565-019-0461-7

Lu, G. (2020). A review of recent research on bio-inspired structures and materials for energy absorption applications. *Composites Part B-Engineering*, *181*. https://doi.org/10.1016/j.compositesb.2019.107496

Lundqvist, M., Stigler, J., Elia, G., Lynch, I., Cedervall, T., & Dawson, K. A. (2008). Nanoparticle size and surface properties determine the protein corona with possible implications for biological impacts. *Proceedings of the National Academy of Sciences of the United States of America*, *105*(38), 14265–14270. https://doi.org/10.1073/pnas.0805135105

Lu, Y., Rijzaani, H., Karcher, D., Ruf, S., & Bock, R. (2013). Efficient metabolic pathway engineering in transgenic tobacco and tomato plastids with synthetic multigene operons. *Proceedings of the National Academy of Sciences of the United States of America*, *110*(8), E623–E632. https://doi.org/10.1073/pnas.1216898110

Maliga, P., & Bock, R. (2011). Plastid biotechnology: food, fuel, and medicine for the 21st century. *Plant Physiology*, *155*(4), 1501–1510. https://doi.org/10.1104/pp.110.170969

Mathiot, C., Ponge, P., Gallard, B., Sassi, J.-F., Delrue, F., & Le Moigne, N. (2019). Microalgae starch-based bioplastics: Screening of ten strains and plasticization of unfractionated microalgae by extrusion. *Carbohydrate Polymers*, *208*, 142–151. https://doi.org/10.1016/j.carbpol.2018.12.057

Matsuo, T., Onai, K., Okamoto, K., Minagawa, J., & Ishiura, M. (2006). Real-time monitoring of chloroplast gene expression by a luciferase reporter: evidence for nuclear regulation of chloroplast circadian period. *Molecular and Cellular Biology*, *26*(3), 863–870. https://doi.org/10.1128/MCB.26.3.863-870.2006

Mayfield, S., & Golden, S. S. (2015). Photosynthetic bio-manufacturing: food, fuel, and medicine for the 21st century. *Photosynthesis Research*, *123*(3), 225–226. https://doi.org/10.1007/s11120-014-0063-z

McQualter, R. B., Bellasio, C., Gebbie, L. K., Petrasovits, L. A., Palfreyman, R. W., Hodson, M. P., Plan, M. R., Blackman, D. M., Brumbley, S. M., & Nielsen, L. K. (2016). Systems biology and metabolic modelling unveils limitations to polyhydroxybutyrate accumulation in sugarcane leaves; lessons for C4 engineering. *Plant Biotechnology Journal*, *14*(2), 567–580. https://doi.org/10.1111/pbi.12399

Medipally, S. R., Yusoff, F. M., Banerjee, S., & Shariff, M. (2015). Microalgae as sustainable renewable energy feedstock for biofuel production. *BioMed Research International*, *2015*, 519513. https://doi.org/10.1155/2015/519513

Merchant, S. S., Allen, M. D., Kropat, J., Moseley, J. L., Long, J. C., Tottey, S., & Terauchi, A. M. (2006). Between a rock and a hard place: trace element nutrition in Chlamydomonas. *Biochimica et Biophysica Acta*, *1763*(7), 578–594. https://doi.org/10.1016/j.bbamcr.2006.04.007

Mu, D., Xin, C., & Zhou, W. (2020). Chapter 18 - Life Cycle Assessment and Techno-Economic Analysis of Algal Biofuel Production. In A. Yousuf (Ed.), *Microalgae Cultivation for Biofuels Production* (pp. 281–292). Academic Press. https://doi.org/10.1016/B978-0-12-817536-1.00018-7

O’Neill, B. M., Mikkelson, K. L., Gutierrez, N. M., Cunningham, J. L., Wolff, K. L., Szyjka, S. J., Yohn, C. B., Redding, K. E., & Mendez, M. J. (2012). An exogenous chloroplast genome for complex sequence manipulation in algae. *Nucleic Acids Research*, *40*(6), 2782–2792. https://doi.org/10.1093/nar/gkr1008

O’Neill, C., Horváth, G. V., Horváth, E., Dix, P. J., & Medgyesy, P. (1993). Chloroplast transformation in plants: polyethylene glycol (PEG) treatment of protoplasts is an alternative to biolistic delivery systems. *The Plant Journal: For Cell and Molecular Biology*, *3*(5), 729–738. https://www.ncbi.nlm.nih.gov/pubmed/8397038

Palocci, C., Valletta, A., Chronopoulou, L., Donati, L., Bramosanti, M., Brasili, E., Baldan, B., & Pasqua, G. (2017). Endocytic pathways involved in PLGA nanoparticle uptake by grapevine cells and role of cell wall and membrane in size selection. *Plant Cell Reports*, *36*(12), 1917–1928. https://doi.org/10.1007/s00299-017-2206-0

Parry, M. A. J., Andralojc, P. J., Scales, J. C., Salvucci, M. E., Carmo-Silva, A. E., Alonso, H., & Whitney, S. M. (2013). Rubisco activity and regulation as targets for crop improvement. *Journal of Experimental Botany*, *64*(3), 717–730. https://doi.org/10.1093/jxb/ers336

Pérez-Bueno, M. L., Pineda, M., & Barón, M. (2019). Phenotyping Plant Responses to Biotic Stress by Chlorophyll Fluorescence Imaging. *Frontiers in Plant Science*, *10*, 1135. https://doi.org/10.3389/fpls.2019.01135

Pitek, A. S., Wen, A. M., Shukla, S., & Steinmetz, N. F. (2016). The Protein Corona of Plant Virus Nanoparticles Influences their Dispersion Properties, Cellular Interactions, and In Vivo Fates. *Small* , *12*(13), 1758–1769. https://doi.org/10.1002/smll.201502458

Plesa, C., Sidore, A. M., Lubock, N. B., Zhang, D., & Kosuri, S. (2018). Multiplexed gene synthesis in emulsions for exploring protein functional landscapes. *Science*, *359*(6373), 343–347. https://doi.org/10.1126/science.aao5167

Prakash, S., & Deswal, R. (2020). Analysis of temporally evolved nanoparticle-protein corona highlighted the potential ability of gold nanoparticles to stably interact with proteins and influence the major biochemical pathways in Brassica juncea. *Plant Physiology and Biochemistry: PPB / Societe Francaise de Physiologie Vegetale*, *146*, 143–156. https://doi.org/10.1016/j.plaphy.2019.10.036

Przibilla, E., Heiss, S., Johanningmeier, U., & Trebst, A. (1991). Site-specific mutagenesis of the D1 subunit of photosystem II in wild-type Chlamydomonas. *The Plant Cell*, *3*(2), 169–174. https://doi.org/10.1105/tpc.3.2.169

Sanchez, V. C., Jachak, A., Hurt, R. H., & Kane, A. B. (2012). Biological interactions of graphene-family nanomaterials: an interdisciplinary review. *Chemical Research in Toxicology*, *25*(1), 15–34. https://doi.org/10.1021/tx200339h

Santana, I., Wu, H., Hu, P., & Giraldo, J. P. (2020). Targeted delivery of nanomaterials with chemical cargoes in plants enabled by a biorecognition motif. *Nature Communications*, *11*(1), 2045. https://doi.org/10.1038/s41467-020-15731-w

Scown, C. D., Baral, N. R., Yang, M., Vora, N., & Huntington, T. (2021). Technoeconomic analysis for biofuels and bioproducts. *Current Opinion in Biotechnology*, *67*, 58–64. https://doi.org/10.1016/j.copbio.2021.01.002

Shahiwala, A., Vyas, T. K., & Amiji, M. M. (2007). Nanocarriers for systemic and mucosal vaccine delivery. In *Recent patents on drug*. https://www.ingentaconnect.com/content/ben/ddf/2007/00000001/00000001/art00001

Sinha, R., & Shukla, P. (2019). Current Trends in Protein Engineering: Updates and Progress. *Current Protein & Peptide Science*, *20*(5), 398–407. https://doi.org/10.2174/1389203720666181119120120

Su, T., Li, W., Wang, P., & Ma, C. (2019). Dynamics of Peroxisome Homeostasis and Its Role in Stress Response and Signaling in Plants. *Frontiers in Plant Science*, *10*, 705. https://doi.org/10.3389/fpls.2019.00705

Tran, M., Henry, R. E., Siefker, D., Van, C., Newkirk, G., Kim, J., Bui, J., & Mayfield, S. P. (2013). Production of anti-cancer immunotoxins in algae: ribosome inactivating proteins as fusion partners. *Biotechnology and Bioengineering*, *110*(11), 2826–2835. https://doi.org/10.1002/bit.24966

Tungsuchat-Huang, T., Slivinski, K. M., Sinagawa-Garcia, S. R., & Maliga, P. (2011). Visual spectinomycin resistance (aadA(au)) gene for facile identification of transplastomic sectors in tobacco leaves. *Plant Molecular Biology*, *76*(3-5), 453–461. https://doi.org/10.1007/s11103-010-9724-2

Van Aken, O., De Clercq, I., Ivanova, A., Law, S. R., Van Breusegem, F., Millar, A. H., & Whelan, J. (2016). Mitochondrial and Chloroplast Stress Responses Are Modulated in Distinct Touch and Chemical Inhibition Phases. *Plant Physiology*, *171*(3), 2150–2165. https://doi.org/10.1104/pp.16.00273

Vazquez-Vilar, M., Orzaez, D., & Patron, N. (2018). DNA assembly standards: Setting the low-level programming code for plant biotechnology. *Plant Science: An International Journal of Experimental Plant Biology*, *273*, 33–41. https://doi.org/10.1016/j.plantsci.2018.02.024

Verhounig, A., Karcher, D., & Bock, R. (2010). Inducible gene expression from the plastid genome by a synthetic riboswitch. *Proceedings of the National Academy of Sciences of the United States of America*, *107*(14), 6204–6209. https://doi.org/10.1073/pnas.0914423107

V. Masson-Delmotte, P. Zhai, H. O. Pörtner, D. Roberts, J. Skea, P.R. Shukla, A. Pirani, W. Moufouma-Okia, C. Péan, R. Pidcock, S. Connors, J. B. R. Matthews, Y. Chen, X. Zhou, M. I. Gomis, E. Lonnoy, T. Maycock, M. Tignor, T. Waterfield (eds.). (2018). *IPCC, 2018: Global Warming of 1.5°C. An IPCC Special Report on the impacts of global warming of 1.5°C above pre-industrial levels and related global greenhouse gas emission pathways, in the context of strengthening the global response to the threat of climate change, sustainable development, and efforts to eradicate poverty*. Intergovernmental Panel on Climate Change. https://www.ipcc.ch/sr15/

Wang, H., Cimen, E., Singh, N., & Buckler, E. (2020). Deep learning for plant genomics and crop improvement. *Current Opinion in Plant Biology*, *54*, 34–41. https://doi.org/10.1016/j.pbi.2019.12.010

Wang, J. W., Grandio, E. G., Newkirk, G. M., Demirer, G. S., Butrus, S., Giraldo, J. P., & Landry, M. P. (2019). Nanoparticle mediated genetic engineering of plants [Review of *Nanoparticle mediated genetic engineering of plants*]. *Molecular Plant*. https://doi.org/10.1016/j.molp.2019.06.010

Wang, J., Zhang, X., Chen, Y., Sommerfeld, M., & Hu, Q. (2008). Toxicity assessment of manufactured nanomaterials using the unicellular green alga Chlamydomonas reinhardtii. *Chemosphere*, *73*(7), 1121–1128. https://doi.org/10.1016/j.chemosphere.2008.07.040

Wang, Z., Zhu, W., Qiu, Y., Yi, X., von dem Bussche, A., Kane, A., Gao, H., Koski, K., & Hurt, R. (2016). Biological and environmental interactions of emerging two-dimensional nanomaterials. *Chemical Society Reviews*, *45*(6), 1750–1780. https://doi.org/10.1039/c5cs00914f

Wannathong, T., Waterhouse, J. C., Young, R. E. B., Economou, C. K., & Purton, S. (2016). New tools for chloroplast genetic engineering allow the synthesis of human growth hormone in the green alga Chlamydomonas reinhardtii. *Applied Microbiology and Biotechnology*, *100*(12), 5467–5477. https://doi.org/10.1007/s00253-016-7354-6

Williams, R. M., Taylor, H. K., Thomas, J., Cox, Z., Dolash, B. D., & Sooter, L. J. (2014). The Effect of DNA and Sodium Cholate Dispersed Single-Walled Carbon Nanotubes on the Green Algae Chlamydomonas reinhardtii. *Journal of Nanoscience and Nanotechnology*, *2014*. https://doi.org/10.1155/2014/419382

Wilson, R. H., Martin-Avila, E., Conlan, C., & Whitney, S. M. (2018). An improved Escherichia coli screen for Rubisco identifies a protein-protein interface that can enhance CO2-fixation kinetics. *The Journal of Biological Chemistry*, *293*(1), 18–27. https://doi.org/10.1074/jbc.M117.810861

Wong, M. H., Giraldo, J. P., Kwak, S.-Y., Koman, V. B., Sinclair, R., Lew, T. T. S., Bisker, G., Liu, P., & Strano, M. S. (2017). Nitroaromatic detection and infrared communication from wild-type plants using plant nanobionics. *Nature Materials*, *16*(2), 264–272. https://doi.org/10.1038/nmat4771

Wong, M. H., Misra, R. P., Giraldo, J. P., Kwak, S.-Y., Son, Y., Landry, M. P., Swan, J. W., Blankschtein, D., & Strano, M. S. (2016). Lipid Exchange Envelope Penetration (LEEP) of Nanoparticles for Plant Engineering: A Universal Localization Mechanism. *Nano Letters*, *16*(2), 1161–1172. https://doi.org/10.1021/acs.nanolett.5b04467

Woodward, J., Kennel, S. J., Mirzadeh, S., Dai, S., & Rondinone, A. J. (2007). Biodistribution of radioactive Cd 125m Te/ZnS nanoparticles targeted with antibody to murine lung endothelium. *Nanotechnology*, *18*(17), 175103. https://inis.iaea.org/search/search.aspx?orig_q=RN:40024102

Wu, H., Nißler, R., Morris, V., Herrmann, N., Hu, P., Jeon, S.-J., Kruss, S., & Giraldo, J. P. (2020). Monitoring Plant Health with Near-Infrared Fluorescent H2O2 Nanosensors. *Nano Letters*, *20*(4), 2432–2442. https://doi.org/10.1021/acs.nanolett.9b05159

Wu, H., Shabala, L., Shabala, S., & Giraldo, J. P. (2018). Hydroxyl radical scavenging by cerium oxide nanoparticles improves Arabidopsis salinity tolerance by enhancing leaf mesophyll potassium retention. *Environmental Science: Nano*, *5*(7), 1567–1583. https://doi.org/10.1039/C8EN00323H

Wu, Y.-L., Putcha, N., Ng, K. W., Leong, D. T., Lim, C. T., Loo, S. C. J., & Chen, X. (2013). Biophysical responses upon the interaction of nanomaterials with cellular interfaces. *Accounts of Chemical Research*, *46*(3), 782–791. https://doi.org/10.1021/ar300046u

Wu, Y., You, L., Li, S., Ma, M., Wu, M., Ma, L., Bock, R., Chang, L., & Zhang, J. (2017). In vivo Assembly in Escherichia coli of Transformation Vectors for Plastid Genome Engineering. *Frontiers in Plant Science*, *8*, 1454. https://doi.org/10.3389/fpls.2017.01454

Xu, Z., Shimizu, H., Yagasaki, Y., Ito, S., Zheng, Y., & Zhou, G. (2013). Interactive Effects of Elevated CO2, Drought, and Warming on Plants. *Journal of Plant Growth Regulation*, *32*(4), 692–707. https://doi.org/10.1007/s00344-013-9337-5

Young, R. E. B., & Purton, S. (2016). Codon reassignment to facilitate genetic engineering and biocontainment in the chloroplast of Chlamydomonas reinhardtii. *Plant Biotechnology Journal*, *14*(5), 1251–1260. https://doi.org/10.1111/pbi.12490

Yu, Q., Lutz, K. A., & Maliga, P. (2017). Efficient Plastid Transformation in Arabidopsis. *Plant Physiology*, *175*(1), 186–193. https://doi.org/10.1104/pp.17.00857

Zhang, H., Zhang, H., Demirer, G. S., González-Grandío, E., Fan, C., & Landry, M. P. (2020). Engineering DNA nanostructures for siRNA delivery in plants. *Nature Protocols*, *15*(9), 3064–3087. https://doi.org/10.1038/s41596-020-0370-0

Zhu, G., Kurek, I., & Liu, L. (2010). Chapter 20 Engineering Photosynthetic Enzymes Involved in CO2–Assimilation by Gene Shuffling. In C. A. Rebeiz, C. Benning, H. J. Bohnert, H. Daniell, J. K. Hoober, H. K. Lichtenthaler, A. R. Portis, & B. C. Tripathy (Eds.), *The Chloroplast: Basics and Applications* (pp. 307–322). Springer Netherlands. https://doi.org/10.1007/978-90-481-8531-3_20

Chapter 3: Catalytic Scavenging of Plant Reactive Oxygen Species *In Vivo* by Anionic Cerium Oxide Nanoparticles

Gregory Michael Newkirk*[1,2], Honghong Wu*[1], Israel Santana[1], Juan Pablo Giraldo[1,2]

[1] Department of Botany and Plant Sciences, University of California

[2] Department of Microbiology and Plant Pathology, University of California

*These authors contributed equally

Abstract

Reactive oxygen species (ROS) accumulation is a hallmark of plant abiotic stress response. ROS play a dual role in plants by acting as signaling molecules at low levels and damaging molecules at high levels. Accumulation of ROS in stressed plants can damage metabolites, enzymes, lipids, and DNA, causing a reduction of plant growth and yield. The ability of cerium oxide nanoparticles (nanoceria) to catalytically scavenge ROS in vivo provides a unique tool to understand and bioengineer plant abiotic stress tolerance.

Here, we present a protocol to synthesize and characterize poly (acrylic) acid coated nanoceria (PNC), interface the nanoparticles with plants via leaf lamina infiltration, and monitor their distribution and ROS scavenging in vivo using confocal microscopy. Current molecular tools for manipulating ROS accumulation in plants are limited to model species and require laborious transformation methods. This protocol for in vivo ROS scavenging has the potential to be applied to wild type plants with broad leaves and leaf structure like Arabidopsis thaliana.

Video Link

The video component of this article can be found at https://www.jove.com/video/58373/

Introduction

Cerium oxide nanoparticles (nanoceria) are widely used in living organisms, from basic research to bioengineering, due to their distinct catalytic reactive oxygen species (ROS) scavenging ability(Gupta et al., 2016; Nelson et al., 2016; C. Xu & Qu, 2014). Nanoceria have ROS scavenging abilities due to a large number of surface oxygen vacancies that alternate between two oxidation states ($Ce3^{+}$ and $Ce4^{+}$)(P. Dutta et al., 2006; Pulido-Reyes et al., 2015; Walkey et al., 2015). The $Ce3^{+}$ dangling bonds effectively scavenge ROS while the lattice strains at the nanoscale promote the regeneration of these defect sites via redox cycling reactions(Boghossian et al., 2013). Nanoceria have also been recently used for studying and engineering plant function(Giraldo et al., 2014; Wu, Tito, et al., 2017). Plants under abiotic stress experience accumulation of ROS, causing oxidative damage to lipids, proteins, and DNA(Demidchik, 2015). In *A. thaliana* plants, nanoceria catalytic scavenging of ROS in vivo leads to improved plant photosynthesis under high light, heat, and chilling stresses(Wu, Tito, et al., 2017). Applying nanoceria to soil also increases shoot biomass and grain yield of wheat (*Triticum aestivum*)(Rico et al., 2014); canola (*Brassica napus*) plants treated with nanoceria have higher plant biomass under salt stress (Rossi et al., 2016).

Nanoceria offer bioengineers and plant biologists a nanotechnology-based tool to understand abiotic stress responses and enhance plant abiotic stress tolerance. Nanoceria's *in vivo* ROS scavenging capabilities are independent of plant species, and the facile delivery into plant tissues has the potential to enable broad application outside of model organisms. Unlike other genetically-based methods, nanoceria do not require generating plant lines with the overexpression of antioxidant enzymes for higher ROS scavenging ability(J. Xu et al., 2013). Leaf lamina infiltration of nanoceria to plants is a practical approach for lab-based research.

The overall goal of this protocol is to describe 1) the synthesis and characterization of negatively charged poly (acrylic) acid nanoceria (PNC), 2) the delivery and tracking of PNC throughout leaf cells, and 3) the monitoring of PNC-enabled ROS scavenging *in vivo*. In this protocol, negatively charged poly (acrylic) acid nanoceria (PNC) are synthesized and characterized by their absorption spectrum, hydrodynamic diameter, and zeta potential. We describe a simple leaf lamina infiltration method to deliver PNC into plant leaf tissues. For *in vivo* imaging of nanoparticle distribution within mesophyll cells, a fluorescent dye (DiI) was used to label PNC (DiI-PNC) and observe the nanoparticles via confocal fluorescence microscopy. Finally, we explain how to monitor *in vivo* PNC ROS scavenging through confocal microscopy.

Protocol

1. Growing A. thaliana Plants

    1.1. Sow *A. thaliana* seeds in 5 cm x 5 cm disposable pots filled with standard soil mix. Put 32 of these pots into a plastic tray filled with water (~0.5 cm depth) and transfer the plastic tray with the plants into a plant growth chamber.

        1.1.1. Set the growth chamber settings as follows: 200 µmol/ms photosynthetic active radiation (PAR), 24 ± 1 °C day and 21 ± 1 °C night, 60% humidity, and 14/10 h day/night light regime, respectively.

    1.2. Thin each pot to leave only one individual plant after one week of germination. Take note to keep the seedlings with similar size in each pot.

    1.3. Water the pots by pouring tap water directly on the plastic tray once every two days. Grow the plants for four weeks. *A. thaliana* plants are ready for further use.

2. Synthesis and Characterization of PNC

    2.1. Weigh 1.08 g of cerium (III) nitrate and dissolve it in 2.5 mL of molecular biology grade water in a 50 mL conical tube.

    2.2. Weigh 4.5 g of poly (acrylic) acid and dissolve it in 5 mL of molecular biology grade water in a 50 mL conical tube.

    2.3. Mix these two solutions thoroughly at 2,000 rpm for 15 min using a digital vortex mixer.

2.4. Transfer 15 mL of ammonium hydroxide solution (7.2 M) to a 50 mL glass beaker.

2.5. While stirring at 500 rpm, add the mixture from Step 2.3 dropwise to the ammonium hydroxide solution and stir at 500 rpm at room temperature for 24 hr in a fume hood.

2.6. Cover the beaker with a piece of paper to avoid the substantial loss of solution during the overnight reaction.

2.7. After 24 h, transfer the resulting solution to a 50 mL conical tube and centrifuge it at 3,900 x g for 1 h to remove any possible debris and large agglomerates.

2.8. Transfer this 22.5 mL of supernatant solution into three 15 mL 10 kDa filters and fill the remainder of the filter with molecular grade water to make a total dilution of 45 mL.

2.9. Purify the supernatant solution from free polymers and other reagents with a benchtop centrifuge by adding the supernatant to a 15 mL 10 kDa filter and centrifuge at 3,900 x g for 15 min. Repeat this step at least six times.

2.10. Measure the absorbance of the eluent in each cycle with a UV-VIS spectrophotometer from 220-700 nm to ensure no free polymers and other reagents are present in the final PNC solution.

2.11. Take the collected PNC solution into the 5 mL syringe and filter it against a 20 nm pore size syringe filter. Collect the filtered PNC solution in a 50 mL conical tube.

2.12. Take a diluted final PNC solution in a plastic cuvette and measure its absorbance with the UV-VIS spectrophotometer from 220-700 nm. PNC absorbance peak is at 271 nm.

2.13. Calculate its concentration by using Beer-Lambert's law: A = εCL. A is the absorbance of the peak value for a given sample, ε is the molar absorption coefficient of PNC (cm^{-1} M^{-1}), L is the optical path length (cuvette width, 1 cm in this method), and C is the molar concentration of measured nanoparticles.

2.14. Measure the hydrodynamic diameter and zeta potential of the synthesized PNC using a particle size and zeta potential analyzer (Figure 3.1).

2.15. Store the final PNC solution in a refrigerator (4 °C) until further use. NOTE: Please refer to Wu et al. for more protocol details about PNC characterization (Wu, Tito, et al., 2017).

3. Labeling PNC with DiI Fluorescent Dye

3.1. Mix 0.4 mL of 5 mM (58 mg/L) PNC with 3.6 mL of molecular biology grade water in a 20 mL glass vial and stir at 500 rpm.

3.2. Add 24 µL 1,1'-dioctadecyl-3,3,3',3'-tetramethylindocarbocyanine perchlorate dye solution (DiI, 2.5 mg/mL; dilute in DMSO) into 176 µL of DMSO (dimethyl sulfoxide) to make the DiI dye solution.

3.3. Add the DiI dye dropwise to the PNC solution, stirring at 1,000 rpm for 1 min at ambient temperature.

3.4. Transfer this resulting mixture into a 15 mL 10 kDa filter and fill the tube to the top with molecular biology grade water to make the total dilution 15 mL.

3.5. Purify the DiI labeled PNC (DiI-PNC) solution from DMSO and any possible free DiI dye by a benchtop centrifugation with the 15 mL 10 kDa filter at 3,900 x g for 5 min.

3.5.1. Repeat Step 3.5 at least five times.

3.6. Filter the final DiI-PNC solutions through a 20 nm pore size syringe filter.

3.7. Measure the absorbance of final DiI-PNC by UV-VIS spectrophotometry and calculate its concentration according to Beer-Lambert's law (Figure 3.2). See Step 2.13 for more details.

3.8. Store it in a refrigerator at 4 °C for further use.

4. Infiltration of Plant Leaves with PNC

4.1. Add 0.1 mL of infiltration buffer (100 mM TES, 100 mM $MgCl_2$, pH 7.5, adjusted by HCl) into 0.9 mL of 0.5 mM PNC or DiI-PNC solution and vortex it. Use a solution of 10 mM TES infiltration buffer as a negative control.

4.2. Transfer 0.2 mL of the PNC or DiI-PNC infiltration solution to a 1 mL sterile needleless syringe. Tap to remove any possible air bubbles.

4.3. Retrieve the plant from the growth chamber just before infiltration with nanoparticles to avoid possible stomata closure under room light conditions.

4.4. Before infiltration, measure the chlorophyll content from A. thaliana leaves with similar size using a chlorophyll meter. Measure each leaf with three replicates (each replicate consisting of at least three measurements)(Wu et al., 2015). Choose the *A. thaliana* leaves with similar chlorophyll content for the infiltration experiment.

4.5. Infiltrate the leaves slowly with the recently prepared PNC or DiI-PNC solution by gently pressing the tip of the needleless syringe against the bottom of the leaf lamina (abaxial side) and depress the plunger (Figure 3.3A).

4.6. Gently wipe off the excess solution that remains on the surface of leaf lamina (Figure 3.3B) using a delicate task wiper (Figure 3.3C) and label the plant. Use new delicate task wipes for each group of leaves.

4.7. Keep the infiltrated *A. thaliana* plants on the bench for leaf adaptation and incubation with PNC or DiI-PNC for 3 h. NOTE: Infiltrated *A. thaliana* plants are then ready for further use (Figure 3.3D).

5. Preparation of Leaf Samples for Confocal Microscopy

5.1. Roll a pea-size amount of observation gel to about a 1 cm radius (Figure 3.4A) and then spread it out until it is 1 mm thin on a glass slide (Figure 3.4B).

5.2. Use a cork borer (diameter 0.3 cm) to cut out a circular section at the center of the observation gel on the glass slide (Figure 3.4C).

5.3. Fill the cut well entirely with perfluorodecalin (PFD) for deeper and better confocal imaging resolution in leaf tissues.

5.4. Use a cork borer (diameter 0.2 cm) to collect leaf discs from the adapted DiI-PNC infiltrated *A. thaliana* plants (Figure 3.4D).

5.5. Mount the leaf disc in the PFD filled well; face the infiltrated (abaxial) side of the leaf up.

5.6. Put a square coverslip on top of the leaf disc and gently press on the slide coverslip evenly to seal it with the well of observation gel and ensure no air bubbles remain trapped (Figure 3.4E).

6. Imaging DiI-PNC in Leaf Tissues by Confocal Microscopy

6.1. Use a 40X objective lens in an inverted laser scanning confocal microscope.

6.2. Drop two to three drops of ddH_2O on the top of the 40X objective lens.

6.3. Place the prepared DiI-PNC infiltrated leaf sample slide on top of the inverted 40X objective lens.

6.3.1. Make sure the coverslip side but not the glass slide contact directly with the ddH_2O on the lens.

6.4. Find a region of interest in the sample under the microscope with either laser light or bright field.

6.5. Start the microscope software and turn on the Argon laser (set at 20%).

6.6. Set the pinhole to collect an optical slice less than 2 μm and a line average of 4.

6.7. Image the sample with confocal microscope settings: 514 nm laser excitation (30 %); Z-Stack section thickness: 2 μm; PMT1: 550-615 nm (for DiI-PNC imaging); PMT2: 700-800 nm (for chloroplast imaging).

6.8. Take representative confocal images of leaf samples from different individuals, a minimum of three biological replicates.

7. Imaging PNC in vivo ROS Scavenging by Confocal Microscopy

7.1. Prepare 25 µM 2',7'-dichlorodihydrofluorescein diacetate (H_2DCFDA, a dye for indicating a general ROS) and 10 µM dihydroethidium (DHE, a dye for indicating superoxide anion) dyes in TES infiltration buffer (pH 7.5) in 1.5 mL microcentrifuge tubes, separately.

7.2. Use a cork borer (diameter 0.2 cm) to collect leaf discs from the adapted PNC infiltrated *A. thaliana* plants.

7.2.1. Use the sharp tip of the forceps to make three to four holes on the leaf discs to accelerate dye loading process.

7.3. Transfer the leaf discs to microcentrifuge tubes with H_2DCFDA and DHE separately and incubate for 30 min under darkness.

7.4. After incubation, rinse the leaf discs with ddH_2O three times and mount it into the glass slide with observation gel (see Protocol Section 5).

7.5. Put the slide on the confocal microscope and manually focus to a region of leaf mesophyll cells. See Protocol Section 6 for details.

7.6. Expose the leaf discs to the UV-A (405 nm) laser for 3 min to generate ROS and record the ROS signal intensity change in time-series ("xyt") per leaf disc.

7.7. Image the leaf disc with confocal microscope settings: 40X water objective; 496 nm laser excitation; PMT1: 500-600 nm (for DHE and DCFDA dye detection); PMT2: 700-800 nm (for chloroplasts detection). Use a plant infiltrated with only infiltration buffer solution as the negative control.

8. PNC Scavenging of H_2O_2 *in vitro*

8.1. Conduct the CAT (catalase) mimetic activity of the synthesized PNC in vitro by following the methods in previous publications3,8,15

8.2. Add 45.4 μL of 1x TES infiltration buffer (10 mM TES, 10 mM $MgCl_2$, pH 7.5, adjusted by HCl), PNC (60 nM, 3 μL), and H_2O_2 (2 μM, 1 μL) into a well (white round bottom 96 well plate), and gently mix it by pipetting.

8.3. Add 10-acetyl-3,7-dihydroxyphenoxazine (working concentration 100 μM, 0.5 μL) and horseradish peroxidase (HRP; working concentration 0.2 U/mL, 0.1 μL) into the well, gently mix it by pipetting, and incubate it for 30 min. 10-acetyl-3,7-dihydroxyphenoxazine reacts with H_2O_2 and is converted into resorufin in the presence of HRP.

8.3.1. Wrap the plate with aluminum foil to avoid light during the incubation.

8.3.2. Prepare a negative control by using reaction buffer or water to replace H_2O_2.

8.3.3. Except for the stock solution, prepare all other solutions at ambient temperature.

8.4. After the incubation, with a plate reader, monitor the absorbance at 560 nm to use resorufin for indicating the level of H_2O_2. Set time regime at 0, 2, 5, 10, 20, and 30 min.

Representative Results

PNC synthesis and characterization

PNC were synthesized, purified and characterized following the method described in Protocol Section 2. Figure 3.1A shows the coloration of the solutions of cerium nitrate, PAA, the mixture of cerium nitrate and PAA, and PNC. A color change from white to light yellow is seen after PNC is synthesized. After purification with a 10 kDa filter, PNC were characterized with a UV-VIS spectrophotometer. A peak of absorbance for PNC was observed at 271 nm (Figure 3.1B). The final eluent was also measured with UV-VIS to confirm that the non-reacted chemicals were washed during the purification. The hydrodynamic diameter and zeta potential of the synthesized PNC were measured with a particle sizer and zeta potential analyzer (Figure 3.1C).

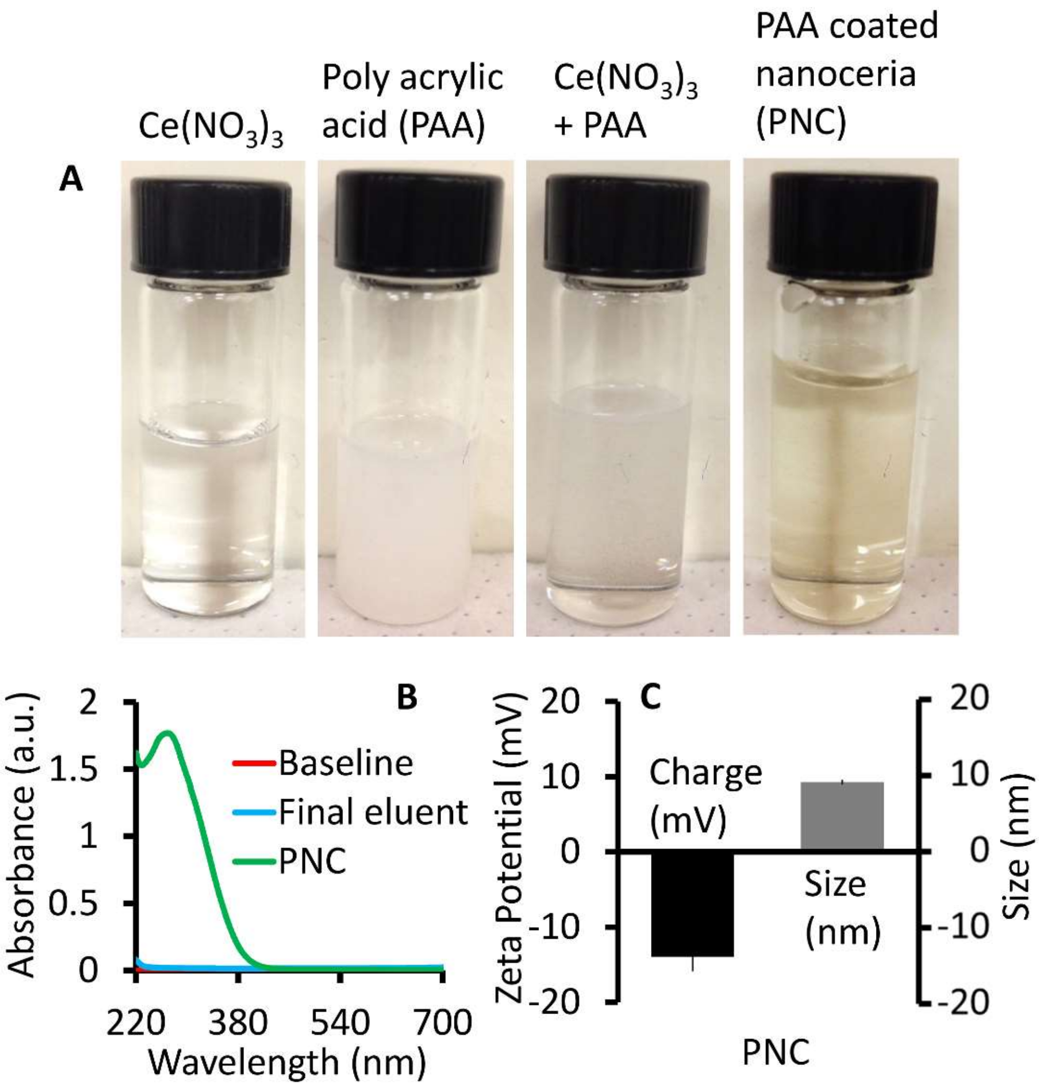

Figure 3.1. Synthesis and characterization of PNC. A. Coloration of cerium nitrate, poly acrylic acid (PAA), mixture of cerium nitrate and PAA, and the synthesized PNC (PAA coated cerium oxide nanoparticles, light yellow). B. Absorbance spectrum of PNC measured by UV-VIS spectrophotometry. C. Hydrodynamic diameter and zeta potential of the synthesized PNC. Mean ± standard error (n = 4).

PNC labeling with DiI dye

To determine the distribution of the nanoparticles in vivo, PNC were labeled with a fluorescent DiI dye following the method described in Protocol Section 3. DiI dye embeds within the PNC coating spontaneously since it can encapsulate into the hydrophobic domains inside the polymer coatings of nanoceria(Asati et al., 2010). After adding DiI dye to the PNC solution, a rapid color change to pink was observed (Figure 3.2A). The DiI labeled PNC were then purified with a 10 kDa filter and characterized by a UV-VIS spectrophotometry. Three clear peaks of absorbance for the DiI labeled PNC were observed (Figure 3.2B). The final eluent was measured by UV-VIS spectrophotometry to confirm that the non-reacted chemicals were washed out during the purification.

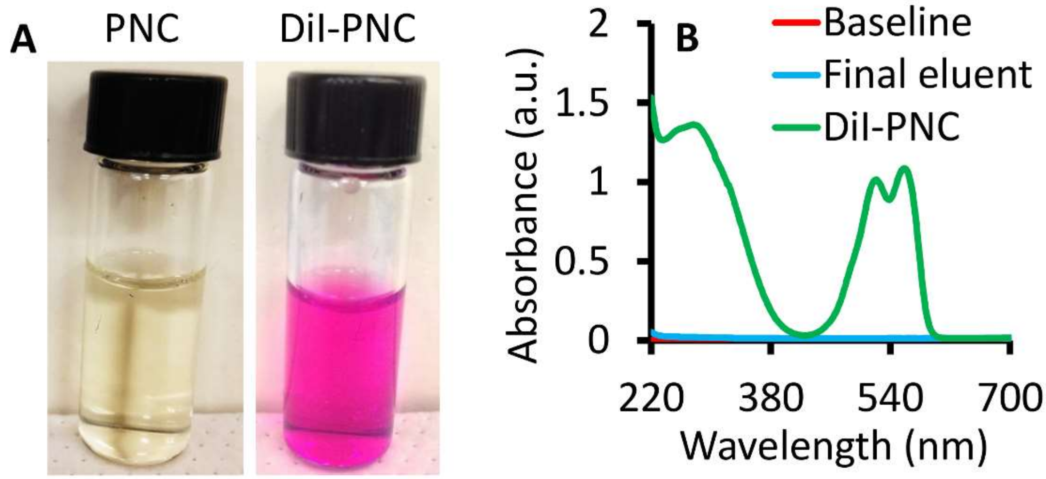

Figure 3.2: PNC labeling with DiI fluorescent dye. A. PNC (light yellow) and DiI dye labelled PNC solution (DiI-PNC, pink). B. Absorbance spectrum of DiI-PNC solution.

Leaf Lamina infiltration

PNC or DiI-PNC were delivered into A. thaliana leaf via leaf lamina infiltration method as described in Protocol Section 4. Leaf was infiltrated at four different spots to ensure the full leaf area was perfused with PNC solution (Figure 3.3A). Any remaining solution was removed from the leaf surface (Figure 3.3B and 3.3C). The leaf color changed during infiltration from green to darker green (Figure 3.3D). The syringe was gently pressed against the leaf to avoid any physical damage.

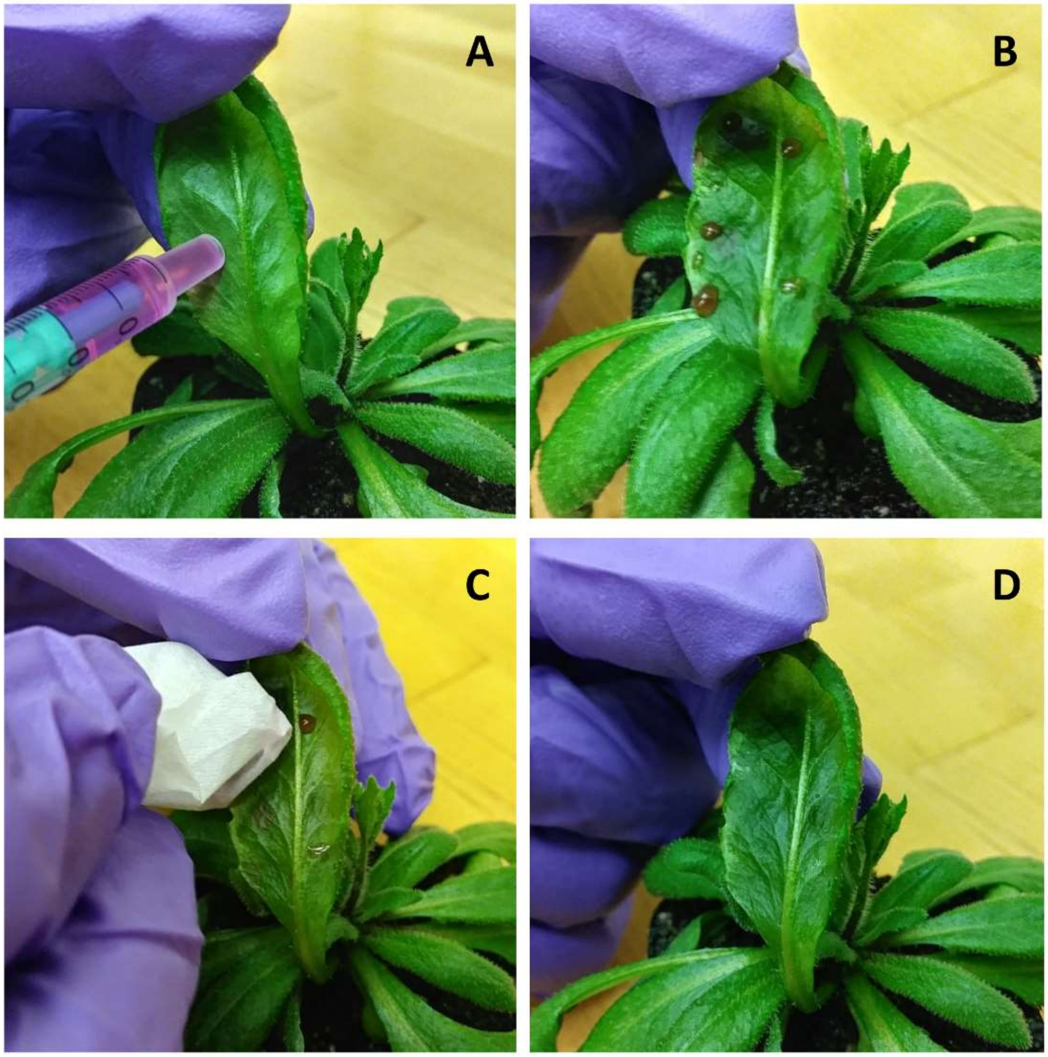

Figure 3.3. Leaf lamina infiltration of PNC or DiI-PNC. A. A. thaliana leaf before infiltration. The solution inside the syringe is DiI-PNC. B. Leaf infiltrated with DiI-PNC. C. Cleaning the remaining solution from the leaf surface with delicate task wipes. D. Cleaned A. thaliana leaf infiltrated with DiI-PNC.

Leaf sample preparation for fluorescence microscopy

Leaf samples were mounted on glass slides within an observation gel made well filled with PFD. After rolling the pea size observation gel on the slide (Figure 3.4A and 3.4B), a well was made in the middle of the flat gel (Figure 3.4C). Then, the freshly prepared leaf disc was transferred to the well previously filled with PFD solution (Figure 3.4D). A coverslip was used to immobilize the leaf sample on the slide (Figure 3.4E).

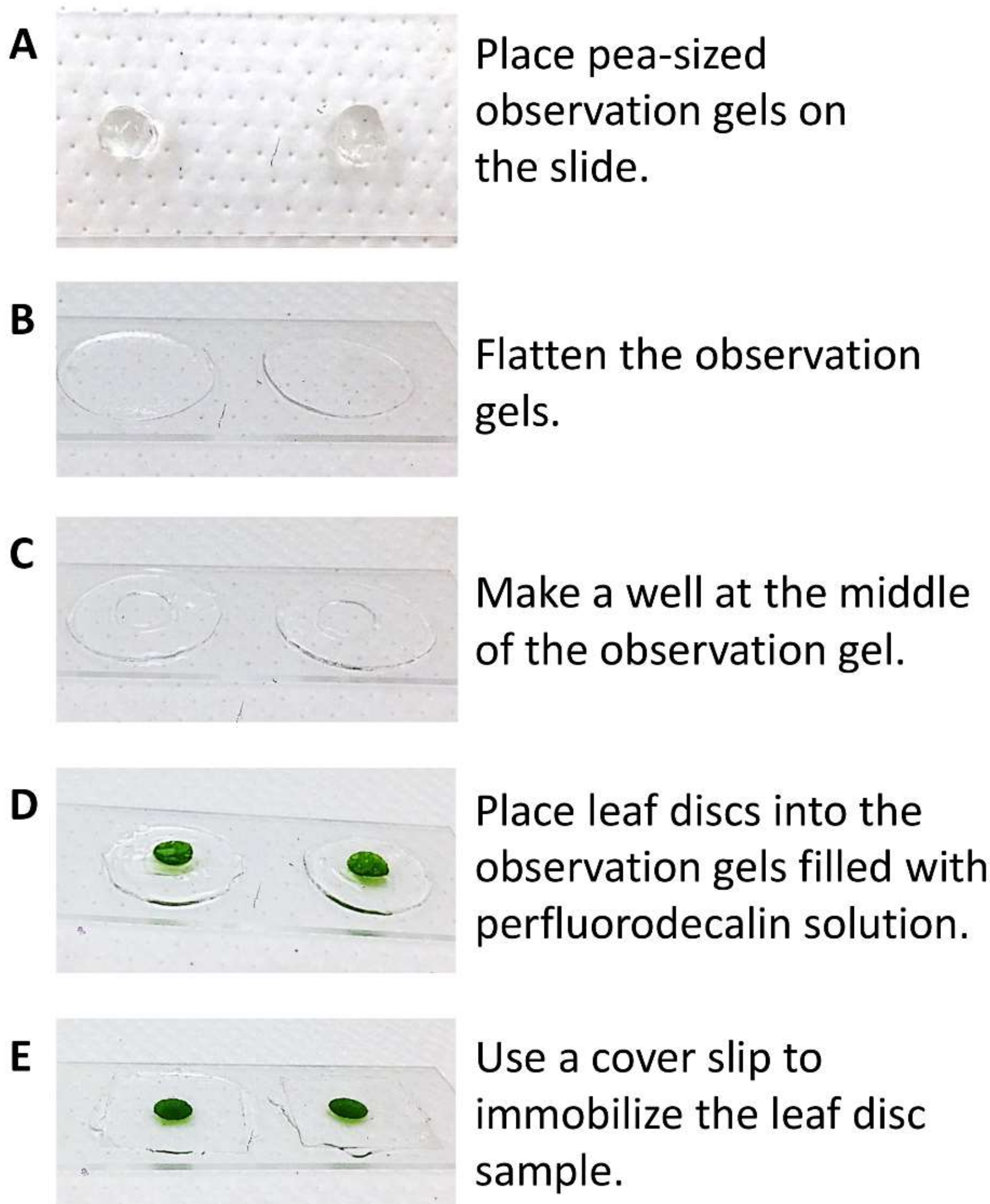

Figure 3.4. Preparation of leaf sample slides. A. Microscopy glass slide with pea size observation gels. B. Slide with flat observation gels. C. Slide with flat observation gel having a well at the middle. D. Slide with leaf discs in the observation gel well filled with perfluorodecalin (PFD) solution. E. Slide with leaf discs immobilized by cover slip.

Confocal imaging of DiI-PNC *in vivo*

DiI-PNC infiltrated A. thaliana leaves were used for determining the distribution of DiI-PNC in leaf mesophyll cells via confocal imaging (Figure 3.5A and 5B). To visualize colocalization between the DiI-PNC and chloroplasts, DiI-PNC infiltrated leaf samples were excited with a 514 nm laser. The emission of DiI-PNC was set at 550-615 nm to avoid the possible interference of chloroplast pigments signals after ~650 nm (Li et al., 2018). The chlorophyll auto-fluorescence from chloroplasts were detected from 700-800 nm. The confocal imaging settings were set (laser power and gain) to make sure no DiI dye signals were detected in the control leaf sample (infiltrated with only buffer) (Figure 3.5C). The colocalization of DiI-PNC with chloroplasts in leaf mesophyll cells can be observed by the overlay image of detected DiI-PNC and chloroplast pigment autofluorescence (Figure 3.5D).

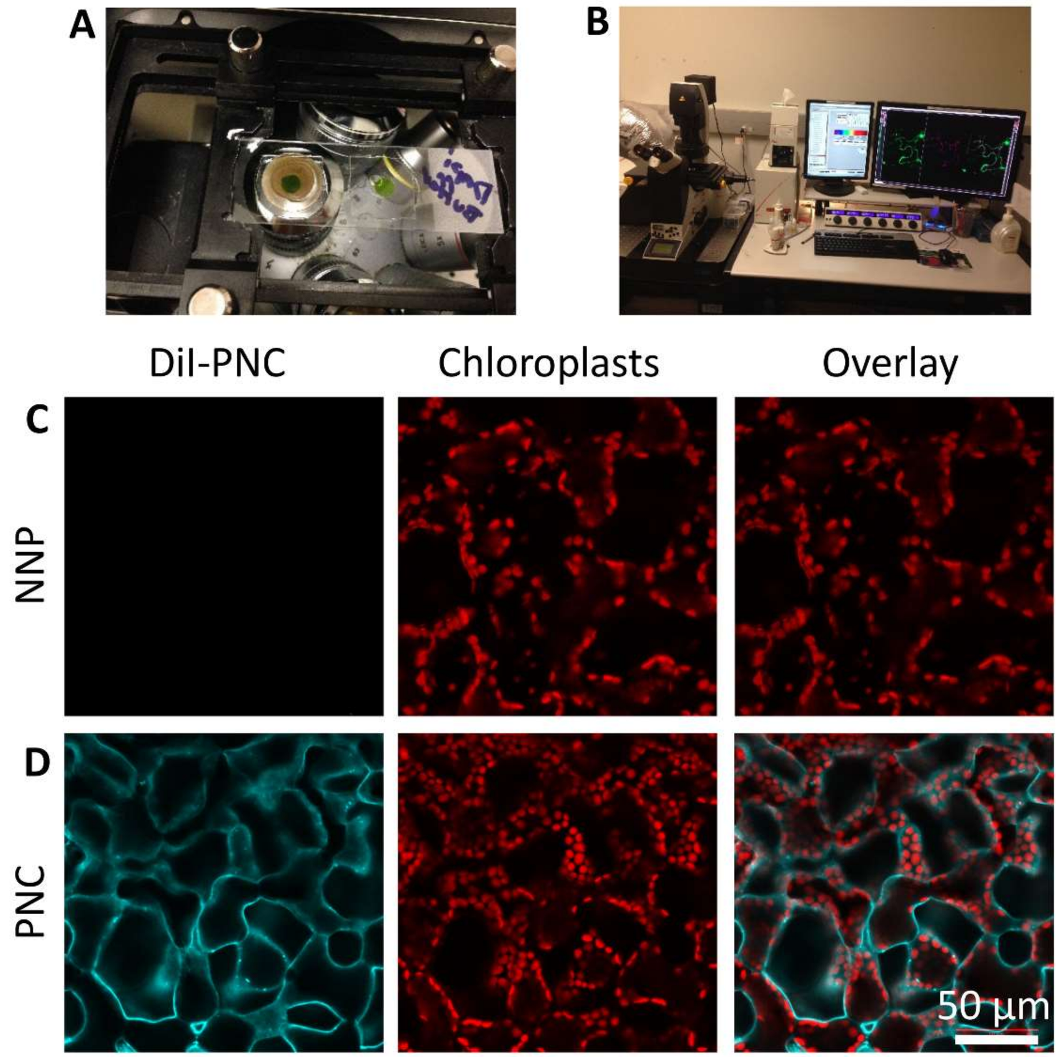

Figure 3.5. Imaging DiI-PNC in leaf mesophyll cells via confocal microscopy. A. Leaf sample is mounted on an inverted confocal microscope having a 40X water immersion lens. B. A confocal microscope is used for imaging DiI-PNC and chloroplasts. C. Chloroplast auto-fluorescence is recorded in buffer infiltrated leaf samples without nanoparticles (NNP). D. DiI-PNC signal and chloroplast auto-fluorescence is imaged in DiI-PNC infiltrated leaf samples.

Confocal imaging of PNC ROS scavenging *in vivo*

PNC in 10 mM TES buffer solution were delivered into A. thaliana leaves via the leaf lamina infiltration method as described in Protocol Section 7. DHE (dihydroethidium) and H_2DCFDA (2′,7′-dichlorodihydrofluorescein diacetate) fluorescent dyes are used to visualize ROS in plant tissues(Wu et al., 2018; Wu, Tito, et al., 2017). H_2DCFDA is known to be converted to fluorescent DCF (2′,7′-dichlorofluorescein, an indicator of the degree of general oxidative stress) due to the cleavage of the acetate groups by ROS(Merad-Boudia et al., 1998). DHE is a more specific dye for superoxide anion having its fluorescent product (2-hydroxyethidium) increase upon reaction with a superoxide anion(Zhao et al., 2005). *In vivo* ROS scavenging enabled by PNC was monitored in leaf discs measuring DHE and DCF dye fluorescence intensity changes (Figures 6A and 6B). PNC infiltrated leaf samples were excited with 496 nm laser. The emission of DHE and DCF dye was set at 500-600 nm to avoid the possible interference with chloroplast auto-fluorescence signals. Pigment auto-fluorescence from chloroplasts were detected from 700-800 nm. After 3 minutes of UV stress, the ROS dye signals in PNC and buffer- infiltrated leaf samples were monitored separately. Compared to the no-nanoparticle buffer control (NNP), PNC infiltrated leaves showed significantly less ROS-activated fluorescent DCF dye signal (Figure 3.6A). Similar results were also found with the superoxide anion-activated DHE dye, where PNC infiltrated leaves had significantly less DHE dye intensity than buffer infiltrated control leaves (Figure 3.6B).

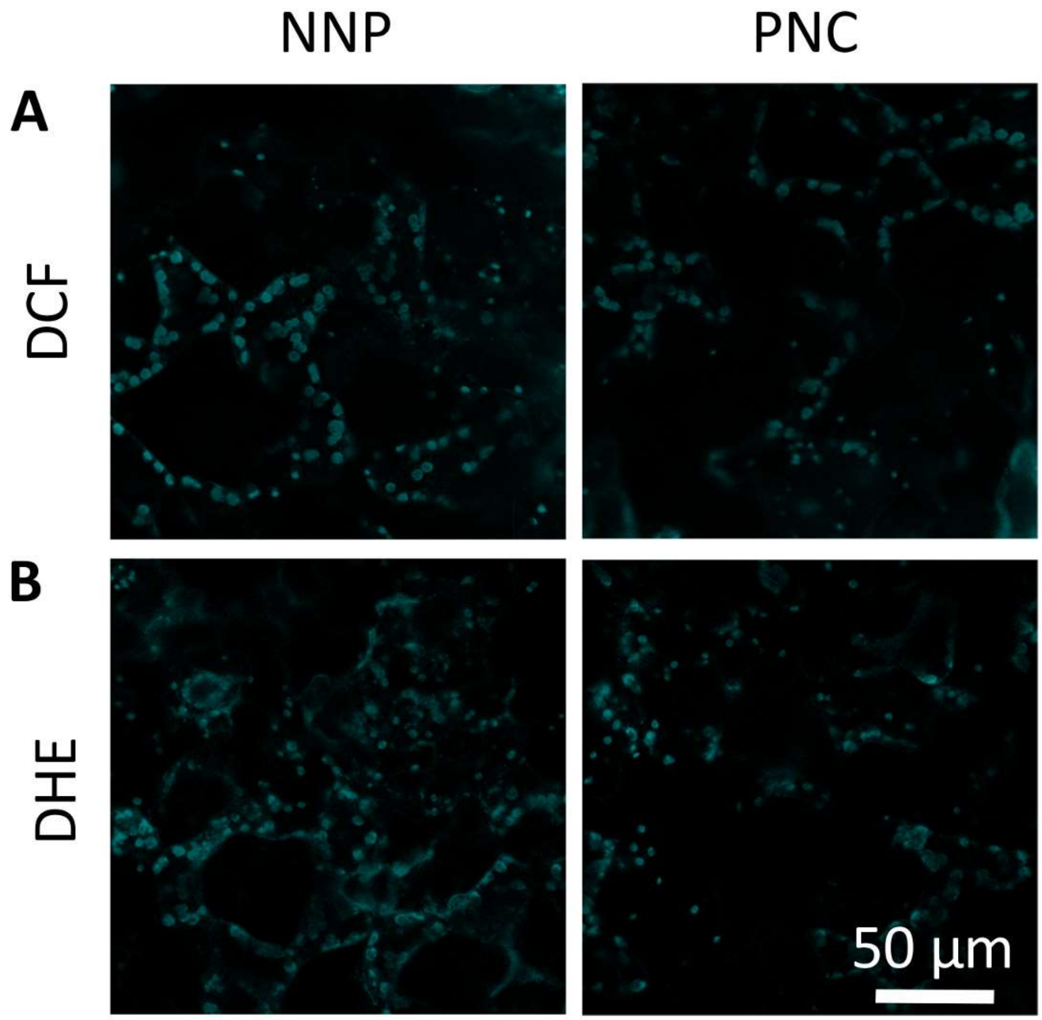

Figure 3.6. **Monitoring PNC ROS scavenging in planta via confocal microscopy.** A. DCF fluorescent dye (for monitoring general ROS signal) is significantly lower in mesophyll cells of PNC infiltrated plants than buffer control (no nanoparticles, NNP). B. Reduced DHE fluorescent dye (for monitoring superoxide anion) in mesophyll cells of PNC infiltrated plants relative to that of buffer control (NNP).

PNC CAT mimetic activity assay

Assay of PNC scavenging of H_2O_2 was described in Protocol Section 8. A decrease of resorufin which indicates H_2O_2 level in the reaction mixture containing PNC was observed (Figure 3.7), confirming the CAT mimetic activity of the synthesized PNC.

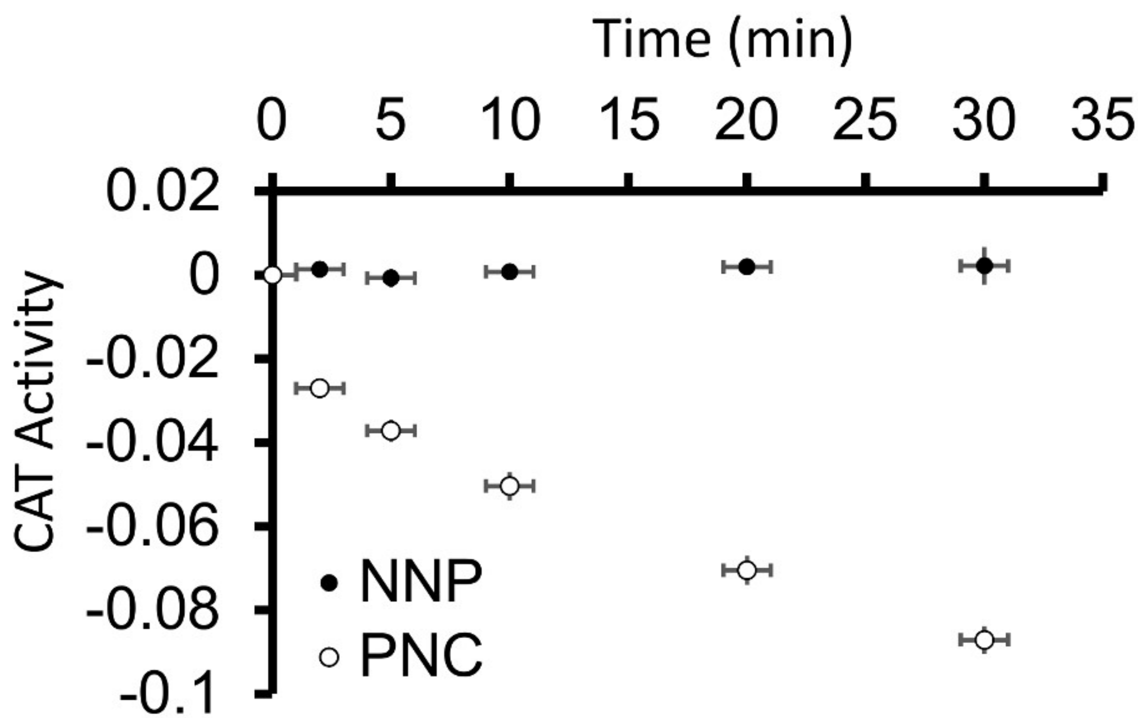

Figure 3.7. **Catalase (CAT) mimetic activity of PNC.** In the presence of horseradish peroxidase, the fluorescent probe reacts with hydrogen peroxide and is converted to resorufin (absorbance 560 nm). Absorbance of resorufin, which is indicative of hydrogen peroxide levels, was monitored at 560 nm. PNC showed a CAT mimetic activity. Mean ± SE (standard error) (n = 4).

Discussion

In this protocol, we describe PNC synthesis, characterization, fluorescent dye labeling, and confocal imaging of the nanoparticles within plant mesophyll cells to exhibit their *in vivo* ROS scavenging activity. PNC are synthesized from a mixture of cerium nitrate and PAA solution in ammonium hydroxide. PNC are characterized by absorption spectrophotometry and the concentration determined using Beer-Lamberts law. Zeta potential measurements confirmed the negatively charged surface of PNC for enhancing delivery to chloroplasts(Wu, Tito, et al., 2017). Labeling of PNC with a fluorescent DiI dye enables in vivo imaging by confocal microscopy within leaf mesophyll cells where the nanoparticles show high levels of colocalization with chloroplasts. Using DHE and DCF fluorescent dyes, we confirmed that PNC act as a potent scavenger of superoxide anion and ROS *in vivo*.

The method for synthesizing PNC is a simple step-wise procedure that generates cerium oxide nanoparticles with controlled size, negative charge, and ROS scavenging capabilities(Asati et al., 2010). Other methods, such as thermal hydrolysis, require high temperatures and expensive chemistry equipment(Hirano & Inagaki, 2000; Sun et al., 2012). The synthesis and characterization of PNC is a low-cost method performed with common laboratory equipment. It does not require a steep learning curve compared with molecular methods in plants based on overexpression of an antioxidant enzyme, e.g., SOD, APX, and CAT, for scavenging ROS species in model systems(Xi et al., 2010). PNC is a robust, water-soluble ROS catalytic scavenger that will not require laborious cloning and transformation methods that are dependent on the plant's genetic tractability and available molecular toolkit.

A critical step in this protocol is the syringe-based infiltration of leaf mesophyll cells with PNC. Infiltration of nanoparticles into live plants should be done gently to avoid physical damage to the leaf (Wu, Santana, et al., 2017). Thus, as in Protocol Step 4 of the methods, gently push against the leaf surface with the syringe to avoid tearing or puncturing the abaxial leaf surface. It is better to infiltrate from the abaxial surface of *A. thaliana* leaf since it has higher stomatal density than the adaxial surface(Fukushima & Hasebe, 2014; Monda et al., 2016). Furthermore, a buffered solution of PNC or DiI-PNC within the physiological pH range (~ pH 7.5) should be used during leaf lamina infiltration. Another critical step in this protocol is to apply the appropriate concentration of PNC to the studied plant tissue. In this protocol, 50 mg/L of PNC was not toxic to *A. thaliana* leaves while enabling catalytic PNC ROS scavenging. Some limitations of the current nanoparticle delivery method are 1) not applicable to plant species having thick and waxy cuticles or low stomatal densities, 2) not scalable for applications in the field, 3) the high cost of a confocal microscopy system to monitor *in vivo* nanoparticle distribution and ROS scavenging.

This protocol demonstrates the application of ROS scavenging PNC for studying and improving abiotic stress tolerance in plants through a facile method of leaf lamina infiltration. ROS accumulation is accompanied by abiotic stresses in plants, which in turn reduces plant photosynthesis, growth, and yield(Chaves et al., 2009; Petrov et al., 2015;

Wu, Tito, et al., 2017). Plant genetic modifications methods for ROS manipulation in vivo are often limited to plant model species while PNC ROS-scavenging has the potential to be applied to diverse wild type plant species. Leaf lamina infiltration is a practical research method to increase ROS scavenging in leaf tissues for understanding and engineering plant abiotic stress tolerance.

References

Asati, A., Santra, S., Kaittanis, C., & Perez, J. M. (2010). Surface-Charge-Dependent Cell Localization and Cytotoxicity of Cerium Oxide Nanoparticles. *ACS Nano*, *4*(9), 5321–5331. https://doi.org/10.1021/nn100816s

Boghossian, A. A., Sen, F., Gibbons, B. M., Sen, S., Faltermeier, S. M., Giraldo, J. P., Zhang, C. T., Zhang, J., Heller, D. A., & Strano, M. S. (2013). Application of Nanoparticle Antioxidants to Enable Hyperstable Chloroplasts for Solar Energy Harvesting. *Advanced Energy Materials*, *3*(7), 881–893. https://doi.org/10.1002/aenm.201201014

Chaves, M. M., Flexas, J., & Pinheiro, C. (2009). Photosynthesis under drought and salt stress: regulation mechanisms from whole plant to cell. *Annals of Botany*, *103*(4), 551–560. https://doi.org/10.1093/aob/mcn125

Demidchik, V. (2015). Mechanisms of oxidative stress in plants: From classical chemistry to cell biology. *Environmental and Experimental Botany*, *109*, 212–228. https://doi.org/10.1016/j.envexpbot.2014.06.021

Fukushima, K., & Hasebe, M. (2014). Adaxial-abaxial polarity: The developmental basis of leaf shape diversity. *Genesis* , *52*(1), 1–18. https://doi.org/10.1002/dvg.22728

Giraldo, J. P., Landry, M. P., Faltermeier, S. M., McNicholas, T. P., Iverson, N. M., Boghossian, A. A., Reuel, N. F., Hilmer, A. J., Sen, F., Brew, J. A., & Strano, M. S. (2014). Plant nanobionics approach to augment photosynthesis and biochemical sensing. *Nature Materials*, *13*(4), 400–408. https://doi.org/10.1038/nmat3890

Gupta, A., Das, S., Neal, C. J., & Seal, S. (2016). Controlling the surface chemistry of cerium oxide nanoparticles for biological applications. *Journal of Materials Chemistry. B, Materials for Biology and Medicine*, *4*(19), 3195–3202. https://doi.org/10.1039/C6TB00396F

Hirano, M., & Inagaki, M. (2000). Preparation of monodispersed cerium(iv) oxide particles by thermal hydrolysis: influence of the presence of urea and Gd doping on their morphology and growth. *Journal of Materials Chemistry*, *10*(2), 473–477. https://doi.org/10.1039/a907510k

Li, J., Wu, H., Santana, I., Fahlgren, M., & Giraldo, J. P. (2018). Standoff Optical Glucose Sensing in Photosynthetic Organisms by a Quantum Dot Fluorescent Probe. *ACS Applied Materials & Interfaces*, *10*(34), 28279–28289. https://doi.org/10.1021/acsami.8b07179

Merad-Boudia, M., Nicole, A., Santiard-Baron, D., Saillé, C., & Ceballos-Picot, I. (1998). Mitochondrial impairment as an early event in the process of apoptosis induced by glutathione depletion in neuronal cells: relevance to Parkinson's disease. *Biochemical Pharmacology*, *56*(5), 645–655. https://doi.org/10.1016/s0006-2952(97)00647-3

Monda, K., Araki, H., Kuhara, S., Ishigaki, G., Akashi, R., Negi, J., Kojima, M., Sakakibara, H., Takahashi, S., Hashimoto-Sugimoto, M., Goto, N., & Iba, K. (2016). Enhanced Stomatal Conductance by a Spontaneous Arabidopsis Tetraploid, Me-0, Results from Increased Stomatal Size and Greater Stomatal Aperture. *Plant Physiology*, *170*(3), 1435–1444. https://doi.org/10.1104/pp.15.01450

Nelson, B., Johnson, M., Walker, M., Riley, K., & Sims, C. (2016). Antioxidant Cerium Oxide Nanoparticles in Biology and Medicine. *Antioxidants & Redox Signaling*, *5*(2), 15. https://doi.org/10.3390/antiox5020015

P. Dutta, S. Pal, A., Seehra*, M. S., Y. Shi, E. M. Eyring, A., & Ernst, R. D. (2006). *Concentration of Ce3+ and Oxygen Vacancies in Cerium Oxide Nanoparticles*. https://doi.org/10.1021/CM061580N

Petrov, V., Hille, J., Mueller-Roeber, B., & Gechev, T. S. (2015). ROS-mediated abiotic stress-induced programmed cell death in plants. *Frontiers in Plant Science*, *6*, 69. https://doi.org/10.3389/fpls.2015.00069

Pulido-Reyes, G., Rodea-Palomares, I., Das, S., Sakthivel, T. S., Leganes, F., Rosal, R., Seal, S., & Fernández-Piñas, F. (2015). Untangling the biological effects of cerium oxide nanoparticles: the role of surface valence states. *Scientific Reports*, *5*(1), 15613. https://doi.org/10.1038/srep15613

Rico, C. M., Lee, S. C., Rubenecia, R., Mukherjee, A., Hong, J., Peralta-Videa, J. R., & Gardea-Torresdey, J. L. (2014). Cerium Oxide Nanoparticles Impact Yield and Modify Nutritional Parameters in Wheat (*Triticum aestivum* L.). *Journal of Agricultural and Food Chemistry*, *62*(40), 9669–9675. https://doi.org/10.1021/jf503526r

Rossi, L., Zhang, W., Lombardini, L., & Ma, X. (2016). The impact of cerium oxide nanoparticles on the salt stress responses of Brassica napus L. *Environmental Pollution* , *219*, 28–36. https://doi.org/10.1016/J.ENVPOL.2016.09.060

Sun, C., Li, H., & Chen, L. (2012). Nanostructured ceria-based materials: synthesis, properties, and applications. *Energy & Environmental Science*, *5*(9), 8475. https://doi.org/10.1039/c2ee22310d

Walkey, C., Das, S., Seal, S., Erlichman, J., Heckman, K., Ghibelli, L., Traversa, E., McGinnis, J. F., & Self, W. T. (2015). Catalytic properties and biomedical applications of cerium oxide nanoparticles. *Environmental Science: Nano*, *2*(1), 33–53. https://doi.org/10.1039/C4EN00138A

Wu, H., Santana, I., Dansie, J., & Giraldo, J. P. (2017). *In Vivo* Delivery of Nanoparticles into Plant Leaves. In *Current Protocols in Chemical Biology* (Vol. 9, pp. 269–284). John Wiley & Sons, Inc. https://doi.org/10.1002/cpch.29

Wu, H., Shabala, L., Shabala, S., & Giraldo, J. P. (2018). Hydroxyl radical scavenging by cerium oxide nanoparticles improves Arabidopsis salinity tolerance by enhancing leaf mesophyll potassium retention. *Environmental Science: Nano*, *5*(7), 1567–1583. https://doi.org/10.1039/C8EN00323H

Wu, H., Shabala, L., Zhou, M., Stefano, G., Pandolfi, C., Mancuso, S., & Shabala, S. (2015). Developing and validating a high-throughput assay for salinity tissue tolerance in wheat and barley. *Planta*, *242*(4), 847–857. https://doi.org/10.1007/s00425-015-2317-1

Wu, H., Tito, N., & Giraldo, J. P. (2017). Anionic Cerium Oxide Nanoparticles Protect Plant Photosynthesis from Abiotic Stress by Scavenging Reactive Oxygen Species. *ACS Nano*, *11*(11), 11283–11297. https://doi.org/10.1021/acsnano.7b05723

Xi, D.-M., Liu, W.-S., Yang, G.-D., Wu, C.-A., & Zheng, C.-C. (2010). Seed-specific overexpression of antioxidant genes in Arabidopsis enhances oxidative stress tolerance during germination and early seedling growth. *Plant Biotechnology Journal*, *8*(7), 796–806. https://doi.org/10.1111/j.1467-7652.2010.00509.x

Xu, C., & Qu, X. (2014). Cerium oxide nanoparticle: a remarkably versatile rare earth nanomaterial for biological applications. *NPG Asia Materials*, *6*(3), e90–e90. https://doi.org/10.1038/am.2013.88

Xu, J., Duan, X., Yang, J., Beeching, J. R., & Zhang, P. (2013). Enhanced Reactive Oxygen Species Scavenging by Overproduction of Superoxide Dismutase and Catalase Delays Postharvest Physiological Deterioration of Cassava Storage Roots. *Plant Physiology*, *161*(3), 1517–1528. https://doi.org/10.1104/pp.112.212803

Zhao, H., Joseph, J., Fales, H. M., Sokoloski, E. A., Levine, R. L., Vasquez-Vivar, J., & Kalyanaraman, B. (2005). Detection and characterization of the product of hydroethidine and intracellular superoxide by HPLC and limitations of fluorescence. *Proceedings of the National Academy of Sciences of the United States of America*, *102*(16), 5727–5732. https://doi.org/10.1073/pnas.0501719102

Chapter 4: DNA delivery by high aspect ratio nanomaterials to algal chloroplasts

Gregory M. Newkirk[1], Su-Ji Jeon, Hye-in Kim, Supreetha Sivaraj, Pedro De Allende, Christopher Castillo, Robert E. Jinkerson[2,3*], Juan Pablo Giraldo[1,2*]

[1]Department of Microbiology and Plant Pathology, University of California, Riverside, CA, USA

[2]Department of Botany and Plant Sciences, University of California, Riverside, CA, USA

[3]Department of Chemical and Environmental Engineering, University of California, Riverside, CA, USA

* Correspondence:

Corresponding Authors

juanpablo.giraldo@ucr.edu

robert.jinkerson@ucr.edu

Abstract

Chloroplast are sites of photosynthesis that have been bioengineered to produce food, biopharmaceuticals, and biomaterials. Current approaches for altering the chloroplast genome rely on inefficient DNA delivery methods, leading to low chloroplast transformation efficiency rates. For algal chloroplasts, there is no modifiable, customizable, and efficient *in situ* DNA delivery chassis. Herein, we investigated polyethylenimine-coated single-walled carbon nanotubes (PEI-SWCNT) as delivery vehicles for DNA to algal chloroplasts. We examined the impact of PEI-SWCNT charge

and PEI polymer size (25k vs 10k) on the uptake into chloroplasts of wildtype and cell wall knockout mutant strains of the green algae *Chlamydomonas reinhardtii*. To assess the delivery of DNA bound to PEI-SWCNT, we used confocal microscopy and colocalization analysis of chloroplast autofluorescence with fluorophore-labeled single-stranded GT_{15} DNA. We found that highly charged DNA-PEI25k-SWNCT have a statistically significant higher percentage of DNA colocalization events with algal chloroplasts (22.28% ± 6.42, 1 hr) over 1-3 hours than DNA-PEI10k-SWNCT (7.23% ± 0.68, 1 hr) ($P<0.01$). We determined the biocompatibility of DNA-PEI-SWCNT through assays for living algae cells, reactive oxygen species (ROS) generation, and *in vivo* chlorophyll assays. Through these assays, it was shown that algae exposed to DNA-PEI25k-SWCNT (30 fg/cell) and DNA-PEI10k-SWCNT (300 fg/cell) were viable over 4 days and had little impact on oxidative stress levels. DNA-coated PEI-SWCNT transiently increased ROS levels within one hour of exposure to nanomaterials (30- 300 fg/cell) both in the wildtype strain and cell-wall knockout strain, followed by ROS decline to normal levels due to reaction with antioxidant glutathione and lipid membranes. PEI-SWCNT can act as biological carriers for delivering biomolecules such as DNA and have the potential to become novel tools for chloroplast biotechnology and synthetic biology.

Introduction

Algae biotechnology's applications range from the manufacturing of biodegradable bioplastics, renewable biofuels, and plant-based sustainable food sources.(Maliga & Bock, 2011; Mathiot et al., 2019; Mayfield & Golden, 2015) Applied and basic research on algae biotechnology could be augmented by exploring emerging nanotechnology approaches. Potential applications of nanomaterials for algae biotechnology include gene delivery, biomolecule sensing, and enhancing photosynthetic efficiency(Giraldo et al., 2019; Newkirk et al., 2021; Wang et al., 2019) Single-walled carbon nanotubes (SWCNTs) have been shown to enter isolated chloroplasts,(Giraldo et al., 2014) plant protoplasts,(Lew et al., 2018) carry plasmid DNA *in planta* for the expression of green fluorescent proteins (GFP) in nuclei without genome integration(Demirer, Zhang, Matos, et al., 2019) and enable chloroplast-specific expression in land plants.(Kwak et al., 2019) SWCNTs are also capable of acting as near-infrared sensors for the detection of stress molecules, for example, by standoff monitoring of plant health though hydrogen peroxide sensing.(Wu et al., 2020) SWCNTs have also been shown to increase plant photosynthetic efficiency by augmenting chloroplast light energy capture and conversion in plant leaves. (Giraldo et al., 2014)

Algae chloroplast biotechnology genetic advancements are currently being stymied by low chloroplast transformation rates due to non-specific and inefficient biomolecule delivery, limiting synthetic biology methods and applications.(Bock, 2015) In theory, each algal cell in a culture could be transformed, allowing for large phenotypic screening and directed evolution experiments using large mutant libraries. However, chloroplast transformation rates are a limiting step and major bottleneck for plastome bioengineering. For example, chloroplast transformation efficiency rates are so limiting for mutant library screening that directed evolution of Ribulose-1,5-bisphosphate carboxylase/oxygenase (RuBisCO) research is currently performed in bacteria.(Wilson et al., 2018; Zhu et al., 2010) The current standard protocol for the delivery of DNA for chloroplast transformation, particle bombardment, uses a microcarrier approach that, once tuned, is fairly universal across algae and plants. However, there are serious limitations with biomolecule delivery through particle bombardment: 1) the particles are unable to be targeted to specific parts of the cell, 2) cause cell and tissue damage, 3) a large amount of DNA is necessary, and 4) high cost of specialized equipment.(Newkirk et al., 2021; Wang et al., 2019) Therefore, there is justification for researching and applying new approaches for biomolecule delivery. Nanotechnology gene delivery approaches have been reported for land plants(Demirer, Zhang, Matos, et al., 2019; Kwak et al., 2019; Santana et al., 2020, 2022; Zhang et al., 2019) but not for algae.

To date, the impact of high aspect ratio nanomaterials on algae, specifically of SWCNTs and multi-walled carbon nanotubes (MWCNTs), has been assessed through the guise of environmental toxicity. In photosynthetic green algae *Dunaliella tertiolecta, Pseudokirchneriella subcapitata,* and *Chlorella* exposure to MWCNTs or SWCNTs result in large aggregates of carbon nanotubes with consequent oxidative stress, low biocompatibility, and inhibition of growth.(Long et al., 2012; Schwab et al., 2011; Thakkar et al., 2016; Wei et al., 2010; Youn et al., 2012) The studies of nanomaterial applications to the algal model species *Chlamydomonas reinhardtii,* a staple of biology research for photosynthetic eukaryotic organisms, are limited to research focused on addressing environmental toxicology questions. SWCNTs with no functionalization or coating were shown to have an inhibitory effect on growth, chlorophyll fluorescence, and quantum yield.(Matorin et al., 2010) In contrast, salmon sperm DNA bound to sodium cholate-coated SWCNTs, at a 1:1 mass ratio, showed no inhibitory effect on *Chlamydomonas reinhardtii* growth or chlorophyll content at concentrations ranging from 0.1 to 100 µg/mL for an exposure duration of 10 days. (Williams et al., 2014) More recently, SWCNT have been reported to protect photosynthetic reactions in *Chlamydomonas* against photoinhibition.(Antal et al., 2022) Taken together, these results suggest that there is large potential in studying the nanotechnology applications for green algae and, specifically, the use of surface functionalized carbon nanotubes in *C. reinhardtii* for advancing biotechnology applications.

SWCNTs have been proposed to translocate across plant cell and chloroplast membranes by a lipid exchange envelope penetration (LEEP) mechanism.(Wong et al., 2016) The LEEP hypothesis posits that temporary pores are created in the chloroplast envelopes when the ionic cloud of highly charged nanomaterials disrupts the lipid membranes. The SWCNTs may become trapped within the outer and inner membranes of the chloroplast and become coated with membrane lipids.(Giraldo et al., 2014; Wong et al., 2016) Using fluorescence microscopy imaging of nanoparticles in extracted chloroplasts, the LEEP model was developed based on a nanoparticle's smallest size dimension and charge as the key factors influencing the translocation through plant lipid bilayers. Lew and colleagues expanded on the original LEEP hypothesis by looking at the uptake of nanoparticles into plant protoplasts via flow cytometry.(Lew et al., 2018) Specifically, the LEEP model hypothesizes that nanoparticles require +/- 20 mV to enter plant protoplasts and for entry into extracted chloroplasts ~+/-30 mV. It is hypothesized that a high concentration of carbon nanotubes could be lethal due to a higher frequency of contact between the nanoparticle and the lipid bilayer, causing an increase in membrane rupturing.(Lew et al., 2018; Wong et al., 2016) In algae, there are multiple obstacles that a nanoparticle must pass through before reaching the chloroplast membrane that were not considered by the LEEP model including the outer algae extracellular matrix and the cell wall.(Newkirk et al., 2021) Semiconducting SWCNTs coated in ssDNA by pi-stacking interactions have been mapped inside plant and algae cells using Raman spectroscopy.(Giraldo et al., 2014; Orlanducci et al., 2020) Due to highly stable and strong pi-stacking interactions, it is very unlikely that these DNA-SWCNT complexes are able to release DNA in organisms. In fact, this type of DNA-SWCNT has been shown to act as stable sensors for animal and plant biomolecules,(Giraldo et al., 2015; Iverson et al., 2013; Wu et al., 2020) indicating the potential to act as tools to image and detect signaling molecules in algae. To date, no studies have investigated SWCNT mediated DNA delivery mechanisms into algae based on physical and chemical properties of nanomaterials. Our study elucidates DNA delivery mechanisms and biocompatibility in algae of oxidized SWCNTs coated by PEI through electrostatic interactions that have been shown to deliver and express transgene DNA in plants.(Demirer, Zhang, Matos, et al., 2019; Santana et al., 2022)

This study focuses on understanding the impact of SWCNT charge and polyethylenimine (PEI) polymer size on the delivery of DNA to *Chlamydomonas* chloroplasts, measuring the effect of the algae cell wall barrier on SWCNT uptake, and SWCNT's influence on oxidative stress, chloroplast photosynthesis, and survivability (Figure 4.1). We coated SWCNT with PEI varying in molecular weight (25k vs. 10k), a coating that has been previously shown to vary in charge and capable of delivering DNA biomolecules to land plants.(Demirer, Zhang, Matos, et al., 2019; Martin-Avila et al., 2020) To determine if PEI-SWCNT coated with DNA (DNA-PEI-SWCNTs) entered into algae cells and chloroplasts, we used high spatial resolution confocal microscopy imaging for tracking a covalently bonded fluorophore to DNA cargo. To assess the impact of DNA-PEI-SWCNTs on *Chlamydomonas* oxidative stress, chloroplast photosynthesis and survivability, we measured the generation of reactive oxygen species (ROS), performed assays of glutathione antioxidant activity and lipid peroxidation, *in vivo* concentrations of chlorophyll and carotenoids, and live cell staining. This study advances our understanding of carbon nanotubes as a tool for nucleic acid delivery in microbial algae and the impact of high aspect ratio nanomaterials on algae function.

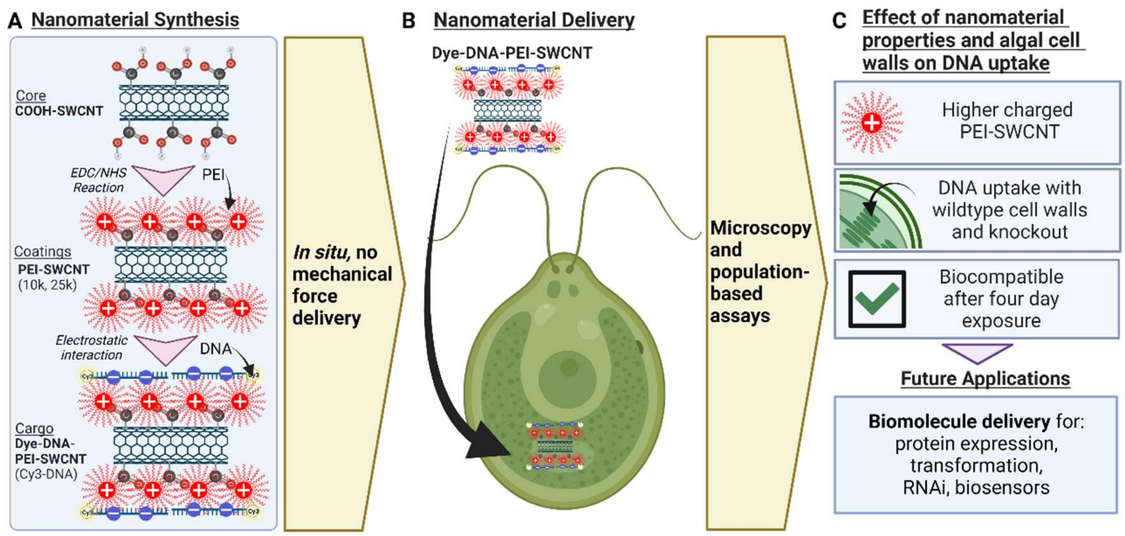

Figure 4.1. Uptake and impact of single-walled carbon nanotubes (SWCNTs) for DNA delivery in algae. a) SWCNTs are functionalized by different molecular weight coatings of polyethylenimine (PEI) and then conjugated with Cy3 dye-labeled single-stranded ssDNA bound for microscopy imaging. **b)** Dye-DNA-PEI-SWCNTs or DNA-PEI-SWCNTs are delivered to *Chlamydomonas reinhardtii* without mechanical aid for colocalization analysis via confocal microscopy or for biocompatibility assays, respectively. **c)** *In situ* uptake of DNA is favored by nanomaterials with higher charge that could be used for multiple synthetic biology and molecular biology research purposes.

Results and discussion

Characterization of DNA-coated PEI-SWCNT

Carboxylated single-walled carbon nanotubes (COOH-SWCNTs, 5 nm d., Sigma-Aldrich, Cat# 652490-250MG) were dispersed into water, suspended in MES buffer (100 mM, pH 6), covered with a PEI coating of either of ~10,000 or ~25,000 molecular weight (PEI10k-SWCNT, PEI25k-SWCNT) through an EDC/NHS reaction, purified, and then finally bound to oligonucleotide DNA through a 30-minute binding reaction at room temperature. We analyzed the changes in height and length of COOH-SWCNTs after coating them with PEI and ssDNA via atomic force microscopy (AFM) (Figure 4.2a-d, S1). The AFM height for PEI25k-SWCNTs (7.60 ± 2.39 nm) was significantly larger (4.08 ± 1.83 nm, $p < 0.0001$) than that of COOH-SWCNTs but only slightly larger for PEI10k-SWCNTs (6.05 ± 1.83 nm, $p > 0.05$) (Figure 4.2c). AFM height for DNA-PEI10k-SWCNTs and DNA-PEI25k-SWCNTs increased to 13.13 ± 5.00 nm and 24.17 ± 9.13 nm ($p < 0.0001$), respectively (Figure 4.2c). In contrast, the average lengths of COOH-SWCNTs (0.87 ± 0.49 μm) decreased after being coated with PEI10k or PEI25k polymer to 0.67 ± 0.43 μm ($p < 0.05$) and 0.64 ± 0.26 μm ($p < 0.01$), respectively (Figure 4.2d).

This can be attributed to a reduction in length during the tip sonication steps performed for suspending SWCNT coated in PEI. Coating PEI10k-/PEI25k - SWCNTs with DNA resulted in non-significant changes in length from 0.79 ± 0.24 μm to 0.82 ± 0.18 μm ($p > 0.05$) (Figure 4.2d). The AFM analysis showed that the thickness of PEI-SWCNT was increased by approximately 7 to 16 nm upon introduction of ssDNA, which is comparable with previous studies,(Ali et al., 2022) and suggested that the surface modification of SWCNTs with PEI 10k or PEI 20k polymer allowed DNA to bind to the surface.

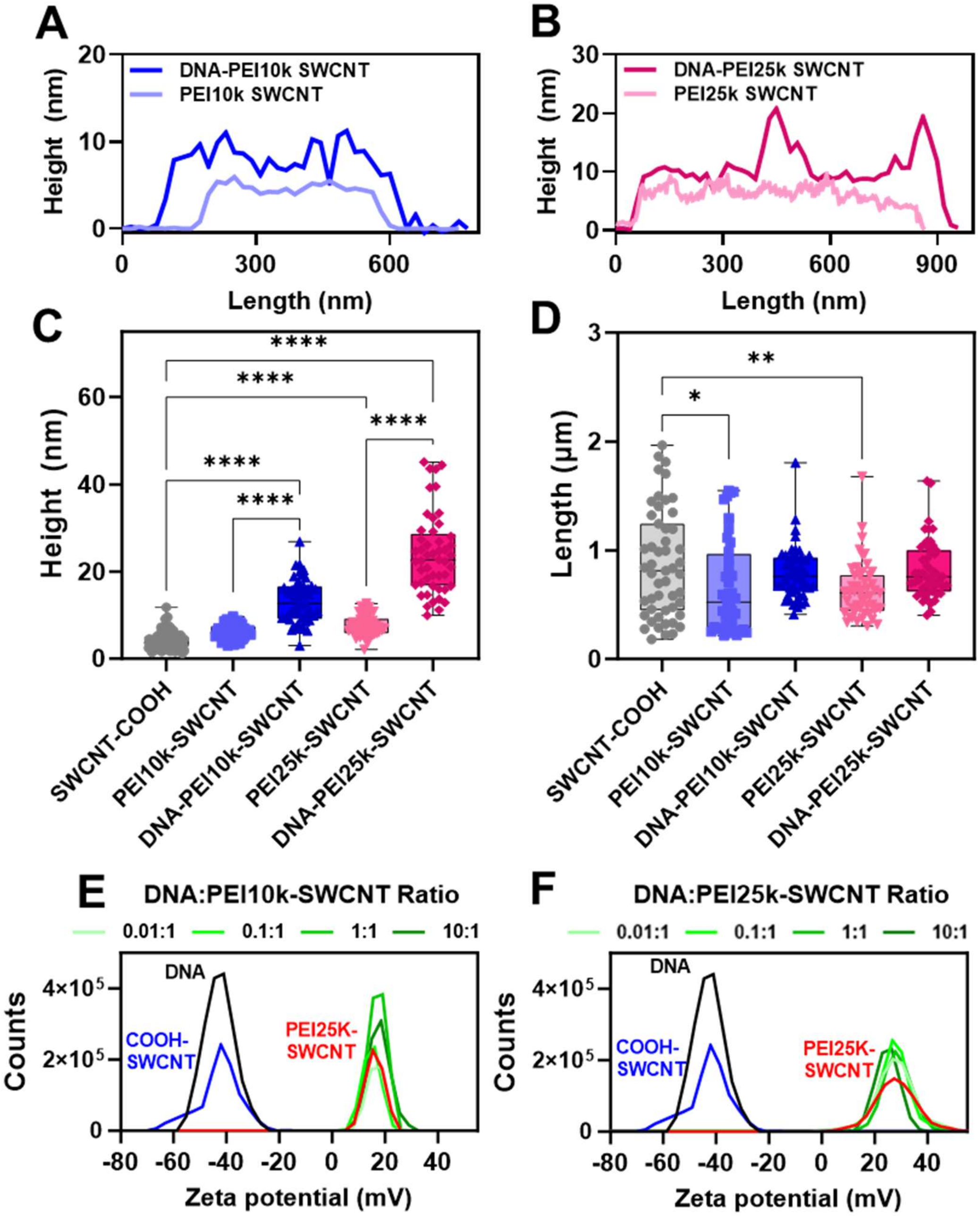
A
DNA-PEI10k SWCNT
PEI10k SWCNT
Height (nm)
Length (nm)
B
DNA-PEI25k SWCNT
PEI25k SWCNT
Height (nm)
Length (nm)
C
Height (nm)
****
SWCNT-COOH
PEI10k-SWCNT
DNA-PEI10k-SWCNT
PEI25k-SWCNT
DNA-PEI25k-SWCNT
D
Length (μm)
*
**
SWCNT-COOH
PEI10k-SWCNT
DNA-PEI10k-SWCNT
PEI25k-SWCNT
DNA-PEI25k-SWCNT
E
DNA:PEI10k-SWCNT Ratio
0.01:1
0.1:1
1:1
10:1
DNA
COOH-SWCNT
PEI25K-SWCNT
Counts
Zeta potential (mV)
F
DNA:PEI25k-SWCNT Ratio
0.01:1
0.1:1
1:1
10:1
DNA
COOH-SWCNT
PEI25K-SWCNT
Counts
Zeta potential (mV)

Figure 4.2. Nanomaterial characterization. a, b) Representative AFM height profiles of PEI10k- and PEI25k-SWCNTs with and without GT15 ssDNA bound at a 1:1 ratio. **c, d)** Average height and length of SWCNT-COOH, PEI10k-/PEI25k- SWCNTs determined from AFM images (*P<0.05, **P<0.01, ****P<0.0001, one way ANOVA, n=50-60). The height of COOH-SWCNT and PEI-SWCNT increased upon coating with PEI and ssDNA, respectively. A slight decrease in length was also observed after coating COOH-SWCNT with PEI by tip sonication. **e, f)** Zeta potential analysis of PEI10k- and PEI25k-SWCNT in the presence of various ssDNA concentrations (10 mM final TE buffer, pH 8.0).

We investigated the zeta potential and ssDNA binding of the nanomaterial complexes to optimize the ratio of DNA to PEI-SWCNTs. Both free DNA and COOH-SWCNT showed highly negative surface charge of -42.6 ± 0.5 mV and -42.5 ± 0.7 mV respectively (Figure 4.2e-f). Once coated with the positively charged PEI, it was observed that the surface charge of the SWCNTs changed to +14.5 ± 2.0 mV and +30.1 ± 2.0 mV for PEI10k-SWCNT and PEI-25k SWCNT, showing a narrow and single-peak shape, which indicated that the carbon nanotubes were successfully coated with these polymers (Figure 4.2e-f, Table 4.1). Interestingly, the PEI-SWCNT zeta potential exhibited minimal change despite the progressive increase in DNA:PEI-SWCNT ratios from 0.01:1, 0.1:1 to 1:1 (Table 4.1). These findings diverge from previously reported interactions involving PEI-SWCNT and dsDNA.(Demirer, Zhang, Matos, et al., 2019; Santana et al., 2022) The observed disparity may be attributed to the distinctive structural properties of single-stranded DNA and plasmid DNA, and their arrangement on the PEI-SWCNT surface that influences the electric potential at the nanomaterial double layer. A DNA-loading assay was used to assess the amount of free GT_{15} oligonucleotide ssDNA that remained after a binding reaction of ssDNA with PEI10k-SWCNTs and PEI25k-SWCNTs at 0.01:1, 0.1:1, 1:1, and 10:1 DNA:PEI-SWCNT, respectively. This binding assay based on gel electrophoresis showed that 100% of DNA was loaded onto the PEI10k- and PEI25k-SWCNT through a 30-minute binding reaction (and further incubation of 1 hour) that mimics experimental conditions (Figure S4.2). The narrow and single-peak shaped zeta potentials of DNA-PEI-SWCNT also indicated that all ssDNA had reacted with PEI-SWCNTs and there was no free ssDNA (Figure 4.2e,f). Zeta potential measurements for DNA:PEI-SWCNT at 10:1 ratio could not be performed due to significant aggregation of the nanomaterial complexes. This ratio indicates the limits for loading of DNA on our PEI-SWCNT without leading to aggregation that could impair delivery of DNA and the nanomaterial complexes (Figure S4.3). Together the zeta potential and ssDNA binding assays pointed out that the optimal reaction ratio was 1:1 DNA:PEI-SWCNT, where DNA adhered well without significant changes in the size of the complex. This 1:1 DNA:PEI-SWCNT ratio was subsequently used for the following experiments.

Table 4.1. Zeta potentials of PEI10k- and PEI25k-SWCNT in the presence of various ssDNA concentrations (10 mM final TE buffer, pH 8.0).

DNA:PEI-SWCNT	**PEI 10k**	**PEI 25k**
No DNA	14.5 ± 2.0	30.1 ± 2.0
0.01:1	14.7 ± 1.8	28.8 ± 2.0
0.1:1	14.6 ± 1.8	29.8 ± 1.7
1:1	17.0 ± 1.6	30.6 ± 2.9

DNA delivery mediated by PEI-SWCNT in algae

We assessed the impact of the algal cell wall and differing PEI coatings of SWCNTs on Cy3-GT_{15} (Dye-DNA) delivery mediated by nanomaterials into chloroplasts. Wildtype algae (CC-124) and a cell wall knockout (CC-4533) were exposed to PEI10k-SWCNTs and PEI25k-SWCNTs (0.1 ng/uL), bound to Dye-DNA at a 1:1 mass ratio, and visualized by confocal microscopy (Figure 4.3a,b); zoomed images for Dye-DNA delivered by PEI10k- and PEI25k-SWCNT to chloroplasts are also shown (Figure S4.4-4.5). The highest rate of Dye-DNA uptake into the chloroplast was determined through colocalization analysis, upon 1 hour of exposure of both PEI10k and PEI25k-SWCNT (300 fg/cell, 1:1 Dye-DNA:SWCNT) with the wildtype and cell wall knockout strain (Figure S4.6-4.8). The delivery of Dye-DNA by PEI25k-SWCNT significantly increased colocalization of Dye-DNA with chloroplasts compared to Dye-DNA-PEI10k-SWCNT in the cell wall knockout strain (****$P<0.0001$)(Figure 4.3c). Orthogonal merged images indicate that after just 1 hour of incubation, Dye-DNA is being delivered and associated with the algae outer membrane and colocalizing with parts of the chloroplast with DNA-PEI10k-SWCNT and DNA-PEI2kk-SWCNT (Figure 4.3a,b). Z-stacks were cell counted and analyzed for colocalization events and it was found that, with both the wildtype and cell knockout strain, DNA-PEI25k-SWCNT had a statistically significant increase in percentage of algae cells with Dye-DNA compared to DNA-PEI10k-SWCNT (****$P<0.0001$)(Figure 4.3d). Both Dye-DNA-PEI10k-SWCNT and Dye-DNA-PEI25k-SWCNT (1-hour incubation) showed increased cell clumping, an indicator of algae experiencing stress or perhaps a result of electrostatic binding between Dye-DNA-PEI-

SWCNT and algae cell walls (Figure S4.7-4.8). A negative control of algae with Dye-DNA without PEI-SWCNTs was used for all confocal experiments to illustrate that the Dye-DNA does not associate with the algae unless the PEI-SWCNT is present (Figure S9). Overall, highly charged DNA-PEI25k-SWCNT (+30.6 ± 2.9 mV) are more effective than DNA-PEI10k-SWCNT (+17.0 ± 1.6 mV) at delivering DNA across algae biosurfaces including the outer matrix, cell wall and lipid membranes into the chloroplasts as reported in land plant studies.(Lew et al., 2018; Santana et al., 2022; Wong et al., 2016)

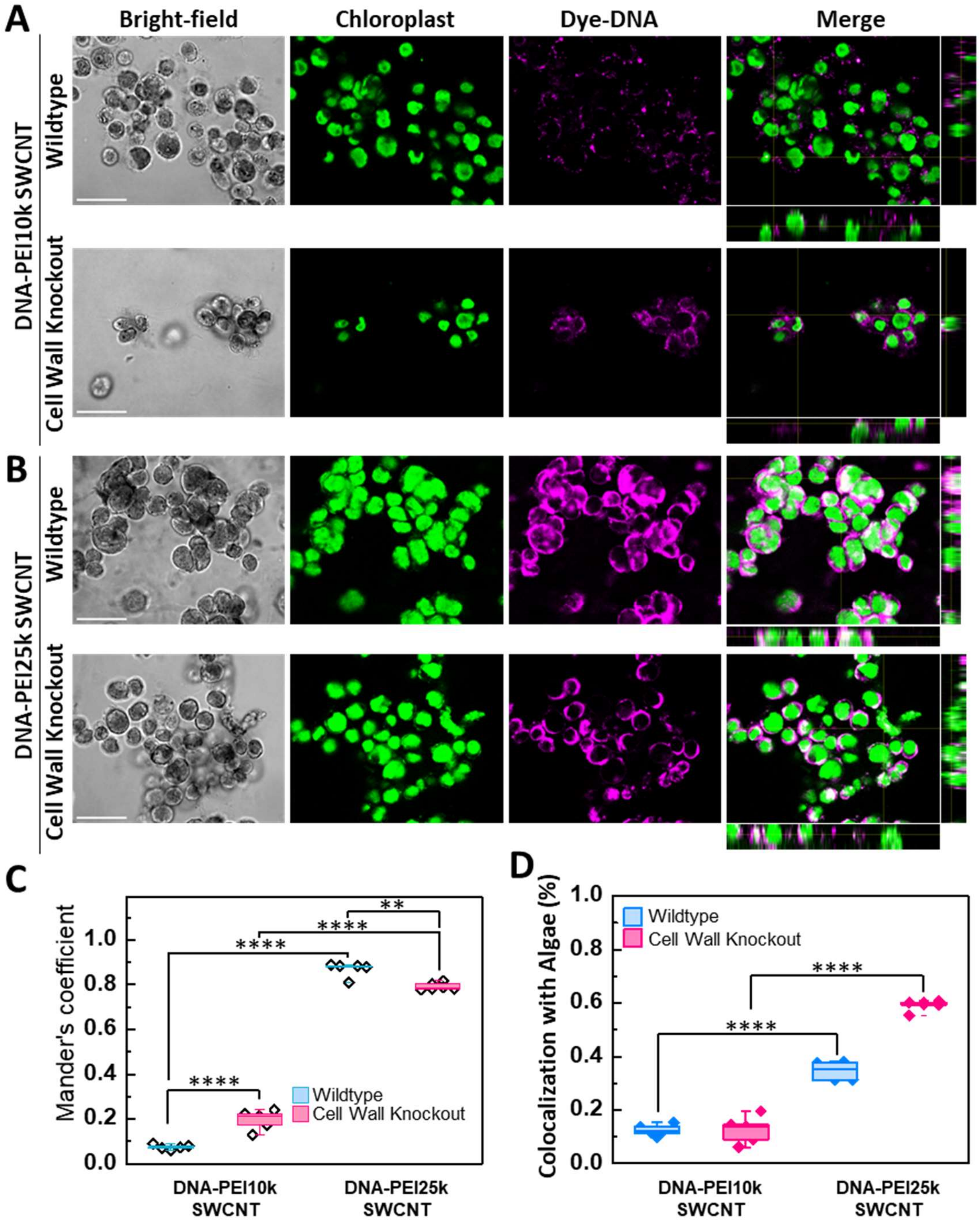
A
Bright-field
Chloroplast
Dye-DNA
Merge
DNA-PEI10k SWCNT
Wildtype
Cell Wall Knockout
B
DNA-PEI25k SWCNT
Wildtype
Cell Wall Knockout
C
Mander's coefficient
1.0
0.8
0.6
0.4
0.2
0.0
****
**
Wildtype
Cell Wall Knockout
DNA-PEI10k SWCNT
DNA-PEI25k SWCNT
D
Colocalization with Algae (%)
1.0
0.8
0.6
0.4
0.2
0.0
Wildtype
Cell Wall Knockout
****
DNA-PEI10k SWCNT
DNA-PEI25k SWCNT

Figure 4.3. DNA delivery to algal chloroplasts mediated by PEI-SWCNT. Confocal microscopy analysis indicated that **a)** PEI10k-SWCNTs and **b)** PEI25k-SWCNTs have distinct capabilities enhancing the delivery of Cy3 dye-labeled ssGT15 DNA (Dye-DNA) (magenta) into chloroplasts (green) of both wild-type and cell-wall knockout algae strains (1 h incubation, 300 fg/cell PEI-SWCNT, 1:1 Dye-DNA:PEI-SWCNT mass ratio). **c)** Population-based analysis of algae using Mander's colocalization coefficient analysis indicated a statistically significant enhancement in the delivery of Dye-DNA to algae chloroplasts when facilitated by PEI25k-SWCNTs compared to PEI10k-SWCNTs. **d)** Algae cell count analysis demonstrated a higher uptake of Dye-DNA when mediated by PEI25k-SWCNTs compared to PEI10k-SWCNTs in both the wild-type (35.22% ± 3.48 vs. 14.60% ± 2.11) and cell-wall knockout strains (59.20 % ± 2.17 vs. 12.56% ± 5.21). **P<0.01, ****P<0.0001; n=5; 1-way ANOVA analysis; box and whisker plot represents the minimum, 25th percentile, median, 75th percentile, and maximum. The scale bar is 20 µm. Overlaps between Dye-DNA and chloroplasts are highlighted in white in the orthogonal views, which represent projections on the z-axis.

Based on the LEEP model we expected the highly charged DNA-PEI25k-SWCNT (~30 mV) to deliver DNA into chloroplasts but not the lower charge (<20 mV) DNA-PEI10k-SWCNT. Both PEI25k and PEI10k SWCNTs are able to translocate and deliver DNA across multiple algae cell barriers including the extracellular matrix, cell wall, cell and organelle lipid membranes into chloroplasts. This indicates that the LEEP model has limitations for determining the delivery of DNA cargoes mediated by SWCNT into algae chloroplasts.(Lew et al., 2018; Wong et al., 2016) Nanomaterial translocation across algae extracellular matrix and cell wall was not tested by the LEEP model developed in plant protoplasts lacking cell walls.(Lew et al., 2018; Wong et al., 2016) Both the algae wildtype and the cell-wall knockout, CC-124 and CC-4533 with *cw15* phenotype, respectively, have a cell wall where the knockout has a highly reduced cell wall. CC-4533 is from a cross between 4A-, whose parental strain was CC-124, and D66+ which produces a *cw15* cell-wall knockout phenotype. (Dent et al., 2005; Schnell & Lefebvre, 1993) Chlamydomonas *cw15* phenotypes are produced from multiple genes and recent research has been unable to identify a genetic locus that produced that specific phenotype. (Gallaher et al., 2015) Entry of nanomaterials through these important algal biological surfaces and the biomolecule coronas that coat the particle thereafter have yet to be included in nanoparticle delivery models.(Newkirk et al., 2021) In addition, there is a significant drop in colocalization after 1 hour of incubation of the highly charged DNA-PEI25k-SWCNTs with the wildtype (Figure S4.6). This is not expected from the LEEP hypothesis that proposes SWCNTs are kinetically trapped within cell lipid membranes after uptake. A possible explanation is that SWCNT is causing reduction in photosynthetic pigments and damage to organelles, as reported previously, (Chen et al., 2019; Du et al., 2016) thus lowering colocalization rates with chloroplast pigments.

Future studies using plasmid DNA or DNA cassettes would allow assessing both delivery and expression of genes into algae chloroplasts mediated by PEI-SWCNTs. It remains to be determined if this study using single-stranded DNA ($ssGT_{15}$) can be extrapolated to understand the delivery of plasmid DNA. A single fully intact molecule of dsDNA is capable of transforming the chloroplast genome, with plasmid DNA being the most compatible.(Bock, 2015) This study demonstrating the delivery of small DNA fragments (30 bp oligonucleotides, 300 fg/cell) across algae cell wall and membrane barriers highlights the potential of PEI-SWCNTs as carriers for plasmid DNA in microalgae. In comparison to our efficiencies for ssDNA delivery with PEI25k-SWCNT (35.22% ± 3.48 in the wildtype and 59.20% ± 2.17 in cell-wall knockout), particle bombardment, the current standard method for chloroplast transformation, has a 0.1-0.3% frequency of cells transiently expressing plasmid DNA after bombardment in cell culture suspensions. (Lacroix & Citovsky, 2020) Another future direction of this research could assist the delivery of RNA by PEI-SWCNTs in algae as it has been demonstrated using gold nanorods in plants.(Zhang et al., 2022)

Effect of DNA-PEI-SWCNT on algae oxidative stress

Reactive oxygen species (ROS), shown previously to be a major contributor of nanomaterial toxicity to algae, were used as a metric to determine oxidative stress levels upon uptake of DNA-PEI-SWCNT. (Chen et al., 2019; Fang et al., 2022) The ROS levels were measured by interfacing algae with H_2DCF-DA (2′,7′-dichlorodihydrofluorescein-diacetate), a cell membrane permeable chemical that is cleaved by cellular esterases forming H_2DCF. The oxidation of H_2DCF by ROS in algae cells yields DCF (2′,7′-dichlorofluorescein). Wildtype algae experienced a significant increase in ROS levels within 2-hour exposure to 300 and 3000 fg/cell of DNA-PEI10k-SWCNTs ($P<0.005$, 2-way ANOVA). The ROS were maintained at similar levels to the control during the 3 hours exposure to the 30 fg/cell of DNA-PEI10k-SWCNTs treatment. In contrast, the 300 and 3000 fg/cell DNA-PEI10k-SWCNT treatment exhibited a significant increase in ROS levels that was followed by a steady decline over time ($P^{****}<0.0001$, 2-way ANOVA) (Figure 4.4a). The DNA-PEI25k-SWCNTs showed a similar trend but with ROS levels increasing for the 30 fg/cell after 2 hr exposure and at a concentration of 3000 fg/cell after 1 hour, followed by a subsequent decline over time (Figure 4.4b). The cell wall knockout strain had higher ROS generation levels than the wildtype and followed a similar trend of peaking ROS levels at 1 hour for both the PEI10k- and PEI25k-SWCNTs (300, and 3000 fg/cell), then declining ROS levels afterwards ($P^{****}<0.0001$, 2-way ANOVA) (Figure 4.4c,d). After 4 days, it was found that the cell wall knockout and wildtype strains had a statistically significant decrease in ROS with both the 300 fg/cell and 3000 fg/cell DNA-PEI10k-SWCNT and DNA-PEI25k-SWCNT ($P^{***}<0.001$, $P^{****}<0.0001$, respectively, 2-way ANOVA) (Figure 4.4a,b). The larger increase in ROS levels in the cell wall knockout strain could be due to higher uptake of DNA-PEI-SWCNT compared to the wild type counterpart. Taken together, transient ROS levels increased after a 1 hour exposure of DNA-PEI-SWCNT but decreased over time, eventually leading to similar values as the negative controls.

The decline in ROS after exposure to DNA-PEI-SWCNT could be the result of ROS reaction with antioxidants or other biomolecules in algae cells upon increase in oxidative stress.(Chen et al., 2019) Glutathione is an antioxidant within algae cells that has been shown to be an important marker for toxicity screening and oxidative stress.(Almeida et al., 2017; Machado & Soares, 2012; Stoiber et al., 2007) Intracellular reduced glutathione (GSH) is seen as a sensitive indicator of healthy cells and lower levels of GSH can be interpreted as decreased cell health due to reaction with ROS. Monochlorobimane (mBCl) is a non-fluorescing cell permeable dye that reacts with intracellular GSH to become fluorescent bimane–glutathione.(Machado & Soares, 2012) After exposure to DNA-PEI10k-SWCNT and DNA-PEI25k-SWCNT, both wildtype and cell-wall knockout strains showed decreases in intracellular GSH (Figure S10; $P<0.0001$), an indicator that GSH was used to mitigate the impact of ROS in algae cells due to nanomaterial exposure.

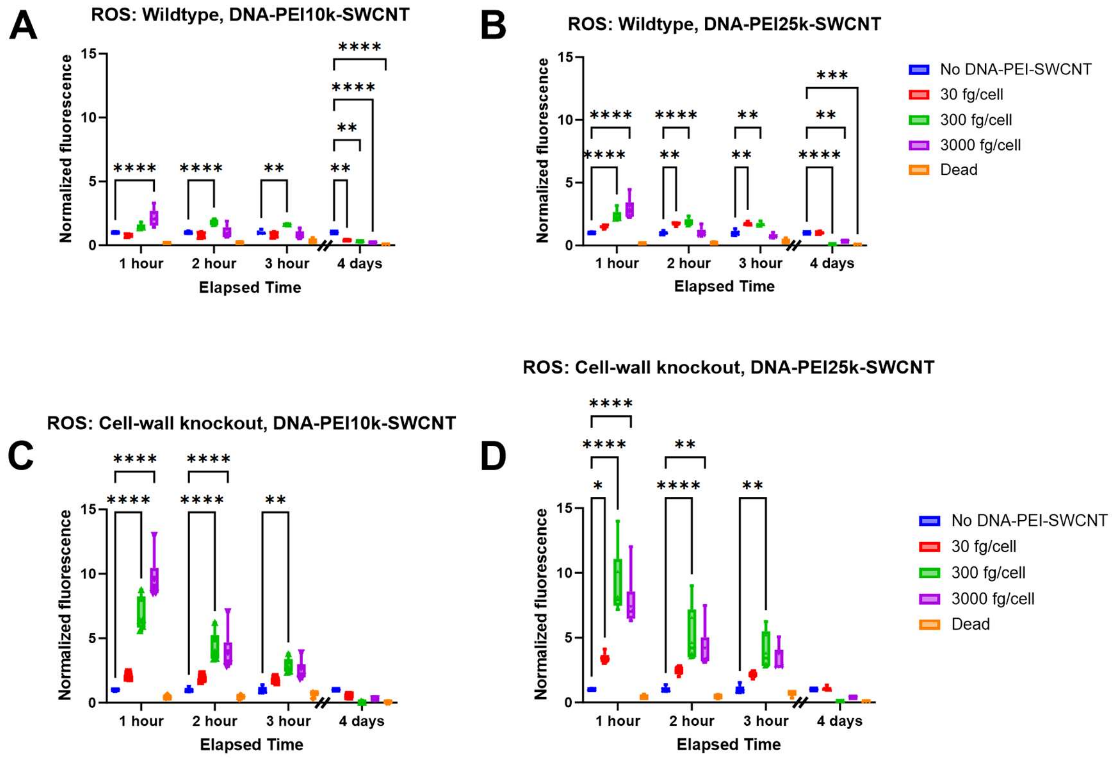

Figure 4.4. Transient increase in reactive oxygen species (ROS) in *C. reinhardtii* exposed to DNA-PEI-SWCNT. a,b) ROS produced by the wildtype strain peaked with both the DNA-PEI10k-SWCNTs and DNA-PEI25k-SWNTs (3000 fg/cell) at 1 hour and subsequently decreased over time (P****<0.0001, 2-way ANOVA). **c,d)** The cell wall knockout generated higher ROS than the wildtype algae but followed the same trend of peaking at 1 hour, then decreasing for DNA-PEI10k-SWCNTs and DNA-PEI25k-SWCNTs at 30, 300, and 3000 fg/cell (P****<0.0001, P**<0.001, 2-way ANOVA). All samples were normalized to algae-only living cell controls and were done in biological and technical triplicate (N = 3, box and whisker plot represents the minimum, 25th percentile, median, 75th percentile, and maximum).

To elucidate the effect of nanomaterial induced ROS generation on lipid membranes, a lipophilic fluorescent dye with a polyunsaturated butadienyl portion, BODIPY™ C11 undecanoic acid, was exposed to the wildtype and cell-wall knockout strains as a lipid peroxidation assay.(Cheloni & Slaveykova, 2013; Martín-de-Lucía et al., 2018) Both PEI10k and PEI25k coatings (300 fg/cell and 1:1 DNA:PEI-SWCNT ratio by mass) produced statistically significant increases in lipid peroxidation in the wildtype and cell wall knockout strains in as little as one hour (Figure S4.11). This lipid peroxidation assay indicates that ROS generated by the DNA-PEI-SWCNT damage lipid membranes compromising their integrity.

Effect of DNA-PEI-SWCNT on algae viability

For a population-based phenotypic assessment of the DNA-PEI-SWCNT impact on *Chlamydomonas reinhardtii* viability, we measured live cell viability staining, chlorophyll *a* and *b*, total carotenoids, and *in vivo* chlorophyll concentrations.(Gomes et al., 2017; Haire et al., 2018; Nguyen et al., 2018; Terashima et al., 2015) Fluorescein diacetate (FDA) was used as a fluorescence-based population-level viability indicator due to its wide use in *C. reinhardtii* research. (Haire et al., 2018) When exposed to the highest concentration of 3000 fg/cell DNA-PEI10k-SWCNTs or DNA-PEI25k-SWCNTs, the wildtype cell's viability dropped significantly over 2 and 3 hr ($P^{****} < 0.0001$, 2-way ANOVA) (Figure 4.5a-b). The cell wall knockout showed a significant decrease in viability at lower concentrations of DNA-PEI SWCNT than the wildtype strain, after being exposed to 30 fg/cell DNA-PEI10k-SWCNTs over 1 and 2 hours (P****<0.0001, 2-way ANOVA) (Figure 4.5c-d). Interestingly, wildtype strain exposure to both DNA-PEI10k-SWCNTs and DNA-PEI25k-SWCNTs resulted in a significant increase in FDA emission at 300 fg/cell starting at 1 hour (P**<0.001, P****<0.0001, respectively, 2-way ANOVA)(Figure 4.5a-b). Increasing concentrations of either DNA-PEI10k-SWCNTs or DNA-PEI25k-SWCNTs in the cell wall knockout also led to higher FDA emission levels than algae controls without nanomaterials. The DNA-PEI-SWCNTs may be facilitating the entry of other molecules besides the DNA cargoes into algae cells, causing higher FDA entry than algae-only samples. This may explain why there is higher FDA emissions from algae exposed to some concentrations of DNA-PEI10k-SWCNTs and DNA-PEI25k-SWCNTs. This population-based FDA analysis also indicates a range of biocompatible concentrations (30-300 fg/cell) of highly charged PEI25k-SWCNT carrier for DNA delivery and the ability for the cell wall of algae to reduce the impact of DNA-PEI-SWCNT on algae viability.

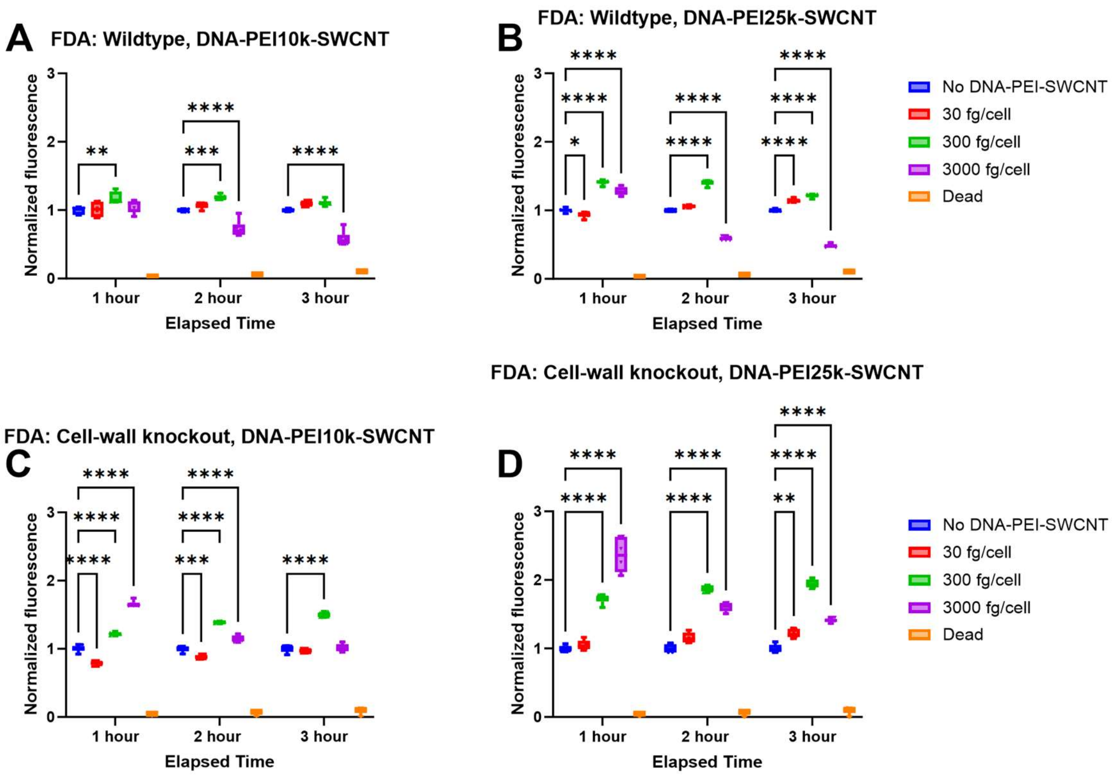

Figure 4.5. Algae population-based DNA-PEI-SWCNT viability assay for algae with and without a cell wall. a,b) Wildtype algae with cell wall showed decreased viability with DNA-PEI10k-SWCNTs and DNA-PEI25k-SWCNTs at 3000 fg/cell over 2 to 3 hours (P****<0.0001, 2-way ANOVA). **c,d)** The cell wall knockout strain exhibited increases in FDA emission after exposure to DNA-PEI10k-SWCNTs and DNA-PEI25k-SWCNTs at concentrations of 300 and 3000 fg/cell after 1 hour and 2 hours (P****<0.0001, P=0.0998, respectively, 2-way ANOVA). All samples were normalized to algae-only living cell controls and were done in biological and technical triplicate, and no DNA-PEI-SWCNT algae-only wells were used for normalization (N = 3, box and whisker plot represents the minimum, 25th percentile, median, 75th percentile, and maximum).

Photosynthetic pigments of chlorophyll and carotenoids are parameters that assess changes in algal phenotype and photosynthesis. (Eullaffroy & Vernet, 2003) The wildtype's chlorophyll *a* content dropped significantly with DNA-PEI10k-SWCNT at a concentration of 3000 fg/cell ($P^* < 0.05$, 2-way ANOVA) but the cell wall knockout was not affected (Figure 6a). At 3000 fg/cell DNA-PEI25k-SWCNT, both the wildtype and cell wall knockout showed a significant decrease in the chlorophyll *a* compared to the algae-only control ($P^{**} < 0.001$, 2-way ANOVA)(Figure 6b). The DNA-PEI10k-SWCNT caused no significant decreases in chlorophyll *b* levels for both the wildtype and cell wall knockout strain (Figure 6c). However, both strains had no detectable chlorophyll *b* levels at 3000 fg/cell of DNA-PEI25k-SWCNT due to dead cells. A significant decrease between the 300 fg/cell of DNA-PEI25k-SWCNT and wildtype algae only controls was also observed ($P^{***} = 0.0001$, 2-way ANOVA)(Figure 6d). No significant differences in total carotenoids of the algal cell were observed ($P > 0.9$, 2-way ANOVA) in wildtype and cell wall knockout strains with DNA-PEI10k-SWCNT relative to controls without nanomaterials (Figure 6e-f). However, wildtype and cell wall knockout algae exposed to DNA-PEI25k-SWCNTs at 3000 fg/cell showed significant differences in total carotenoids relative to algae-only controls ($P^* < 0.003$ for the cell wall knockout, $P^{****} < 0.0001$ for the wildtype, 2-way ANOVA). Overall, both DNA-PEI10k-SWCNTs and DNA-PEI25k-SWCNTs reduced chlorophyll pigments at 3000 fg/cell but DNA-PEI25k-SWCNTs had a larger impact on carotenoids than DNA-PEI10k-SWCNTs in a dose dependent manner. Based on both i*n vivo* chlorophyll and carotenoid content analysis over multiple days, 300 fg/cell of PEI10k-SWCNTs and 30 fg/cell of PEI25k-

SWCNTs were deemed biocompatible with algal cultures. Previously, SWCNT directly coated with salmon testes genomic DNA by Π-stacking interactions at 1:1 mass ratio concentration were shown to be biocompatible with *Chlamydomonas reinhardtii* wild-type strain (cc-1690) at concentrations from 0.1 to 100 μg/mL through growth curves and extracted chlorophyll *a* and *b*. (Williams et al., 2014) SWCNT have also been shown to protect against *Chlamydomonas reinhardtii* photosynthetic PSII inactivations and higher rates of photosynthetic electron transport. (Antal et al., 2022)

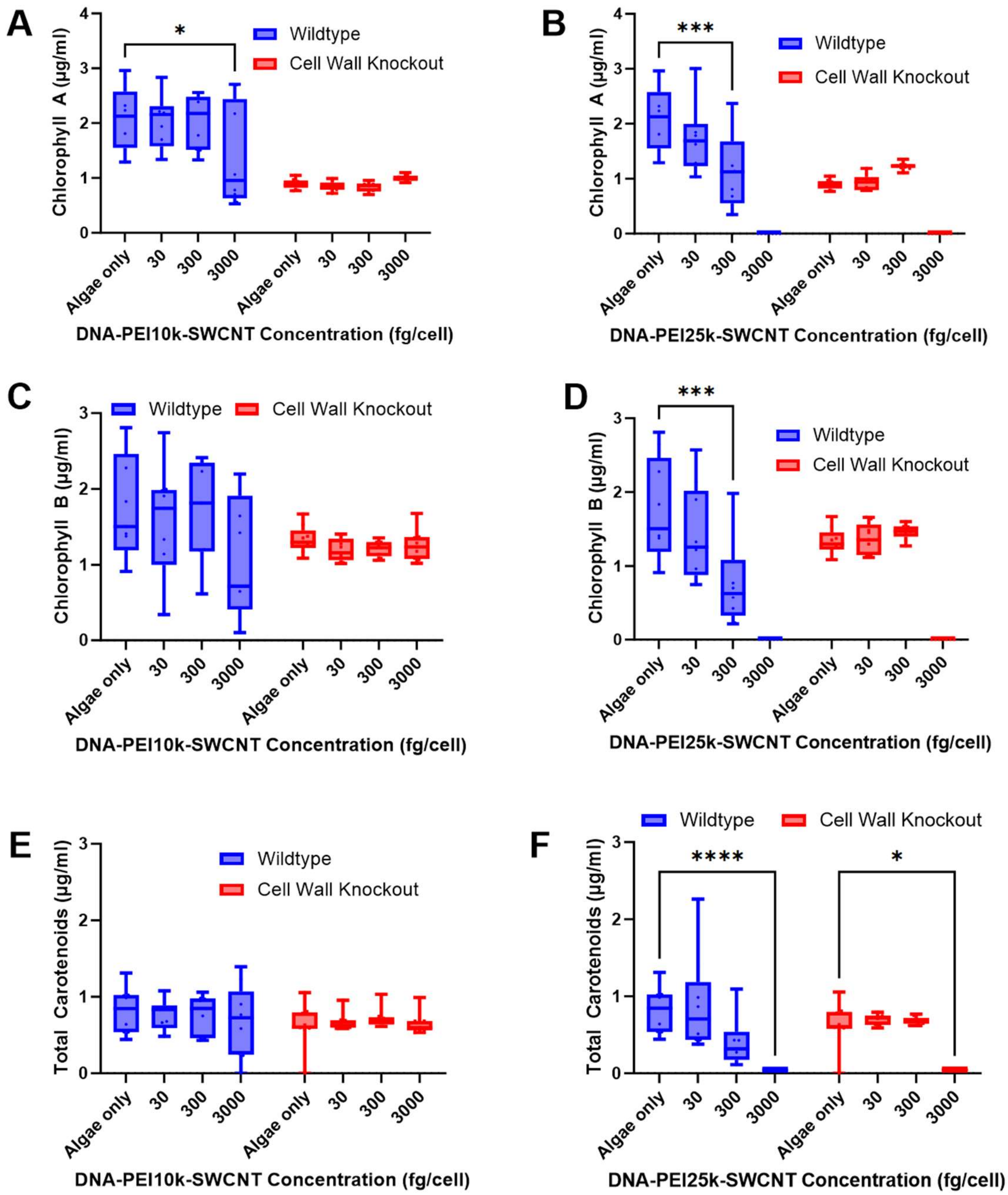
A
Wildtype
Cell Wall Knockout
Chlorophyll A (μg/ml)
Algae only
30
300
3000
DNA-PEI10k-SWCNT Concentration (fg/cell)
B
Chlorophyll A (μg/ml)
DNA-PEI25k-SWCNT Concentration (fg/cell)
C
Chlorophyll B (μg/ml)
DNA-PEI10k-SWCNT Concentration (fg/cell)
D
Chlorophyll B (μg/ml)
DNA-PEI25k-SWCNT Concentration (fg/cell)
E
Total Carotenoids (μg/ml)
DNA-PEI10k-SWCNT Concentration (fg/cell)
F
Total Carotenoids (μg/ml)
DNA-PEI25k-SWCNT Concentration (fg/cell)

Figure 4.6. *In vivo* photopigment concentrations for determining biocompatibility of DNA-PEI-SWCNT. Wildtype (CC-124) and the cell-wall knockout strain (CC-4533) were exposed to 1:1 DNA:PEI-SWCNT in microplates under continuous 100 PAR lighting for 4 days. **a)** DNA-PEI10k-SWCNT caused a decrease in chlorophyll *a* in wildtype algae at 3000 fg/cell (*P<0.05) while showing no significant differences in the cell wall knockout. **b**) The wildtype strain showed a reduction in chlorophyll *a* relative to algae-only control at 300 fg/cell DNA-PEI25k-SWCNT (***P<0.005). **c)** No statistically significant difference in chlorophyll *b* was found between the wildtype or cell wall knockout algae when exposed to DNA-PEI10k-SWCNT (P>0.9, 2-way ANOVA). **d**) At 300 fg/cell, DNA-PEI25k-SWCNT showed a statistically significant decrease in chlorophyll *b* (P***=0.0001, 2-way ANOVA) compared to the algae-only control for the wildtype strain, but both strains had no living cells for measurement at 3000 fg/cell, **e)** No differences in total carotenoids were observed after algae exposure to DNA-PEI10k-SWCNTs at different concentrations. **f)** In contrast, wildtype (****P<0.0001) and cell wall knockout (**P<0.003) experienced a decline in total carotenoid content at 3000 fg/cell DNA-PEI25k-SWCNT. Biological triplicates were performed in technical triplicates and assessed with a 2-way ANOVA analysis; box and whisker plot represents the minimum, 25th percentile, median, 75th percentile, and maximum.

Overall, population-based assays of ROS for oxidative stress, FDA for living cells, and *in vivo* chlorophyll content all pointed to 300 fg/cell of DNA-PEI10k-SWCNT and 30 fg/cell of DNA-PEI25k-SWCNT being the concentrations that were deemed to be biocompatible with algal cultures. This study demonstrates that algae are able to survive upon exposure to nanomaterials (PEI-SWCNT) capable of delivering a biomolecule (DNA). The ROS, FDA and chlorophyll level analyses in combination with the glutathione and lipid peroxidation assays indicate that DNA-PEI-SWCNT mechanism of toxicity is increased oxidative stress and disruption of lipid membranes as they translocate into cell and chloroplast membranes.

Conclusions

This study demonstrates the application of engineered high aspect ratio nanomaterials for biomolecule delivery into algal chloroplasts. We showcased how the molecular weight of the PEI coating for SWCNTs impacts uptake into algae with and without a cell wall. In wild-type algae, the highly charged PEI25k-SWCNT showed higher potential for DNA delivery as evidenced by the higher colocalization rates of Dye-DNA with chloroplasts. We also identified biocompatible exposure conditions for delivery of DNA into *Chlamydomonas reinhardtii*. More than 300 fg/cell of the higher charged PEI25k-SWCNT showed higher lethality through the FDA cell viability assay, higher oxidative stress through the ROS assay, and no biocompatibility through the carotenoid assay. The biocompatibility assay for ROS showed lower generation for the wildtype algae with a cell wall, while the cell-wall knockout algae had higher oxidative stress levels for both PEI10k- and PEI25k-SWCNTs. This highlights the role of the cell wall as a barrier for delivery of nanomaterials with biomolecule cargoes. The PEI-SWCNT mediated delivery of DNA into wildtype cells may lead to new opportunities for plasmid DNA delivery into chloroplasts.

This research into the intersection of nanotechnology and algae biotechnology opens new roads into biomolecule delivery and bioreactor productivity. Future research applications for PEI-coated SWCNTs could include coating with biorecognition peptide sequences for improved localization into chloroplasts. (Santana et al., 2020) Biomolecule delivery of genetic elements to algal chloroplasts can also enable the transient expression of genetic biosensors or synthetic riboswitches. (Mehrshahi et al., 2020) With one of the major bottlenecks of algae chloroplast transformation being DNA delivery efficiency and stable integration into chloroplasts, nanomaterial-mediated delivery could yield a higher number of genetic library mutants to be screened than current standard methods. (Wang et al., 2019) Taken together, these nanotechnology-based advancements in *Chlamydomonas* may also translate to other biofuel research-focused algae species. *Scenedesmus, Monoraphidium*, and *Pichoclorum* have been proposed as strong candidates for algae biofuel production. Nanotechnology approaches are providing tools for improving native photosynthetic performance, stress and health monitoring, and ROS as previously demonstrated in land plants.(Giraldo et al., 2014, 2019; Liu et al., 2020; Wu et al., 2018, 2020)

Materials and Methods

Algae Strain Culturing

Chlamydomonas reinhardtii wildtype strain, CC-124 and cell wall knockout strain, CC-4533 were ordered from the University of Minnesota Chlamy Center. All media contains Kropat's Trace Element mixture and TAP was used for liquid and solid culturing (Kropat et al., 2011). TAP plates supplemented with yeast extract at 4 g/L were used throughout to test for bacterial and yeast contamination. For strain maintenance, algae were grown with Bacto Agar (Cat#214010) at a 1.5% concentration under 50 μE 4K dimmable LED light conditions; a Walz ULM-500 was used to measure light intensity. For liquid culture, an orbital shaker (Cat#89032-100) at room temperature, with 150 rpm under a 100 PAR light with 24-hour photoperiod and Flytianmy drawer dividers were used to organize the shake flasks. All flasks were 50 mL Erlenmeyer flasks with Chemglass silicone sponge closure. Flasks and sponge closures were sterilized by autoclaving before the addition of TAP liquid media, and a second sterilization step of 121ºC for 20 minutes was performed to sterilize the TAP media.

Preparation of SWCNT with PEI and DNA Coating

All SWCNT preparation and PEI reaction steps are followed by previous studies unless otherwise noted (Demirer, Zhang, Goh, et al., 2019; Demirer, Zhang, Matos, et al., 2019). An in-depth protocol reference is available with applicable troubleshooting steps (Demirer, Zhang, Goh, et al., 2019). A solution of COOH-SWCNT is made with 30 mg of dry COOH-SWCNT (Cat# 652490-250MG) and 30 mL molecular quality water

(VWR, Cat# VWRL0201-0500), followed by 10-minute bath sonication. Once finished, samples were tip sonicated at 90% amplitude with the ThermoFisher (Model# FB120) and 6-mm probe tip (Model# CL-18) at ~30 W for 30-minutes in an ice bath. Mixtures were cooled for 10 minutes before ultracentrifugation (Beckman L8-60M) at 18,000 g for 1 hour at 20˚C. A pipette was used to remove the supernatant, carefully not disturbing the pellet, and leaving liquid at the bottom so as to not bring any clumped nanotubes into the next reaction. Using Beer-Lambert's Law ($A = C * E * L$) and a 1:10 dilution in water, the concentration of COOH-SWCNT was calculated using the absorbance value at 632 nm where $E = 0.036$ L/cm*mg and $L = 1$ cm. Typical concentration ranges are around 175 ± 25 mg/L. This solution can be stored for a month at room temperature.

AMES buffer solution was first prepared prior to reaction (500 mM, pH 4.5-5) . Next, a COOH-SWCNT solution was diluted to 100 mg/L. Then, 20 mL of the 100 mg/L COOH-SWCNT solution to a 50 mL conical tube for a final amount of 2 mg and 5 mL of the MES buffer was added to yield a 100 mM final concentration. Solution pH was then adjusted to be between 4.5 to 6 using HCl or NaOH as necessary. In a separate tube, 10 mg EDC and 10 mg NHS were added to 500 uL of 500 mM and 2 mL of molecular quality water and dissolved completely. EDC-NHS solutions were added dropwise to the COOH-SWCNT suspension while stirring, then bath sonicated for 15 minutes and placed on a 150 rpm orbital shaker for 45 minutes. Two 50 mL centrifugal 100,000-MWCO filters (Cat# UFC910024) were pre-washed with 15 mL of 0.1x PBS at 4,000g for 1 minute at room temperature.The COOH-SWCNT solution was then split between the two 50 mL centrifuge tubes and centrifuged at 300g for 8 min at 21˚C. Flow-through was discarded and volume was raised back up to the 50 mL line with 0.1x PBS. Solutions were briefly vortexed, and centrifuged again. This wash step was repeated two additional times to remove excess EDC and NHS. Both filtered solutions were then added to the same tube and filled to 20 mL before MES addition. This solution was bath sonicated for 15 minutes. In a new tube, 40 mg of PEI (PEI10k, Alfa Aesar Cat# 40331; PEI25k Sigma-Aldrich Cat# 408727-100ML) was added to a 15 mL conical tube and fully dissolved with 5 mL of 0.1x PBS. Solution's pH was then adjusted between 7.4 to 7.6. Lastly, activated COOH-SWCNT was added to the PEI solution in a dropwise manner while stirring. Reaction solution pH was then adjusted to between 7 and 8. The reaction solution was then placed on an orbital shaker at 150 rpm for 16 hours.

Two 100,000-MWCO 50 mL centrifugal filter tubes were washed with 15 mL nuclease-free water at maximum speed for 2 minutes. The PEI-SWCNT reaction mixture was split into both tubes, and centrifuged at 1,000g for 15 min at 21˚C. The flow-through was discarded, and the liquid level was brought back up to 15 mL with water, briefly vortexed, and centrifuged again. This wash was repeated 5 additional times. The liquid level was brought up to the previous level (20 mL as previously described). The solution was bath sonicated for 15-minutes, then tip sonicated for 15-minutes with a 6-mm tip in an ice bath at ~30% W, or 90% amplitude for 15 minutes; ice was replaced halfway through this tip sonication. The solution was centrifuged at 18,000 rpm in an ultracentrifuge for 1-hour at room temperature, and pipetted off to not disturb the pellet. The solution was centrifuged with the same parameters two additional times to remove large PEI-SWCNT bundles. Beer-Lambert's Law was then used to calculate the concentration and continue to characterize this PEI-SWCNT solution. The solution can be kept at 4˚C for 1 month.

Coating GT_{15} and Cy3-GT_{15} onto the PEI-SWCNT was done by adding the corresponding concentration of DNA to the microcentrifuge tube first, adding the PEI-SWCNT dropwise, and finally pipetting up and down ten times. The binding reaction was allowed to go on at room temperature for 30 minutes before proceeding and being used.

Characterization of PEI-SWCNT and DNA-PEI-SWCNT

Characterization of the nanomaterials was done immediately after preparation. The nanomaterials can be used experimentally within 30 days if kept at 4 °C. All PEI10k- and PEI25k- were diluted to 30 ng/uL and buffered with 10 mM TE final concentration for zeta potential, gel electrophoresis, and AFM measurements.

Beer-Lambert's Law was used to determine the concentration of SWCNT solution, using a spectrophotometer at 632 nm with a 1:10 dilution, where E = 0.036 L/cm*mg and L = 1 cm. A Malvern Nano-S was used for the zeta potential measurements with a specialized folded capillary cell (Model# DTS1070). All measurements were taken with a final concentration of 100 mM Tris-EDTA buffer. Twelve technical replicates were performed for each sample and the Henry model was used to measure zeta potential and pH measured between 7.4 to 7.5.

Standard gel electrophoresis was performed with 1% TBE gel, SYBR Safe (Cat# S33102), and Invitrogen 1 kb Plus DNA Ladder (Cat#10787018) for Dye-DNA binding assays to PEI-SWCNT. A 60 minute room temperature binding reaction was performed before adding DNA Gel Loading Dye (Cat#R0611) and running of the gel electrophoresis. Analysis of the bands for DNA binding efficiency was performed by GelAnalyzer 19.1.

AFM images of COOH-SWCNTs, and PEI-coated SWCNTs with and without DNA were collected by using a tapping mode with NanoScope 5000C-1 and analyzed with Gwyddion software. A total of 50 individual particles were measured for each sample type. DNA:PEI-SWCNT was bound at a mass ratio of 1:1, pipetted up and down ten times, and then incubated at room temperature for 30 minutes. The 15 uL mixture was then pipetted onto a silica wafer and let to dry at room temperature. The silica wafer was rinsed with distilled water three times, and dried at room temperature for 30 min before AFM measurements.

Dye-DNA-PEI-SWCNT Confocal Microscopy

The PEI-SWCNT solution was first bath sonicated in an Elmasonic P at 37 Hz for 30 minutes to disperse any bundles. Cy3-GT_{15} (Dye-DNA) was ordered and synthesized by IDT and then bound to PEI-SWCNTs at the appropriate mass ratio by adding the PEI-SWCNTs to the Dye-DNA dropwise, to reduce aggregation, and then pipetted up and down 10 times; this was performed at room temperature for 30 min. A liquid algae culture midway through exponential growth was then measured using OD_{550}. All experiments are done at an OD_{550} of 0.5. After the Dye-DNA has been bound to the PEI-SWCNT, algae are then added to the Dye-DNA-PEI-SWCNT solution dropwise in 1.7

mL tubes, and then pipetted up and down ten times. Wrap the tubes in foil to prevent any bleaching and put on an orbital shaker set to 150 rpm for the appropriate exposure time to be tested. Algae was then pelleted at 4000 g for 10 minutes and the supernatant was pipetted off, leaving around 10 µl. Pellet was then resuspended by gently pipetting up and down.

Algae samples were fixed on glass slides for confocal analysis using agarose pads (1%). In brief, 10 µl of room temperature chilled 1% agarose solution was mixed with 10 µl of algae pellet and was mixed by pipetting up and down. Mixture was then dispensed on a microscopy slide and covered using a cover slip. To fix the slide for long-term exposure experiments, nail polish was applied via pipette at the end to seal the sides and prevent evaporation.

On an inverted Zeiss 880 confocal microscope, 2 µm slices and 199 µm pinhole were used with a Cy3-DNA channel exciting with 2% of 514 nm laser and catching the emission from 538-589 nm. Additionally, a chloroplast autofluorescence channel exciting with 2% of 594 nm laser and emission range from 599-690 nm was simultaneously used. 200x was used to capture population-based images, captured in five random places on the slide for statistical significance. 1000x magnification was used to capture the z-stack analyses for confirmation at the organelle-level.

To calculate the thresholded Mander's coefficients for Dye-DNA delivered within chloroplasts in algae, we analyzed the overlap between chloroplast and Dye-DNA pixels using Fiji-ImageJ software. This coefficient was derived from the ratio of chloroplast pixels that colocalized with Dye-DNA to the total number of chloroplast pixels The signal threshold for Dye-DNA (15 for wildtype and 7 for cell-wall knockout strain) and chloroplast (27 for wildtype and 34 for cell-wall knockout strain) were set based on pixel values from algae samples without Dye-DNA within a pixel value range of 0-255. This method provided us with a more precise quantification of the Dye-DNA's location both within the chloroplast and throughout the algae.

Algal PEI-SWCNT *In Vivo* Biocompatibility Assays

A standard mass of DNA-PEI-SWCNT per algae cell (30 to 3000 fg/cell) was used with a concentration of DNA (1:1 ratio, ng/µL), PEI-SWCNT (5 ng/µL), and concentration of algae (OD_{550} = 0.100 = 1.49 x10^6 cells/mL) across assays. (Haire et al., 2018) The algae culture within a 96-well plate completes their growth curve at 4 days and enters into the death phase of the culture thereafter. Therefore, biocompatibility assays were performed for up to 4 days of algae culture growth.

Population-based biocompatibility analysis for *Chlamydomonas* and DNA-PEI-SWCNT was performed with black opaque 96-well plates using fluorescein diacetate (FDA, Cat# F1303; ex: 493 nm, em: 523 nm) final concentration 2.4 µM (1µg/mL). After the 48-hour culture, samples were incubated in the dark for 30 minutes before sampling. Negative controls for cell viability were made by heating samples in a PCR machine for 45 minutes at 90˚C. Percent viability was calculated and OD_{550} was taken for cells/mL. In addition, 2′,7′-dichlorodihydrofluorescein diacetate (H$_2$DCFDA, Cat# D399; ex: 493 nm, em: 523 nm) at a final concentration of 100 μM (48.73 μg/mL) was used to measure the presence of ROS produced from the exposure to DNA-PEI-SWCNTs.

FDA diffuses across the cell membrane of the algae, and if the cell is alive, cytoplasmic esterases cleave FDA to produce anionic fluorescein, becoming excitable and capturable by a plate reader at a specific emission wavelength (λ_{ex} = 475 nm, λ_{em} = 535 nm). PEI-SWCNT was bound to GT_{15} DNA oligonucleotides without a fluorophore for these measurements, with the same room temperature binding reaction. The following plate reader-based culturing and *in vivo* phenotypic screens were adapted from Haire and colleagues (Haire et al., 2018). Using the cells/mL polynomial, cells/ml polynomial =(216944)+(8483581*(OD550))+(46233132*(OD550^2))+(-36516574*(OD550^3)), cells were diluted to OD550 = 0.01 (~3x10^5 cells/mL). These cultures were then grown with 96-well plates at 200 μL for 48 hours under 50 PAR of continuous light on an orbital shaker at 150 rpm. All readings were taken on a Tecan Infinite M Plex with the following settings: 25 flashes, 16 square readings per plate, and 30 seconds of orbital shaking between rounds of readings with a 2 μm radius.

Using clear plates and the above culturing methods, photosynthetic photopigment analysis was performed to assess the impact of DNA-PEI-SWCNTs. After the 48-hour period, *in vivo* carotenoid concentrations were measured spectrophotometrically at 470, 550, 650, 680, and 750 nm (for cells/mL).

The acetone-based chlorophyll extraction was used by Lichtenthaler and colleagues. (Haire et al., 2018; Lichtenthaler, 1987) The formula for Chlorophyll *a* was used: ChlA (μg/ml) = 12.25(A663)–2.79(A647); Chlorophyll *b*: ChlB (μg/ml) = 21.5(A647)–5.1(A663); and finally total carotenoid = [1000(A470)–1.82(ChlA)–85.02(ChlB)]/198.

Monochlorobimane (mBCl; Cat#: M1381MP; stock 50 mM in DMSO) was used to detect changes in intracellular reduced GSH levels and was added at a final concentration of 50 μM to both strains after 1 hour exposure to 300 fg/cell DNA-PEI-SWCNT in TAP buffer - in a 1:1 DNA:PEI-SWCNT mass ratio - then left to incubate in the dark while shaking for 1.5 hours. A black 96-well plate was used to record fluorescent bimane–glutathione (λ_{ex}: 405 nm, λ_{em}: 486 nm) on a plate reader (Tecan Infinite M Plex).

BODIPY™ 581/591 C11 undecanoic acid, 4,4-difluoro-5-(4-phenyl-1,3-butadienyl)-4-bora-3a,4a-diaza-s-indacene-3-undecanoic acid (Cat# D3861; λ_{ex}: 488 nm, λ_{em}: 510 nm; 50 mM stock solution diluted in DMSO), was used at a final concentration of 2 μg mL−1 to evaluate lipid peroxidation due to being oxidized by peroxyl radicals, which can be detected after excitation at 488 nm and an emission peak shift from 590 to 510 nm. PEI10k- and PEI25k-SWCNT was bound to DNA in a 1:1 ratio by mass, exposed to both strains at 300 fg/cell in TAP buffer, and measured in a plate reader with a black 96-well plate (Tecan Infinite M Plex).

Conflict of Interest

The authors declare that the research was conducted in the absence of any commercial or financial relationships that could be construed as a potential conflict of interest.

Author Contributions

G.M.N, J.P.G and R.E.J. conceived the idea and designed the experiments. G.M.N. performed most experiments including synthesis of nanomaterials, DNA delivery, ROS, FDA, and chloroplast pigment analysis. H.K. S.J. and C.C. performed nanoparticle characterizations and colocalization analysis. S.S. assisted biocompatibility assays and P.D.A. with confocal microscopy measurements. All authors contributed to writing the manuscript.

Funding

G.M.N. was supported by a fellowship by the Department of Defense National Science and Engineering Graduate Fellowship Program. This work was supported by the National Science Foundation under the Center for Sustainable Nanotechnology, CHE-2001611. The CSN is part of the Centers for Chemical Innovation Program. The authors are also grateful for funding from Frank G. and Janice B. Delfino Agricultural Technology Research Initiative.

Acknowledgments

All figures are made on Biorender.com.

References

Ali, Z., Serag, M. F., Demirer, G. S., Torre, B., di Fabrizio, E., Landry, M. P., Habuchi, S., & Mahfouz, M. (2022). DNA–Carbon Nanotube Binding Mode Determines the Efficiency of Carbon Nanotube-Mediated DNA Delivery to Intact Plants. *ACS Applied Nano Materials*, *5*(4), 4663–4676. https://doi.org/10.1021/acsanm.1c03482

Almeida, A. C., Gomes, T., Langford, K., Thomas, K. V., & Tollefsen, K. E. (2017). Oxidative stress in the algae Chlamydomonas reinhardtii exposed to biocides. *Aquatic Toxicology* , *189*, 50–59. https://doi.org/10.1016/j.aquatox.2017.05.014

Antal, T. K., Volgusheva, A. A., Kukarskikh, G. P., Lukashev, E. P., Bulychev, A. A., Margonelli, A., Orlanducci, S., Leo, G., Cerri, L., Tyystjärvi, E., & Lambreva, M. D. (2022). Single-walled carbon nanotubes protect photosynthetic reactions in Chlamydomonas reinhardtii against photoinhibition. *Plant Physiology and Biochemistry: PPB / Societe Francaise de Physiologie Vegetale*, *192*, 298–307. https://doi.org/10.1016/j.plaphy.2022.10.009

Bock, R. (2015). Engineering plastid genomes: methods, tools, and applications in basic research and biotechnology. *Annual Review of Plant Biology*, *66*, 211–241. https://doi.org/10.1146/annurev-arplant-050213-040212

Cheloni, G., & Slaveykova, V. I. (2013). Optimization of the C11-BODIPY(581/591) dye for the determination of lipid oxidation in Chlamydomonas reinhardtii by flow cytometry. *Cytometry. Part A: The Journal of the International Society for Analytical Cytology*, *83*(10), 952–961. https://doi.org/10.1002/cyto.a.22338

Chen, F., Xiao, Z., Yue, L., Wang, J., Feng, Y., Zhu, X., Wang, Z., & Xing, B. (2019). Algae response to engineered nanoparticles: current understanding, mechanisms and implications. *Environmental Science: Nano*, *6*(4), 1026–1042. https://doi.org/10.1039/C8EN01368C

Demirer, G. S., Zhang, H., Goh, N. S., González-Grandío, E., & Landry, M. P. (2019). Carbon nanotube–mediated DNA delivery without transgene integration in intact plants. *Nature Protocols*, *14*(10), 2954–2971. https://doi.org/10.1038/s41596-019-0208-9

Demirer, G. S., Zhang, H., Matos, J. L., Goh, N. S., Cunningham, F. J., Sung, Y., Chang, R., Aditham, A. J., Chio, L., Cho, M.-J., Staskawicz, B., & Landry, M. P. (2019). High aspect ratio nanomaterials enable delivery of functional genetic material without DNA integration in mature plants. *Nature Nanotechnology*. https://doi.org/10.1038/s41565-019-0382-5

Dent, R. M., Haglund, C. M., Chin, B. L., Kobayashi, M. C., & Niyogi, K. K. (2005). Functional genomics of eukaryotic photosynthesis using insertional mutagenesis of Chlamydomonas reinhardtii. *Plant Physiology*, *137*(2), 545–556. https://doi.org/10.1104/pp.104.055244

Du, S., Zhang, P., Zhang, R., Lu, Q., Liu, L., Bao, X., & Liu, H. (2016). Reduced graphene oxide induces cytotoxicity and inhibits photosynthetic performance of the green alga Scenedesmus obliquus. *Chemosphere*, *164*, 499–507. https://doi.org/10.1016/j.chemosphere.2016.08.138

Eullaffroy, P., & Vernet, G. (2003). The F684/F735 chlorophyll fluorescence ratio: a potential tool for rapid detection and determination of herbicide phytotoxicity in algae. *Water Research*, *37*(9), 1983–1990. https://doi.org/10.1016/S0043-1354(02)00621-8

Fang, R., Gong, J., Cao, W., Chen, Z., Huang, D., Ye, J., & Cai, Z. (2022). The combined toxicity and mechanism of multi-walled carbon nanotubes and nano copper oxide toward freshwater algae: Tetradesmus obliquus. *Journal of Environmental Sciences* , *112*, 376–387. https://doi.org/10.1016/j.jes.2021.05.020

Gallaher, S. D., Fitz-Gibbon, S. T., Glaesener, A. G., Pellegrini, M., & Merchant, S. S. (2015). Chlamydomonas Genome Resource for Laboratory Strains Reveals a Mosaic of Sequence Variation, Identifies True Strain Histories, and Enables Strain-Specific Studies. *The Plant Cell*, *27*(9), 2335–2352. https://doi.org/10.1105/tpc.15.00508

Giraldo, J. P., Landry, M. P., Faltermeier, S. M., McNicholas, T. P., Iverson, N. M., Boghossian, A. A., Reuel, N. F., Hilmer, A. J., Sen, F., Brew, J. A., & Strano, M. S. (2014). Plant nanobionics approach to augment photosynthesis and biochemical sensing. *Nature Materials*, *13*(4), 400–408. https://doi.org/10.1038/nmat3890

Giraldo, J. P., Landry, M. P., Kwak, S.-Y., Jain, R. M., Wong, M. H., Iverson, N. M., Ben-Naim, M., & Strano, M. S. (2015). A Ratiometric Sensor Using Single Chirality Near-Infrared Fluorescent Carbon Nanotubes: Application to In Vivo Monitoring. *Small* , *11*(32), 3973–3984. https://doi.org/10.1002/smll.201403276

Giraldo, J. P., Wu, H., Newkirk, G. M., & Kruss, S. (2019). Nanobiotechnology approaches for engineering smart plant sensors. *Nature Nanotechnology*, *14*(6), 541–553. https://doi.org/10.1038/s41565-019-0470-6

Gomes, T., Xie, L., Brede, D., Lind, O.-C., Solhaug, K. A., Salbu, B., & Tollefsen, K. E. (2017). Sensitivity of the green algae Chlamydomonas reinhardtii to gamma radiation: Photosynthetic performance and ROS formation. *Aquatic Toxicology* , *183*, 1–10. https://doi.org/10.1016/J.AQUATOX.2016.12.001

Haire, T. C., Bell, C., Cutshaw, K., Swiger, B., Winkelmann, K., & Palmer, A. G. (2018). Robust Microplate-Based Methods for Culturing and in Vivo Phenotypic Screening of Chlamydomonas reinhardtii. *Frontiers in Plant Science*, *9*, 235. https://doi.org/10.3389/fpls.2018.00235

Iverson, N. M., Barone, P. W., Shandell, M., Trudel, L. J., Sen, S., Sen, F., Ivanov, V., Atolia, E., Farias, E., McNicholas, T. P., Reuel, N., Parry, N. M. a., Wogan, G. N., & Strano, M. S. (2013). In vivo biosensing via tissue-localizable near-infrared-fluorescent single-walled carbon nanotubes. *Nature Nanotechnology*, *8*(11), 873–880. https://doi.org/10.1038/nnano.2013.222

Kropat, J., Hong-Hermesdorf, A., Casero, D., Ent, P., Castruita, M., Pellegrini, M., Merchant, S. S., & Malasarn, D. (2011). A revised mineral nutrient supplement increases biomass and growth rate in Chlamydomonas reinhardtii. *The Plant Journal: For Cell and Molecular Biology*, *66*(5), 770–780. https://doi.org/10.1111/j.1365-313X.2011.04537.x

Kwak, S.-Y., Lew, T. T. S., Sweeney, C. J., Koman, V. B., Wong, M. H., Bohmert-Tatarev, K., Snell, K. D., Seo, J. S., Chua, N.-H., & Strano, M. S. (2019). Chloroplast-selective gene delivery and expression in planta using chitosan-complexed single-walled carbon nanotube carriers. *Nature Nanotechnology*. https://doi.org/10.1038/s41565-019-0375-4

Lacroix, B., & Citovsky, V. (2020). Biolistic Approach for Transient Gene Expression Studies in Plants. In S. Rustgi & H. Luo (Eds.), *Biolistic DNA Delivery in Plants: Methods and Protocols* (pp. 125–139). Springer US. https://doi.org/10.1007/978-1-0716-0356-7_6

Lew, T. T. S., Wong, M. H., Kwak, S.-Y., Sinclair, R., Koman, V. B., & Strano, M. S. (2018). Rational Design Principles for the Transport and Subcellular Distribution of Nanomaterials into Plant Protoplasts. *Small* , e1802086. https://doi.org/10.1002/smll.201802086

Lichtenthaler, H. K. (1987). [34] Chlorophylls and carotenoids: Pigments of photosynthetic biomembranes. In *Methods in Enzymology* (Vol. 148, pp. 350–382). Academic Press. https://doi.org/10.1016/0076-6879(87)48036-1

Liu, T., Xiao, B., Xiang, F., Tan, J., Chen, Z., Zhang, X., Wu, C., Mao, Z., Luo, G., Chen, X., & Deng, J. (2020). Ultrasmall copper-based nanoparticles for reactive oxygen species scavenging and alleviation of inflammation related diseases. *Nature Communications*, *11*(1), 2788. https://doi.org/10.1038/s41467-020-16544-7

Long, Z., Ji, J., Yang, K., Lin, D., & Wu, F. (2012). Systematic and quantitative investigation of the mechanism of carbon nanotubes' toxicity toward algae. *Environmental Science & Technology*, *46*(15), 8458–8466. https://doi.org/10.1021/es301802g

Machado, M. D., & Soares, E. V. (2012). Assessment of cellular reduced glutathione content in Pseudokirchneriella subcapitata using monochlorobimane. *Journal of Applied Phycology*, *24*(6), 1509–1516. https://doi.org/10.1007/s10811-012-9811-7

Maliga, P., & Bock, R. (2011). Plastid biotechnology: food, fuel, and medicine for the 21st century. *Plant Physiology*, *155*(4), 1501–1510. https://doi.org/10.1104/pp.110.170969

Martin-Avila, E., Lim, Y.-L., Birch, R., Dirk, L. M. A., Buck, S., Rhodes, T., Sharwood, R. E., Kapralov, M. V., & Whitney, S. M. (2020). Modifying Plant Photosynthesis and Growth via Simultaneous Chloroplast Transformation of Rubisco Large and Small Subunits. *The Plant Cell*, *32*(9), 2898–2916. https://doi.org/10.1105/tpc.20.00288

Martín-de-Lucía, I., Campos-Mañas, M. C., Agüera, A., Leganés, F., Fernández-Piñas, F., & Rosal, R. (2018). Combined toxicity of graphene oxide and wastewater to the green alga Chlamydomonas reinhardtii. *Environmental Science: Nano*, *5*(7), 1729–1744. https://doi.org/10.1039/C8EN00138C

Mathiot, C., Ponge, P., Gallard, B., Sassi, J.-F., Delrue, F., & Le Moigne, N. (2019). Microalgae starch-based bioplastics: Screening of ten strains and plasticization of unfractionated microalgae by extrusion. *Carbohydrate Polymers*, *208*, 142–151. https://doi.org/10.1016/j.carbpol.2018.12.057

Matorin, D. N., Karateyeva, A. V., Osipov, V. A., Lukashev, E. P., Seifullina, N. K., & Rubin, A. B. (2010). Influence of carbon nanotubes on chlorophyll fluorescence parameters of green algae Chlamydomonas reinhardtii. *Nanotechnologies in Russia*, *5*(5), 320–327. https://doi.org/10.1134/S199507801005006X

Mayfield, S., & Golden, S. S. (2015). Photosynthetic bio-manufacturing: food, fuel, and medicine for the 21st century. *Photosynthesis Research*, *123*(3), 225–226. https://doi.org/10.1007/s11120-014-0063-z

Mehrshahi, P., Nguyen, G. T. D. T., Gorchs Rovira, A., Sayer, A., Llavero-Pasquina, M., Lim Huei Sin, M., Medcalf, E. J., Mendoza-Ochoa, G. I., Scaife, M. A., & Smith, A. G. (2020). Development of Novel Riboswitches for Synthetic Biology in the Green Alga Chlamydomonas. *ACS Synthetic Biology*, *9*(6), 1406–1417. https://doi.org/10.1021/acssynbio.0c00082

Newkirk, G. M., de Allende, P., Jinkerson, R. E., & Giraldo, J. P. (2021). Nanotechnology Approaches for Chloroplast Biotechnology Advancements. *Frontiers in Plant Science*, *12*, 1496. https://doi.org/10.3389/fpls.2021.691295

Nguyen, N. H. A., Padil, V. V. T., Slaveykova, V. I., Černík, M., & Ševců, A. (2018). Green Synthesis of Metal and Metal Oxide Nanoparticles and Their Effect on the Unicellular Alga Chlamydomonas reinhardtii. *Nanoscale Research Letters*, *13*(1), 159. https://doi.org/10.1186/s11671-018-2575-5

Orlanducci, S., Fulgenzi, G., Margonelli, A., Rea, G., Antal, T. K., & Lambreva, M. D. (2020). Mapping Single Walled Carbon Nanotubes in Photosynthetic Algae by Single-Cell Confocal Raman Microscopy. *Materials*, *13*(22). https://doi.org/10.3390/ma13225121

Santana, I., Jeon, S.-J., Kim, H.-I., Islam, M. R., Castillo, C., Garcia, G. F. H., Newkirk, G. M., & Giraldo, J. P. (2022). Targeted Carbon Nanostructures for Chemical and Gene Delivery to Plant Chloroplasts. *ACS Nano*. https://doi.org/10.1021/acsnano.2c02714

Santana, I., Wu, H., Hu, P., & Giraldo, J. P. (2020). Targeted delivery of nanomaterials with chemical cargoes in plants enabled by a biorecognition motif. *Nature Communications*, *11*(1), 2045. https://doi.org/10.1038/s41467-020-15731-w

Schnell, R. A., & Lefebvre, P. A. (1993). Isolation of the Chlamydomonas regulatory gene NIT2 by transposon tagging. *Genetics*, *134*(3), 737–747. https://doi.org/10.1093/genetics/134.3.737

Schwab, F., Bucheli, T. D., Lukhele, L. P., Magrez, A., Nowack, B., Sigg, L., & Knauer, K. (2011). Are carbon nanotube effects on green algae caused by shading and agglomeration? *Environmental Science & Technology*, *45*(14), 6136–6144. https://doi.org/10.1021/es200506b

Stoiber, T. L., Shafer, M. M., Karner Perkins, D. A., Hemming, J. D. C., & Armstrong, D. E. (2007). Analysis of glutathione endpoints for measuring copper stress in Chlamydomonas reinhardtii. *Environmental Toxicology and Chemistry / SETAC*, *26*(8), 1563–1571. https://doi.org/10.1897/06-534r.1

Terashima, M., Freeman, E. S., Jinkerson, R. E., & Jonikas, M. C. (2015). A fluorescence-activated cell sorting-based strategy for rapid isolation of high-lipid Chlamydomonas mutants. *The Plant Journal: For Cell and Molecular Biology*, *81*(1), 147–159. https://doi.org/10.1111/tpj.12682

Thakkar, M., Mitra, S., & Wei, L. (2016). Effect on Growth, Photosynthesis, and Oxidative Stress of Single Walled Carbon Nanotubes Exposure to Marine Alga Dunaliella tertiolecta. *Journal of Nanomaterials*, *2016*. https://doi.org/10.1155/2016/8380491

Wang, J. W., Grandio, E. G., Newkirk, G. M., Demirer, G. S., Butrus, S., Giraldo, J. P., & Landry, M. P. (2019). Nanoparticle mediated genetic engineering of plants [Review of *Nanoparticle mediated genetic engineering of plants*]. *Molecular Plant*. https://doi.org/10.1016/j.molp.2019.06.010

Wei, L., Thakkar, M., Chen, Y., Ntim, S. A., Mitra, S., & Zhang, X. (2010). Cytotoxicity effects of water dispersible oxidized multiwalled carbon nanotubes on marine alga, Dunaliella tertiolecta. *Aquatic Toxicology* , *100*(2), 194–201. https://doi.org/10.1016/j.aquatox.2010.07.001

Williams, R. M., Taylor, H. K., Thomas, J., Cox, Z., Dolash, B. D., & Sooter, L. J. (2014). The Effect of DNA and Sodium Cholate Dispersed Single-Walled Carbon Nanotubes on the Green Algae Chlamydomonas reinhardtii. *Journal of Nanoscience and Nanotechnology*, *2014*. https://doi.org/10.1155/2014/419382

Wilson, R. H., Martin-Avila, E., Conlan, C., & Whitney, S. M. (2018). An improved Escherichia coli screen for Rubisco identifies a protein-protein interface that can enhance CO2-fixation kinetics. *The Journal of Biological Chemistry*, *293*(1), 18–27. https://doi.org/10.1074/jbc.M117.810861

Wong, M. H., Misra, R. P., Giraldo, J. P., Kwak, S.-Y., Son, Y., Landry, M. P., Swan, J. W., Blankschtein, D., & Strano, M. S. (2016). Lipid Exchange Envelope Penetration (LEEP) of Nanoparticles for Plant Engineering: A Universal Localization Mechanism. *Nano Letters*, *16*(2), 1161–1172. https://doi.org/10.1021/acs.nanolett.5b04467

Wu, H., Nißler, R., Morris, V., Herrmann, N., Hu, P., Jeon, S.-J., Kruss, S., & Giraldo, J. P. (2020). Monitoring Plant Health with Near-Infrared Fluorescent H2O2 Nanosensors. *Nano Letters*, *20*(4), 2432–2442. https://doi.org/10.1021/acs.nanolett.9b05159

Wu, H., Shabala, L., Shabala, S., & Giraldo, J. P. (2018). Hydroxyl radical scavenging by cerium oxide nanoparticles improves Arabidopsis salinity tolerance by enhancing leaf mesophyll potassium retention. *Environmental Science: Nano*, *5*(7), 1567–1583. https://doi.org/10.1039/C8EN00323H

Youn, S., Wang, R., Gao, J., Hovespyan, A., Ziegler, K. J., Bonzongo, J.-C. J., & Bitton, G. (2012). Mitigation of the impact of single-walled carbon nanotubes on a freshwater green algae: Pseudokirchneriella subcapitata. *Nanotoxicology*, *6*(2), 161–172. https://doi.org/10.3109/17435390.2011.562329

Zhang, H., Demirer, G. S., Zhang, H., Ye, T., Goh, N. S., Aditham, A. J., Cunningham, F. J., Fan, C., & Landry, M. P. (2019). DNA nanostructures coordinate gene silencing in mature plants. *Proceedings of the National Academy of Sciences of the United States of America*, *116*(15), 7543–7548. https://doi.org/10.1073/pnas.1818290116

Zhang, H., Goh, N. S., Wang, J. W., Pinals, R. L., González-Grandío, E., Demirer, G. S., Butrus, S., Fakra, S. C., Del Rio Flores, A., Zhai, R., Zhao, B., Park, S.-J., & Landry, M. P. (2022). Nanoparticle cellular internalization is not required for RNA delivery to mature plant leaves. *Nature Nanotechnology*, *17*(2), 197–205. https://doi.org/10.1038/s41565-021-01018-8

Zhu, G., Kurek, I., & Liu, L. (2010). Chapter 20 Engineering Photosynthetic Enzymes Involved in CO2–Assimilation by Gene Shuffling. In C. A. Rebeiz, C. Benning, H. J. Bohnert, H. Daniell, J. K. Hoober, H. K. Lichtenthaler, A. R. Portis, & B. C. Tripathy (Eds.), *The Chloroplast: Basics and Applications* (pp. 307–322). Springer Netherlands. https://doi.org/10.1007/978-90-481-8531-3_20

Chapter 5: Major Contributions and Prospects

In Chapter 2, we reviewed the need for chloroplast biotechnology improvements, compared synthetic biology tools to advance the field, the benefit of chloroplast research, and the current state of nanotechnology-enabled abilities to augment and deliver biomolecules to plant chloroplasts. With a central role in producing sustainable and reliable food, biomaterial, and biofuels, chloroplasts are uniquely capable of taking advantage of advances in synthetic biology (Figure 2.1). Thus, nanotechnology-mediated delivery of biomolecules is an application that will unlock advances in chloroplast biotechnology through synthetic biology approaches.

In our review, we found many papers that dealt with nanoparticles and microbes, but none that functionalized those nanoparticles and applied this nanotechnology for research. Environmental toxicology is a large aspect nanoparticle and microbiology research due to the human-caused runoff. Researching how these particles enter into microbes can help create new products that would be as impactful for their human uses, but not allow them to enter into cells, for example; conversely, studying nanoparticle uptake could help the environment by targeting specific types of microbes during toxic algae blooms. Entry mechanism research could also help researchers apply *in situ* methods of delivery that have yet to be explored but may yield higher efficiencies than standard protocols.

A missing gap in knowledge was identified in the application of these next-generation nanotechnology delivery techniques that had been used in land plants previously (Figure 2.3). With each algae being a single plant, a single-celled organism may be the best host for high throughput screening of a mutant library, for example. Additionally, single-walled carbon nanotubes and the LEEP model hypotheses that high aspect ratio and highly charged nanomaterials could enter through membranes, and this had yet to be explored in wildtype cell walls or cell wall knockouts of algae (Figure 2.2). Future work exploring the use of microbial nanotechnology may look at other organisms that have interesting material or biofuel value. Going further, nanotechnology-mediated delivery of biomolecules may be a method to explore new uncultured microorganisms through synthetic biology approaches. These new approaches could enable a microbial community-based health monitoring approach just as they are currently being used to watch plant health (Figure 2.5). In addition, new nanotechnology approaches could be used for microbes, and their related endosymbiotic organelles chloroplasts, to improve natural functions like photosynthesis in plants (Figure 2.6).

Chapter 3 develops a reliable and reproducible method for anionic cerium oxide nanoparticles, which scavenge reactive oxygen species and were shown to protect plant photosynthesis from abiotic stresses. As the abiotic stresses from climate change increase, reproducible protocols that can be used to research ways to deal with excessive reactive oxygen species will be in demand. This protocol can make an anionic, spherical, sub-11 nm cerium oxide nanoparticle that can scavenge ROS in leaf mesophyll cells and protect photosynthetic functions.

Future use of these ROS-scavenging cerium oxide nanoparticles could include algae bioreactors. Inside the algae fermenters, dissolved oxygen concentrations get very high. It may be possible for algae to live at higher concentrations of dissolved oxygen if nanoparticles like cerium oxide scavenged the reactive oxygen species that were generated; this is a frequent problem with current photobioreactors that are grown at high algal densities (Figure 3.6). Additionally, it may be possible to culture previously unculturable microorganisms by reducing their reactive oxygen species generated from the inevitable selection that happens during the culturing process. While pure cultures would be the desired end product, it has yet to be explored if nanotechnology can help ease the transition to a managed cultured state for a microbial community.

Chapter 4 of this dissertation shows proof of concept biomolecule delivery by engineered nanotechnology to algal chloroplasts. There is enormous potential for the nanomaterial delivery of biomolecules to algae chloroplasts through chloroplast transformation. If long pieces of DNA can be delivered to chloroplasts and incorporated into the plastome at high efficiency, large mutant libraries could be screened at higher efficiencies for more efficient lipid production for biofuels or new research into biodegradable materials. The tools developed in this Chapter are a critical step in delivering plasmid DNA to chloroplast, and also a steppingstone for future nanotechnology-based research on how to make the nanomaterial and its functionalization biocompatible in a high throughput manner. PEI was used as a coating for single-walled carbon nanotubes and found to have the highest charge with 25,000 MW but no additional length added (Figure 4.2). Translocation into algae was then confirmed with confocal microscopy and colocalization analysis - between the Cy3-ssGT$_{15}$ (Dye-DNA) and chloroplast autoflourescence - at a Dye-DNA:PEI-SWCNT ratio of 1:1, with the highest rates coming from the higher charged PEI25k coating. Interestingly and very importantly, there was colocalization between the Dye-DNA and algal chloroplasts even in the wildtype strain with a fully intact cell wall. Currently, cell wall knockouts are the preferred strains to be used for chloroplast transformation. If there was a chloroplast transformation capable of working with intact cell walls, as demonstrated here that may be possible, a vast majority of new strains would be usable for applications in chloroplast biotechnology. After analysis of Z-stacks for the number of colocalization events per algae, the wildtype strain was found to have 22.28% ± 6.42 of the algae undergoing an uptake event (Figure 4.3). With current chloroplast transformation rates being around 1:1,000,000 efficiency, this finding would have dramatic effects even if 1% of those 22.28% were deemed to be a viable colony forming unit after DNA uptake.

The remaining of Chapter 4 validates a high throughput assay to ascertain biocompatibility with nanomaterials and algae. Using this high throughput plate-based method, new coatings and ratios of DNA:nanomaterial could be performed and assayed before chloroplast transformation attempts. ROS generation, one of the biggest things to have been found to be lethal to algae after nanoparticle uptake, was assayed in serial dilution to ascertain lethal concentrations quickly and easily (Figure 4.4). Also importantly, ROS generation was found to be transient. Future assays should check to insure that ROS generation is transient by running a test 3-4 days after first exposure.

Running the same concentrations in our live-cell viability assay allowed us to see the peak concentrations and how they were impacting the cells in just three hours (Figure 4.5). These two assays get fairly quick results in 3 hours, but longer term viability must be measured as well. Here we tested, again in a high throughput manner, longer-term biocompatibility with *in vivo* photopigment concentrations (Figure 4.6). All of these tests combined to show us the upper limit of biocompatibility: 30 fg/cell of DNA-PEI25k-SWCNT and 300 fg/cell of DNA-PEI10k-SWCNT.

Not explored here are two assays that may be of interest to future researchers who are exploring chloroplast transformations by nanotechnology: *in situ* delivery and expression of a fluorescent reporter protein, and subsequent plating for colony-forming units. Delivery of a chloroplast-specific fluorescent reporter protein may be readable on a 96-well plate reader; an example of this would be using the *Chlamydomonas* prrn promoter to drive GFP biochemically linked to *aaDa*, which confers spectinomycin resistance; pATV1, a chloroplast-specific fluorescence reporter plasmid used in *Arabidopsis* chloroplast transformations, would be a good plasmid backbone for this vector. This could be a good way to test different coatings and DNA:nanomaterial ratios. Higher fluorescence would indicate higher biomolecule uptake. The viability of those cells could be done by plating them on selective and non-selective media, with additional colony-forming unit calculations. Selection on plate media would give the added benefit of allowing for the picking and verifying transformants directly - colony PCR followed by sequencing - after re-streaking.

Future research that extends the research explored in this thesis would be transformations and RNA-seq or mRNA expression analysis exploring the impact these PEI-SWCNT have on the cell. The goal of Chapter 4 was to produce a biocompatible concentration for the eventual use of chloroplast transformation. To eventually accomplish this goal, we believe that the PEI25k is a suitable coating of SWCNT and that it is capable of delivery plasmid DNA to the chloroplast of *Chlamydomonas*, just as SWCNT has delivered DNA to chloroplasts of land plants as previously reviewed. The conclusion of Chapter 4 is that the LEEP mechanism does seem to hold for *Chlamydomonas* just as it has with isolated chloroplasts and plant protoplasts. Therefore, the goal would be to use a highly charged high-aspect ratio nanoparticle like the SWCNT. Plasmid DNA-PEI-SWCNT (pDNA-PEI-SWCNT) would have to be validated with a biocompatible assay just like the ones presented in Chapter 4; our recommendation would be to use a concentration of around 30-300 fg/cell. It cannot be strongly stated that the characterization of PEI-SWCNT and pDNA-PEI-SWCNT must be done thoroughly, i.e. size, charge, DNA binding assay; this is where reproducibility of the nanotechnology-based biomolecule delivery chassis comes from. Algae should be grown to log phase growth, and cell counts should be performed. The exact concentration of pDNA-PEI-SWCNT used will matter based on the cell/mL concentration of the culture. pDNA-PEI-SWCNT should be added to algae already inside a tube, and then there are several delivery options: pipette up and down 10 times (as done in Chapter 4), vortexing, or reproducing previously explored methods that have been done, such as glass bead vortexing or even using the pDNA-PEI-SWCNT in lieu of gold particles within a particle bombardment chamber. The plasmid used should be encoding a resistance marker, i.e. *aaDa* for spectinomycin resistance, or restoring photosynthetic mutants from a knockout line. The main problem with resistance is that only some of the chloroplast genome copies could be transformed, leading to the need for culturing of the transformants until homoplasy has been confirmed. Theoretically, the drive for photosynthesis is so strong within a chloroplast genome that there are no chimeric plastomes produced within the photosynthetic knockout restoration. Once the algae are exposed to pDNA-PEI-SWCNT, we believe that successful DNA delivery is capable of happening within one hour, so anything further may just damage the cells. Something that has not been explored is the addition of a sucrose recovery stage (1 hour on an orbital shaker) in order to help the cells survive; we do not believe that this would hurt the cells in any way but may be superfluous if the pDNA-PEI-SWCNT is already biocompatible. Our hypothesis is that the SWCNT that entered the cell would stay there but will be diluted over time due to cellular division. After plating, successful transformants could be screened with standard cell biology colony PCR and sequencing. This same approach could be applied to nuclear transformations with another selectable antibiotic resistance marker, however the need for a highly efficient for multiple species is lower for nuclear transformations than it is with chloroplasts.

The next steps in terms of biocompatibility would be to analyze the transcription rates of the cell when exposed to the DNA-delivery chassis, PEI-SWCNT in this case. Aliquots of exposed cultures could be taken right after exposure, and then at 1-hour after exposure since we showed that entry could happen during that time. RNA-seq could be done to analyze the entire cell, or mRNA expression analysis could be performed on specific genes that have already been associated with ROS response in *Chlamydomonas*. For example as discussed in Chapter 4, *APX1* encodes for ascorbate peroxidase and is known to be involved in the ROS response of *Chlamydomonas*, but the exact mechanism is still unknown for how it deals with nanoparticle-specific damage; *MSD1* encodes for Manganese-superoxide dismutase in a large range of prokaryotes and eukaryotes that is capable of converting mitochondrial-generated ROS to hydrogen gas. Under the guise of environmental toxicology, these ROS-specific genes being upregulated may be an early sign of nanoparticle stress in aquatic and terrestrial microbes.

Conclusion

Uncultured microbes are the final frontier of biology research. Humans are in desperate need of new approaches for sustainable material and renewable biofuel production. Synthetic biology approaches have already been applied to great success in bacteria, but chloroplast biotechnology is falling behind. Nanotechnology-based approaches represent a new avenue to explore these uncultured microbial communities *in situ* or in high throughput applications with already cultured microbes. Additionally, nanotechnology research can be used to combat the problems humans are causing to the environment by protecting existing sustainable food sources and targeting harmful algal blooms. Biomolecule delivery into microbes can unlock new avenues to sensor existing microbial communities and explore new unculturable ones. Chloroplasts could become biomanufacturing devices for bioengineers that seek to make new biodegradable materials, high concentrations of renewable biofuels, and create new biopharmaceuticals through exploring vast mutant libraries.

This dissertation demonstrates methods to safely interface nanomaterials with *Arabidopsis thaliana* and *Chlamydomonas reinhardtii*, how they can be used for chloroplast bioengineering through increased photosynthetic protection to abiotic stresses, and the capability for them to delivery biomolecules to the algal chloroplast. By determining the biocompatible concentration of nanomaterial for land plant and algae, these approaches can be applied in the next wave of cutting-edge approaches.

Appendixes

Supplementary Figures: Chapter 4

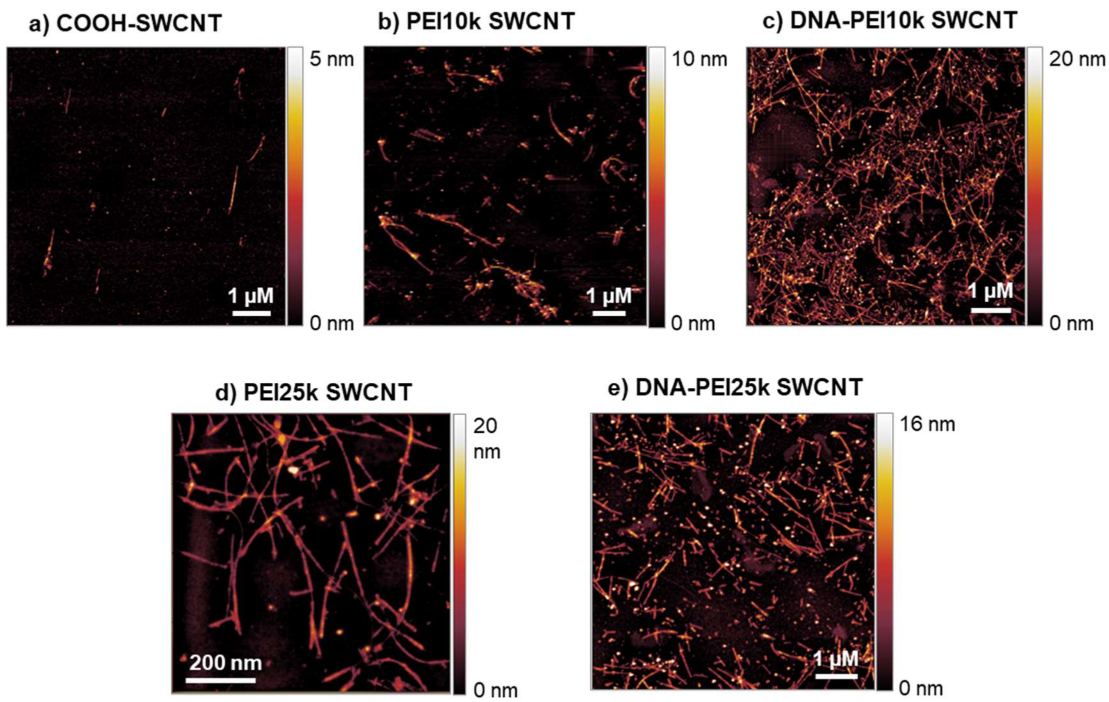

Supplementary Figure 4.1. AFM images of a) COOH-SWCNT, b) PEI10k SWCNT c) GT_{15} ssDNA coated PEI10k-SWCNT, d) PEI25k SWCNT, e) GT_{15} ssDNA coated PEI25k-SWCNT collected by tapping mode.

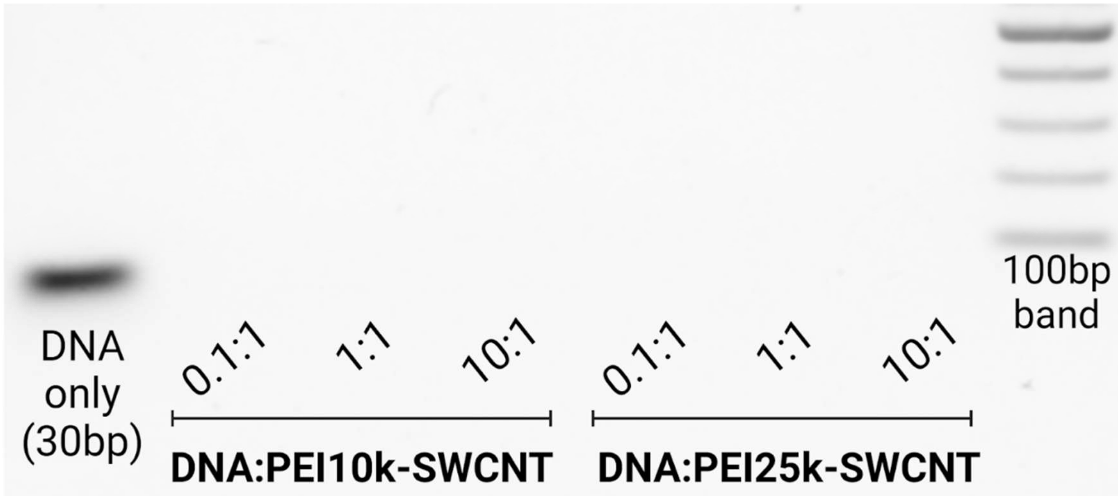

Supplementary Figure 4.2. Nanomaterial characterization of ssDNA binding efficiency. Gel electrophoresis with 1% TBE agarose gel of 0.1:1, 1:1 and 10:1 mass ratios of GT_{15}:PEI-SWCNT for DNA loading efficiency quantification after a 1 hour binding reaction shows 100% binding to PEI10k- and PEI25k-SWCNT.

.

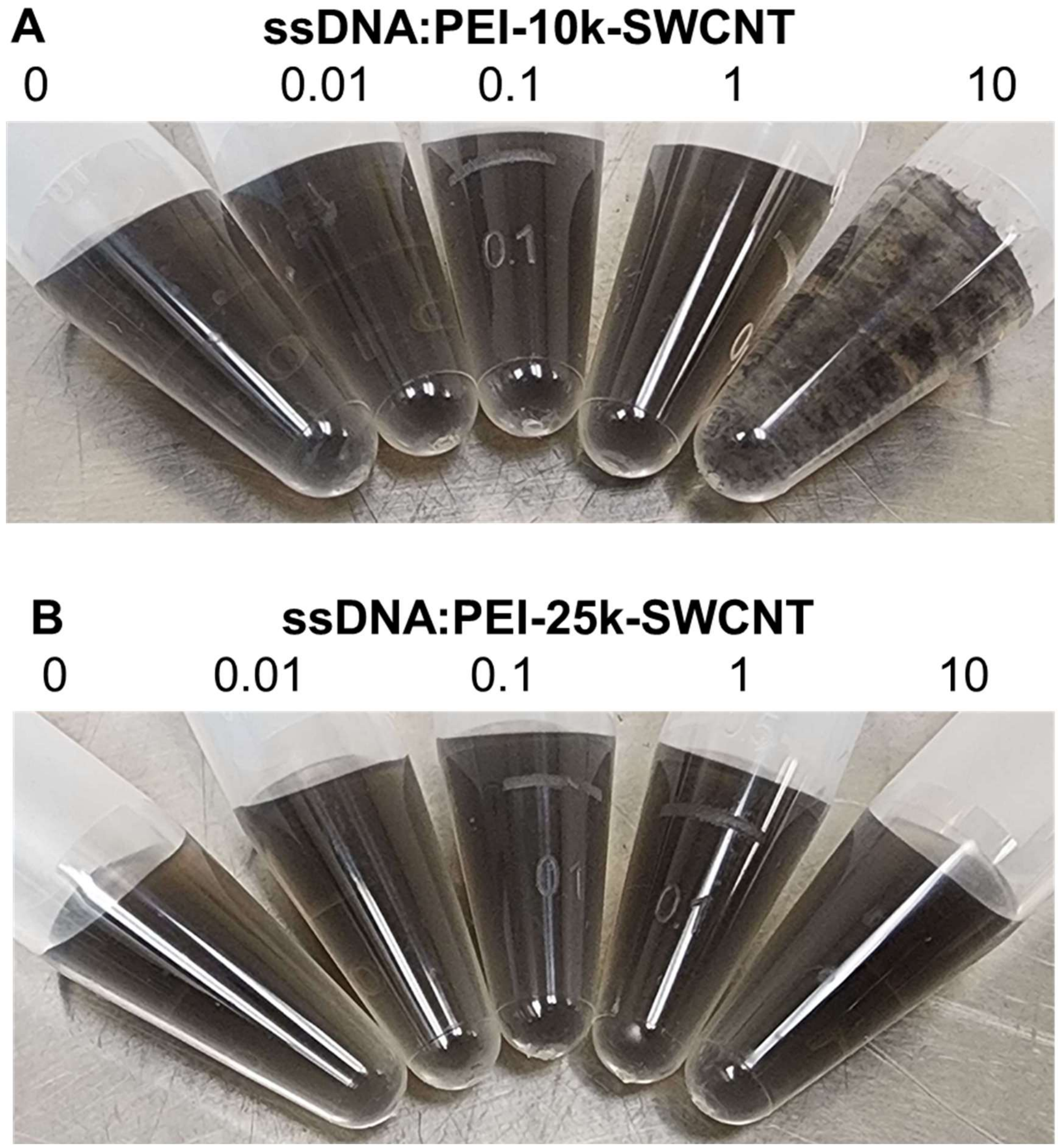

Supplementary Figure 4.3. Aggregation of ssDNA-PEI-SWCNT at high ssDNA:PEI-SWCNT ratio. a) PEI10k-SWCNT visibly aggregated at a 10:1 ratio of ssDNA:PEI-SWCNT, while b) PEI25k-SWCNT did not show any visible signs of aggregation at any of the testing ratios.

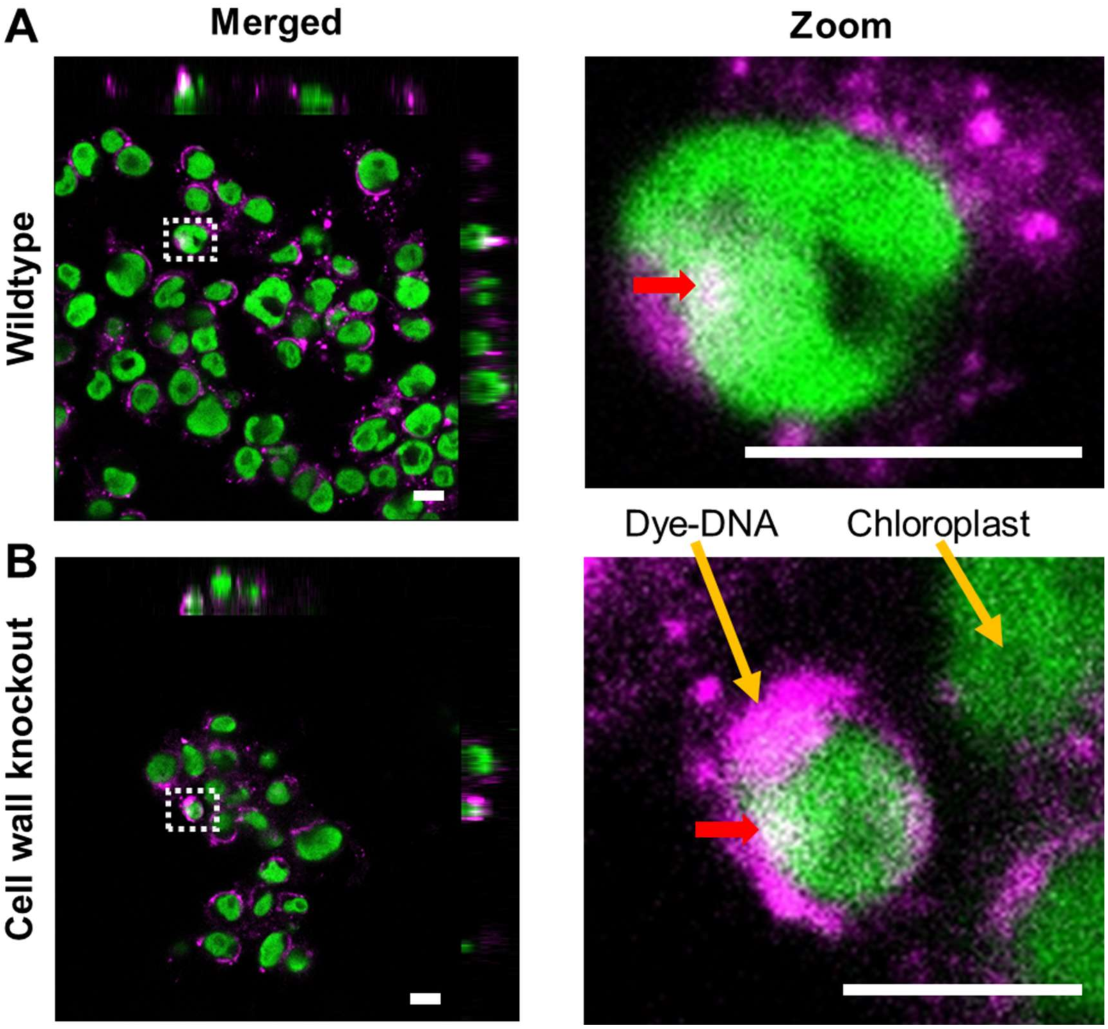

Supplementary Figure 4.4. Colocalization of Dye-DNA delivered by PEI10k-SWCNT within algae chloroplasts. Dye-DNA-PEI10k-SWCNTs colocalization with chloroplasts in the a) wildtype and b) cell wall knockout strain, after 1 hour incubation with 300 fg/cell of PEI10k-SWCNTs at a 1:1 Dye-DNA:SWCNT ratio (n=5).The scale bar is 10 µm. Overlap between Dye-DNA and chloroplasts is highlighted in the orthogonal views representing projections on the z-axis. Red arrows indicate areas of overlap.

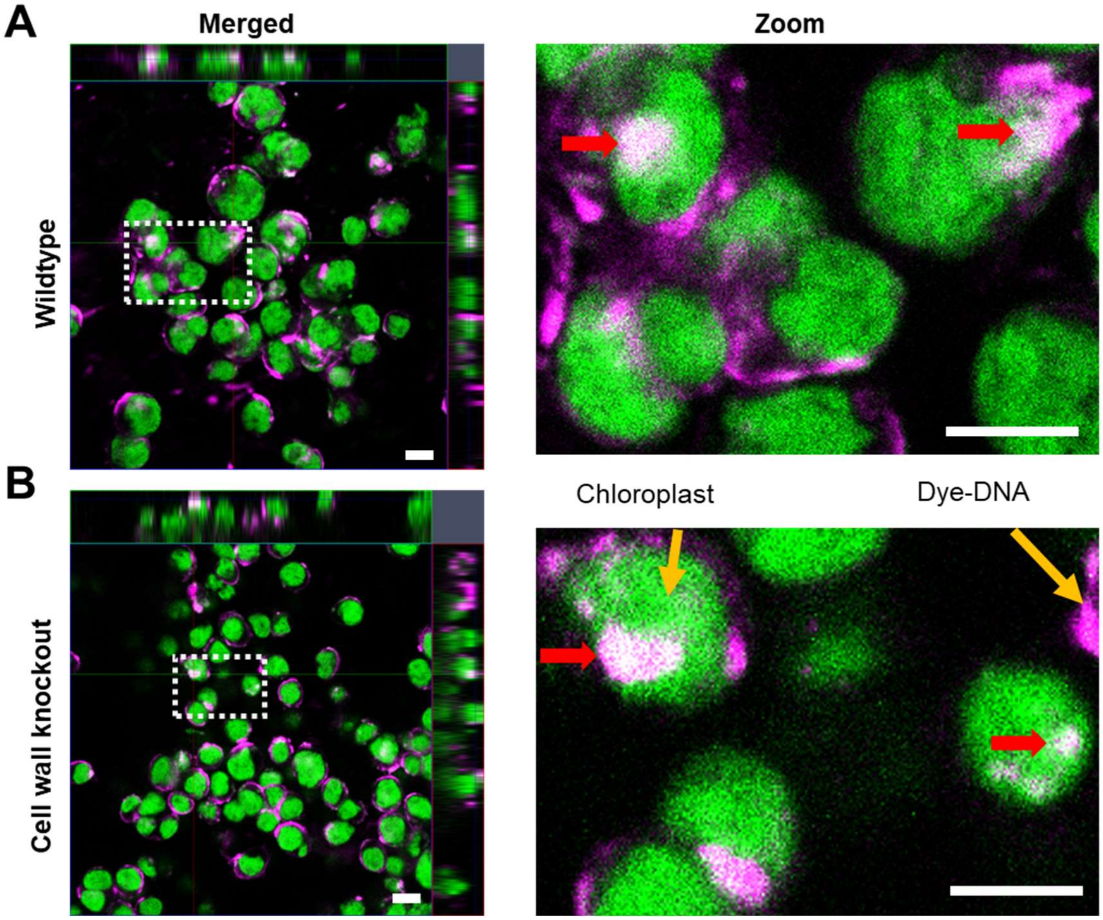

Supplementary Figure 4.5. Colocalization of Dye-DNA delivered by PEI25k-SWCNT within algae chloroplasts. Dye-DNA-PEI25k-SWCNTs colocalization with chloroplasts in the a) wildtype and b) cell wall knockout strain, after a 1 hour incubation with 300 fg/cell of PEI25k-SWCNTs with a 1:1 Dye-DNA:SWCNT ratio (n=5).The scale bar is 10 µm. Overlap between Dye-DNA and chloroplasts is highlighted in the orthogonal views representing projections on the z-axis. Red arrows indicate areas of overlap.

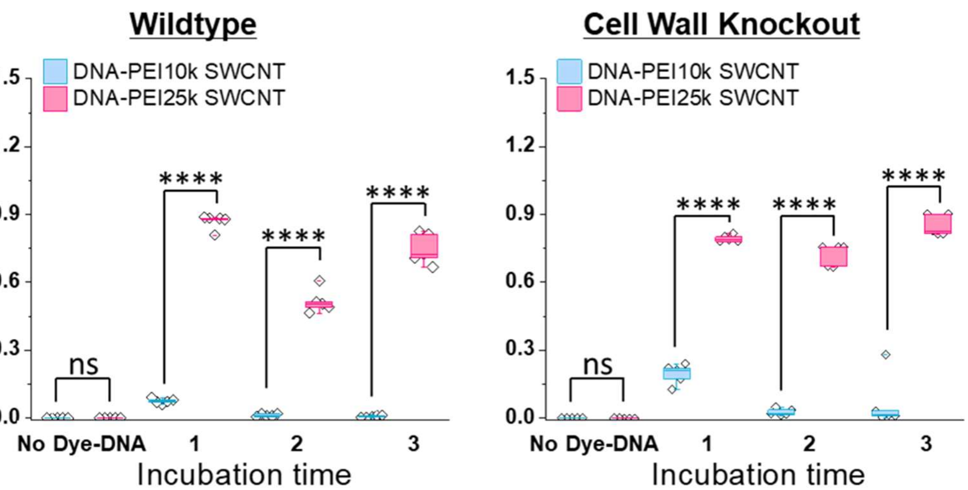

Supplementary Figure 4.6. Dye-DNA-SWCNT uptake into algae chloroplasts over time. DNA-PEI25k-SWCNT increased colocalization of Dye-DNA with chloroplasts (P*<0.05, ****<0.0001) to a larger extent than DNA-PEI10k-SWCNT in the wildtype and cell wall knockout strain after 1, 2 and 3 hour incubation (300 fg/cell of PEI-SWCNT with a 1:1 Dye-DNA:SWCNT ratio) (n=5; 1-way ANOVA analysis; box and whisker plot represents the minimum, 25th percentile, median, 75th percentile, and maximum)

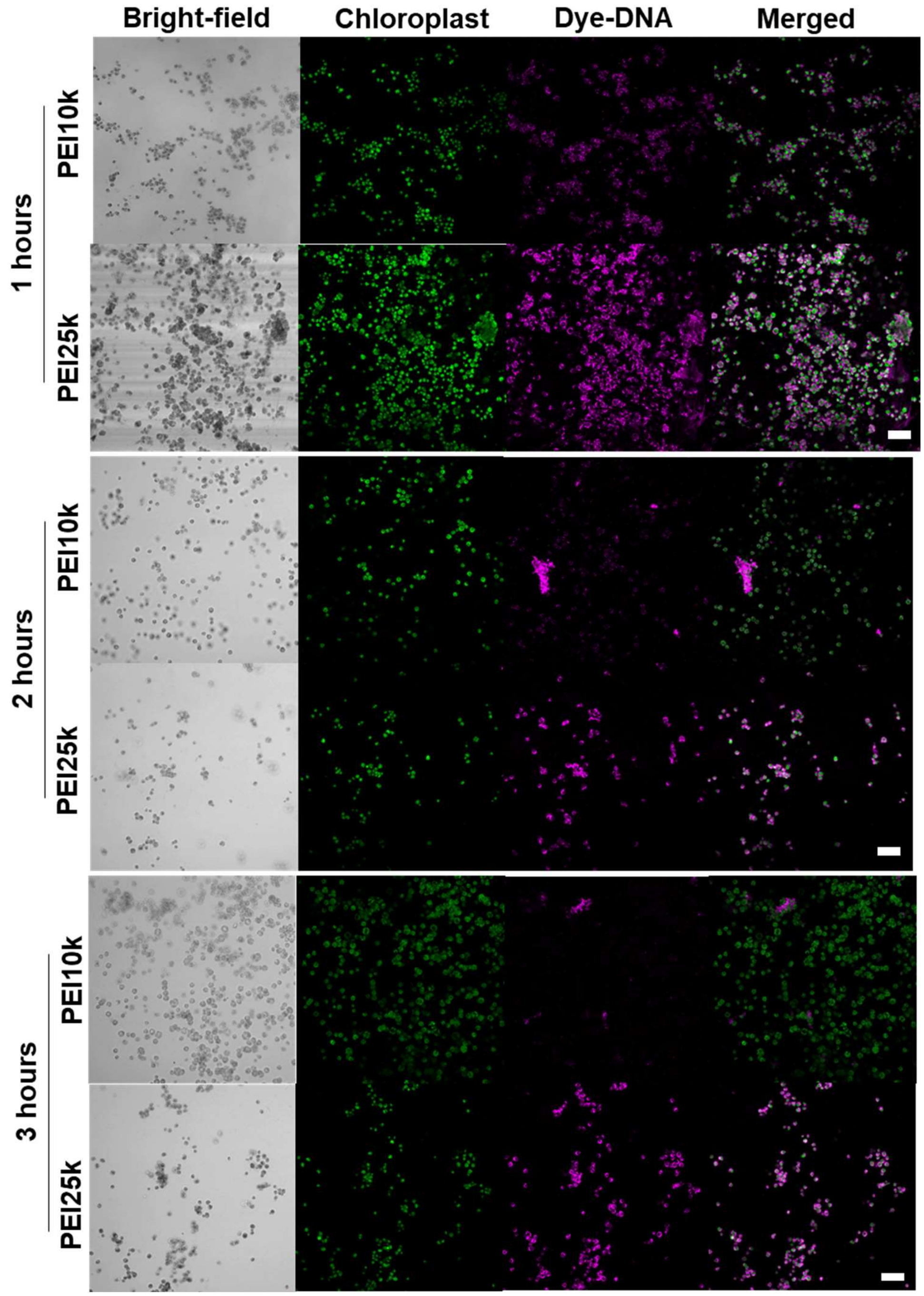

Supplementary Figure 4.7. Population-level wildtype algae with Dye-DNA-PEI10k-SWCNT and -PEI25k-SWCNT confocal microscopy across multiple time points. Higher colocalization between chloroplasts and dye-DNA is observed in PEI25k than in PEI10k SWCNT-treated algae at 300 fg/cell and 1:1 mass ratio of DNA:PEI-SWCNT. Representative population-level image; scale bar is 50 uM.

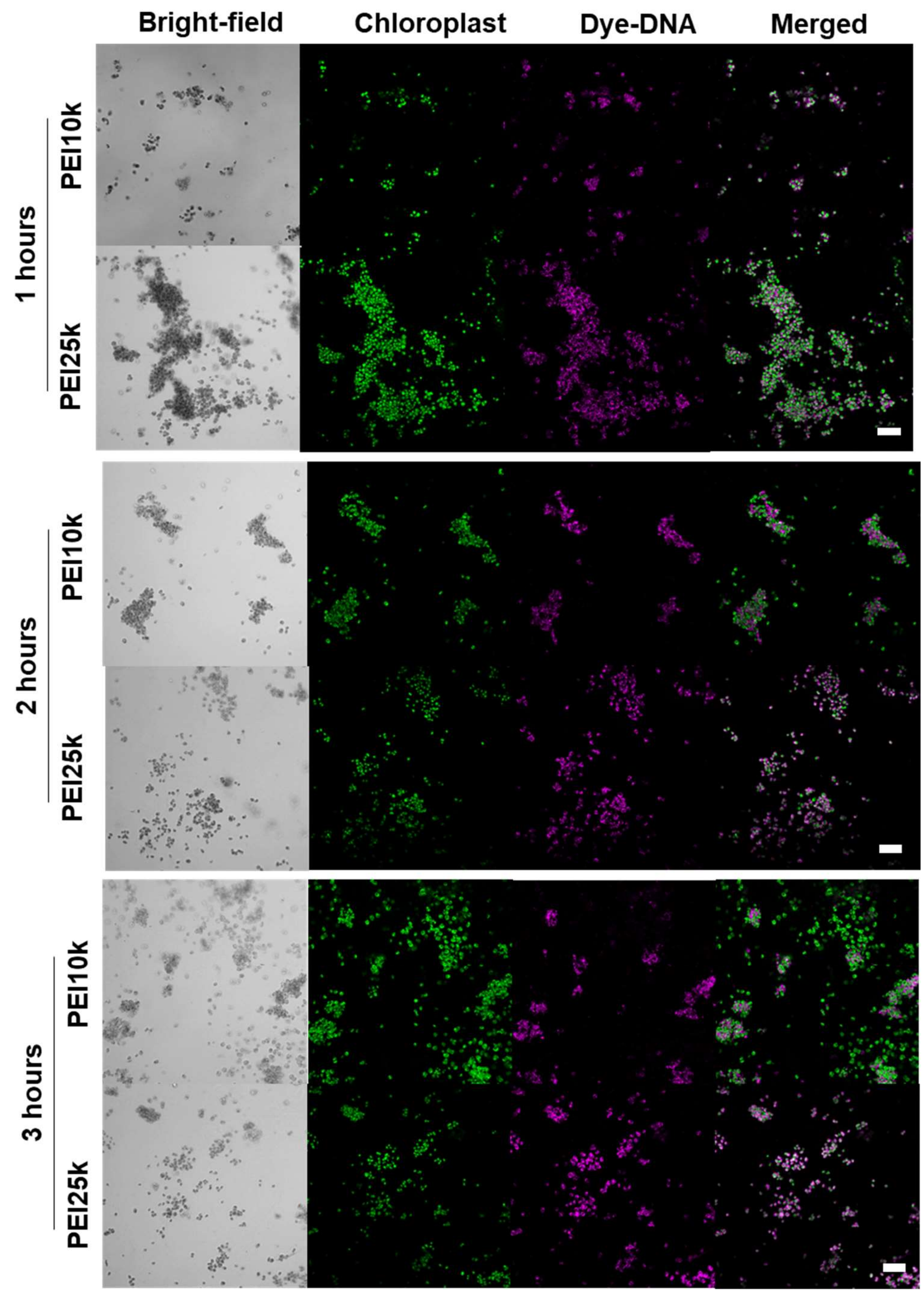

Supplementary Figure 4.8. Population-level cell wall knockout algae with Dye-DNA-PEI10k-SWCNT and -PEI25k-SWCNT confocal microscopy across multiple time points. Higher colocalization between chloroplasts and dye-DNA is observed in PEI25k than in PEI10k SWCNT-treated algae at 300 fg/cell and 1:1 mass ratio of DNA:PEI-SWCNT. Representative population-level image; scale bar is 50 uM.

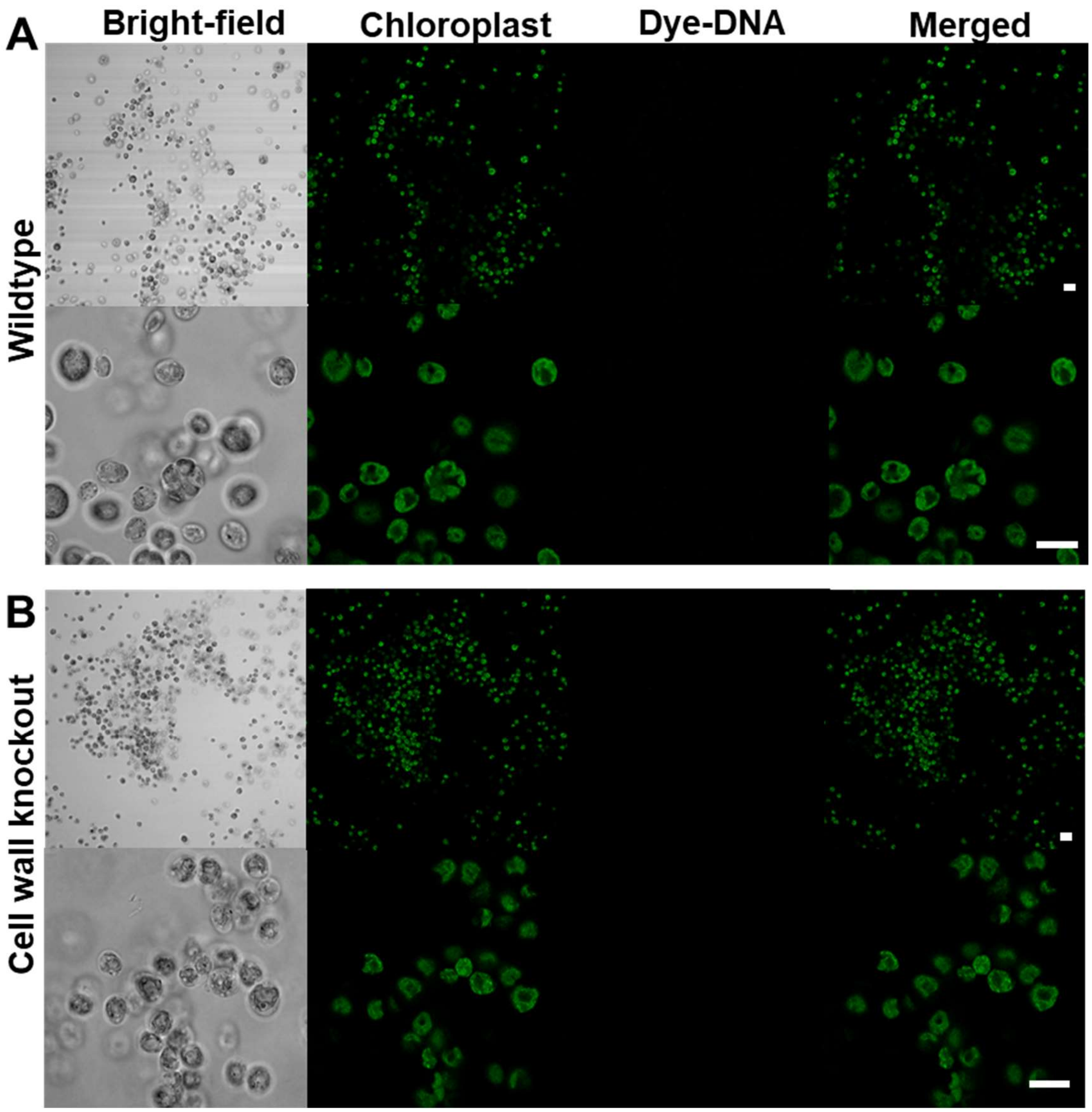

Supplementary Figure 4.9. Dye-DNA without PEI-SWCNT does not associate with algae. No Dye-DNA fluorescence was found in either a) wildtype or b) cell wall knockout algae exposed to the negative control without PEI-SWCNTs. The scale bar is 20 µm.

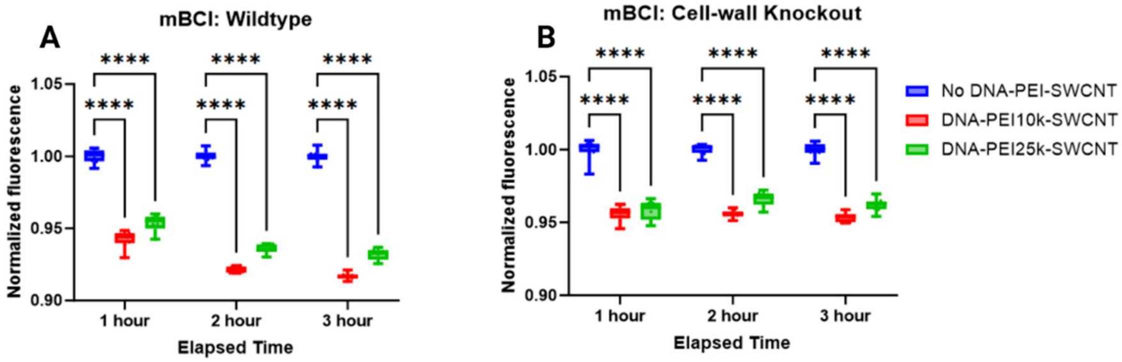

Supplementary Figure 4.10. Reduced Glutathione (GSH) upon reaction with ROS generated after DNA-PEI-SWCNT exposure. Monochlorobimane (mBCl) assay indicated that intracellular reduced Glutathione (GSH) levels decrease within one hour in response to both DNA-PEI10k- and DNA-PEI25k-SWCNT in a) wildtype and b) cell wall knockout strain (ANOVA one way test, ****P < 0.0001)(n=3). Glutathione is an antioxidant molecule used by algae cells to regulate ROS levels.

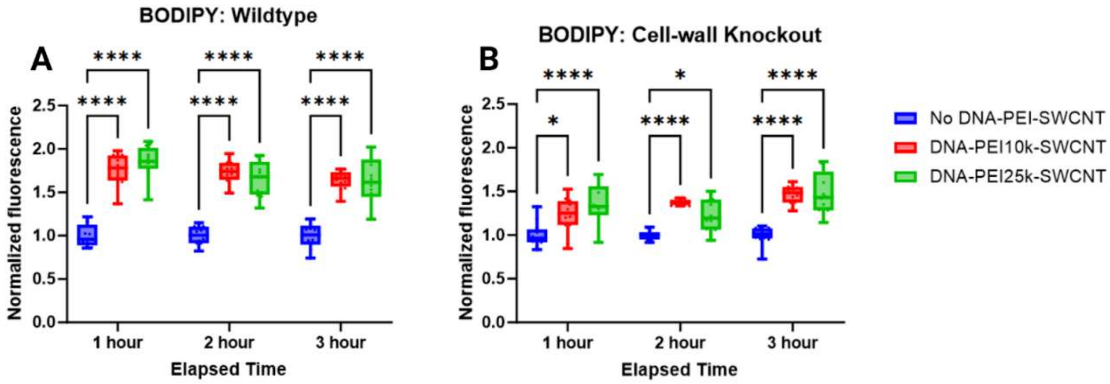

Supplementary Figure 11. Lipid peroxidase assay detects damage to lipid membranes due to reaction with ROS**.** BODIPY C11 identified an increase in lipid oxidation in algae after exposure to 300 fg/cell DNA-PEI-SWCNT in 1:1 ratio to DNA:PEI-SWCNT by mass. a) Wildtype and b) cell-wall knockout strains both showed statistically significant higher levels of lipid peroxidation, *P< 0.05 and ****P < 0.0001, respectively, when exposed to PEI-10k-SWCNT and PEI-25k-SWCNT (ANOVA one-way test; n=3, technical triplicate) indicating ROS damage in lipid membranes and impact on membrane integrity.